universität wien

Masterarbeit

Titel der Masterarbeit

Enlightening the sulfate-reducing microbiota in an acidic fen ecosystem: Dynamics of specific microbial groups in anoxic incubations with individual carbon degradation intermediates and enrichment of a novel, rare *Desulfosporosinus* species

verfasst von

Martin Huemer, BSc

angestrebter akademischer Grad

Master of Science (MSc)

Wien, 2014

Studienkennzahl lt. Studienblatt:	A 066 833
Studienrichtung lt. Studienblatt:	Masterstudium Ökologie
Betreut von:	Assoz. Prof. Dipl.-Biol. Dr. Alexander Loy

Table of contents

Index of figures

Index of tables

1 Introduction

Sulfur constitutes about 0.5 % of the earths chemical composition (Allègre et al., 2001) and is an essential elemental building block of all life forms. Its catalytic reactivity is speculated to be linked to the development of first molecular entities exhibiting surface metabolism and being capable of Darwinian evolution on early earth (Wächtershäuser, 1990).The variety of oxidation states ranging from −II to +VI implies diverse chemical properties and explains the suitability of this element as a constituent in a all major classes of biomolecules including nucleotides (Chen et al., 2010; Zhou et al., 2005). Not surprisingly, this flexibility in oxidation states was evolutionary exploited to fuel energy generation and carbon degradation via the biological redox cycling of sulfur species. The sulfur cycle (Sievert et al., 2007) is tightly coupled to the transformation and mineralization of carbon andsulfur metabolizing microorganisms, which make use of reduced and oxidized sulfur species, are phylogenetically widespread amongst *Bacteria* and *Archaea*. Moreover, the cycling of sulfur also gives rise to intermediate products such as dimethylsulfide, which is suspected to affect global climate on a large scale (Oduro et al., 2012) through the formation of oxidation products in the atmosphere that can act as cloud condensation nuclei according to the CLAW hypothesis (Ayers and Cainey, 2007).

Dissimilatory sulfate reduction refers to a step in the cycle, where sulfate acts as a terminal electron acceptor in the respiratory chain of anaerobic microorganisms. Phylogenetic evidence suggests that this process is ancient as it can be found both in *Archaea* and *Bacteria,* which are thus typically summarized as sulfate-reducing microorganisms (SRM) (Muyzer and Stams, 2008). Despite their unifying feature of using sulfate as an electron acceptor for respiration, these organisms are physiologically truly heterogeneous and can make use of a variety of carbon sources (Henstra et al., 2007; Kniemeyer et al., 2007; Musat et al., 2009), other electron acceptors (Dalsgaard and Bak, 1994; Park et al., 2008), employ different carbon assimilation strategies for growth, performing a syntrophic lifestyle (Plugge et al., 2011; Sousa et al., 2007), or form associations with *Archaea* in a consortium performing the anaerobic oxidation of methane (Boetius et al., 2000). At the global scale the functional importance of this microbial guilde is related to the degradation of carbon in marine systems. Estimates of the total oceanic sulfate pool depict sulfate as second most abundant anion (after chloride) with a total mass of 1.3×10^9 Tg and an average concentrationof 29 mM (Vairavamurthy Murthy A. et al., 1995). Calculations of gross sulfate reduction and global net sulfate reduction rates range between 75 Tmol (Jørgensen and Kasten, 2006) and 11.3 Tmol per year respectively (Bowles et al., 2014). Dissimilatory sulfate reduction in marine sediments as the major biological sink of sulfate is thus predicted to account for 12 to 29 % of the global organic carbon flux to the sea floor (Bowles et al., 2014), which strongly emphasizes the importance of SRM as autocatalytic units in this process.

On the contrary, SRM in terrestrial ecosystems such as freshwater wetlands are considered to face a scenario of low sulfate concentrations (in the micromolar range) but display sulfate reduction rates that can peak at levels comparable to those of marine sediments (Jørgensen, 1982; Pester et al., 2012). Wetlands are candidate environments for SRM, due to their water satured character and the resulting anoxic zones. In the anoxic layer the oxidative capacity of the system is constituted by nitrate, Fe (III), sulfate and complex organic substances such as humic acids (Limpens et al., 2008). Input of sulfate in marine sediments can be explained through flux of the external sources of ambient seawater and

oxidative biological recycling of the resulting sulfur at the oxic - anoxic interface. Although in marine sediments the cycling of redox states of sulfur can also exhibit complex recycling mechanisms (Nielsen et al., 2010; Pfeffer et al., 2012), the prevalence of this cycle is generally the default assumption in models. The observed high turnover rates in wetland ecosystems (Pester et al., 2012) can typically not be fully explained by external input sources (Wieder et al., 1990).This observation triggered the proposal of an internal recovery pathway of sulfate via an enigmatic hidden sulfur cycle. The foundation of this concept is, that reduced inorganic sulfur arising from dissimilatory sulfate reduction is re - oxidized with an internal, yet unknown redox mediator such as humic acids, quinone moieties and in particular Fe (III) (for further details refer to (Blodau et al., 2007; Klüpfel et al., 2014; Knorr and Blodau, 2009; Pester et al., 2012)).

On a global scale, two premises justify the importance of assessing SRM identity and activity in peatlands. First, wetlands and in particular peatland soil is functionally ambivalent when it comes to ecosystem services. Peatlands harbor one third of terrestrial organic carbon, sequester atmospheric CO_2 and thus can act as a net carbon sink if carbon degradation is recalcitrant (Limpens et al., 2008). On the opposite, emission of the potent greenhouse gas methane and the implied increased radiative forcing renders them as a potential threat for climate change (Frolking et al., 2006). Natural wetlands (e.g. peatland, marshes and swamps) and anthropogenic wetlands (e.g. rice paddies) are reported to account for 10 to 20 % of global methane emission (Wuebbles and Hayhoe, 2002) and their response in terms of carbon balance to changes in agricultural land use, global warming and other causalities of industrialism and post industrialism is uncertain. Second, methanogenesis is the result of metabolizing methanongenic archaea (MA), which populate the anoxic zones of wetlands. Importantly, when sulfate is available (non – limiting conditions) as an electron acceptor, SRM outcompete MA for the same substrates (e.g. H_2 and acetate) due to lower K_s values and thus higher substrate affinity (Kristjansson and Schönheit, 1983). Consequentely, elevated sulfate concentrations in wetlands, for instance caused by the deposition of sulfuric acid in acid rain, potentially divert the carbon balance away from methane emission. Estimates for this mitigating effect postulate a decrease of up to 14 % (Gauci et al., 2004). Logically, knowledge of the microbial community variables and their interaction is imperative to understand carbon balances in these ecosystems.

Here, the assessment of potential core taxa of SRM and a rare biosphere *Desulfosporosinus* species, that has the potential to be a key species in carbon degradation in peatland soil is reported. This work follows up on previous research conducted on SRM in the model peatland system Schlöppnerbrunnen II. The peatland (classified as acidic minerotrophic fen) is located in the catchment of the Lehstenbach river at the Czech – German Border Fichtelgebirge mountains (50° 08’ 38’’ N, 11° 51’ 41’’ E) and serves as an attractive model due to increased deposition of sulfuric acid caused by soft coal burning (Steger, 2010) and extensive sets of studies conducted. The mitigating effect of methane emission due to increased sulfate reduction was successfully demonstrated in *in vitro* studies (Loy et al., 2004) and taxonomic repertoires of SRM communities as well as biogeochemical parameters in the system were monitored for almost a decade (Küsel et al., 2008; Loy et al., 2004; Paul et al., 2006; Schmalenberger et al., 2007a; Steger et al., 2011). Briefly, the fen can be described as acidic (pH 4 to 5), with a mean groundwater table of 0.1 m, rich in iron, low sulfate concentrations (µM) and low concentrations of short chain fatty acids (SCFAs) and other carbonic acids (e.g. lactate) (µM). Various biogeochemical transformations of carbon have been identified in the system and linked to the reduction of Fe (III), methanogenesis and dissimilatory sulfate reduction. Despite the sparse availability of sulfate, the rapid turnover rate of the total sulfate pool (1.2 to 1.6 days) emphasizes the

importance of SRM in this process (Knorr and Blodau, 2009). Obviously, carbon transformation in a biogeochemically stratified natural ecosystem is performed by several functional entities and shall not be approached by a narrow investigation of only one particular unit of interest (such as SRM). From a naïve rationale it can be speculated that abundant organisms entail functional relevance for a given system. The application of 16S rRNA gene qPCR as well as amplicon and metagenomic DNA sequencing revealed that bacteria of the phylum of *Acidobacteria* are abundant in this fen ecosystem (Hausmann, 2014; Steger, 2010). Despite their high relative abundance *in situ* (up to 26 % only for subdivision 1) their functional role was not yet revealed. In order to get a glimpse into their response to conditions of anoxia and the availability of various small organic compounds, the abundance of *Acidobacteria* subdivisions 1, 2, and 3 was assessed by 16S rRNA gene-targeted qPCR here.

A major limitation when it comes to identifying unknown SRM in the environment is, that they do not constitute a coherent systematic group (Muyzer and Stams, 2008). Based on 16S rRNA analysis of cultivated sulfate reducers, this guild can taxonomically be classified in *Deltaproteobacteria, Firmicutes, Nitrospirae, Thermodesulfobacteria, Thermodesulfobiaceae, Euryarchaeota* and *Crenarchaeota* (Müller et al., in preparation; Muyzer and Stams, 2008). Due to observations, that these lineages can also harbor taxa that are clearly not capable to reduce sulfate, functional capacity cannot universally be inferred from 16S rRNA sequence data alone (Kendall et al., 2006).

A promising approach is to combine 16S rRNA gene information with the use of a functional marker gene that is universally found within the functional group of interest and meets the criteria for phylogenetic analysis (Wagner et al., 2005). Research of Wagner et al. (1998) indicated, that the evolution of the gene encoding dissimilatory (bi)sulfite reductase (*dsrAB*) in *Bacteria* and *Archaea* (Rabus et al., 2006), largely coincides with their evolutionary relationships postulated from 16S rRNA gene analysis and that they evolved from a common ancestor. By assessing *dsrAB* diversity and abundance distribution in the *in situ* fen ecosystem, a glimpse of the potential SRM diversity could be exposed. 53 species level operational taxonomic units (OTU) could be identified via *dsrAB* based screenings (Pester et al., 2012). qPCR analysis suggested for two particular OTUs (1 and 2), which constitute a dominant fraction of *dsrAB* diversity and represent core taxa of the Schlöppnerbrunnen microbiota, with relative abundance estimates of 1-2 % (Steger et al., 2011). A detailed assessment of known *dsrAB* diversity indicated that these OTUs are members of family level lineages with no closely related cultured representative (Pester et al., 2012).

In a DNA-stable isotope probing (DNA-SIP) incubation experiment, the response of the Schlöppnerbrunnen SRM community at the *dsrAB* and 16S rRNA gene level was investigated in incubations with sulfate and substrate (SCFAs and lactate) (Pester et al., 2010). No response of these "core" taxa could be observed, however a set of novel *Desulfosporosinus* species was shown to be the only relevant SRMs responding to the treatment with an increase in relative abundance and strong ^{13}C label incorporation. Surprisingly, *Desulfosporosinus* entities *in situ* could be classified as rare biosphere members (defined as a relative abundance below 0.1 to 1 % (Fuhrman, 2009; Sogin et al., 2006)) in Schlöppnerbrunnen II, with a relative abundance of only 0.006 % of the total bacterial and archaeal 16S rRNA gene pool. On the contrary, the DNA-SIP experiment suggested for a selective response of members of this genus to the sulfate amendment with an estimated cell specific sulfate reduction rate (csSRR) of 341 fmol of sulfate per day (Pester et al., 2010). The authors concluded, that the autochthonous *Desulfosporosinus* community has, despite its low abundance, the potential to catalyze a considerable part of sulfate reduction in the peatland.

As a consequence these SRM could representkey organisms in the competitive relationship for carbon with methanogenic *Archaea*. So far activity of this *Desulfosporosinus* species could only be confirmed in anoxic soil slurry incubations of Schlöppnerbrunnen II (Hausmann, 2014) and only a *Syntrophobacter* related *dsrAB* OTU (OTU 6) had been shown to be another autochthonous SRM member of the rare biosphere (Loy et al., 2004; Steger et al., 2011).The genus *Desulfosporosinus* currently comprises eight type strains (*D. lacus* (Ramamoorthy et al., 2006), *D. burensis* (Mayeux et al., 2013), *D. acidiphilus* (Alazard et al., 2010a), *D. orientis* (Stackebrandt et al., 1997), *D. youngiae* (Lee et al., 2009), *D. meridiei* (Robertson et al., 2001), *D. hippie* (Vatsurina et al., 2008) and *D. auripigmenti* (Newman et al., 1997)) isolated from various habitats ranging from soil, to freshwater wetlands, gasoline contaminated water and acid mine drainage sediments. Importantly, evidence is accumulating that this genus might contain members being well adapted to low pH environments, such as constructed wetlands (Lee et al., 2009) or acid mine drainage systems (Senko et al., 2009; Karnachuk et al., 2009; Sánchez-Andrea et al., 2013), which has rendered it an important candidate for biotechnological application such as acid mine drainage effluent remediation (Bertel et al., 2012; Kolmert and Johnson, 2001). The above described features of the novel *Desulfosporosinus* species in Schlöppnerbrunnen II (namely the potential for extraordinary high csSRR under acidic conditions) make this microorganism also valuable for biotechnological efforts such as bioremediation of acidic systems in constructed wetlands (Hallberg and Johnson, 2005).

The outlined observations induced the proposal of the major aims of this study.

1. Development of an effective, specific screening and detection strategy for the uncultured *Desulfosporosinus* species (*DSP SbII*) from Schlöppnerbrunnen II soil.
2. Development of a cultivation based approach to enrich the rare biosphere member *DSP SbII* from the background of the total microbial consortium.
3. Isolation and purification of *DSP SbII* strains for genome sequencing and characterization of basic physiological parameters.
4. Assessment of the response of the Schlöppnerbrunnen II core SRM microbiota (OTU1 and 2) and a rare biosphere member (OTU6) to the amendment of sulfate and carbon sources (Hausmann, 2012) via quantitative PCR based screening of *dsrA* genes.
5. Monitoring the change in 16S rRNA gene abundance of *Acidobacteria* subdivisions 1, 2 and 3 under different conditions of amendment of sulfate and carbon sources (Hausmann, 2012) via quantitative PCR.
6. Examine the effect of pH on growth of a *Desulfovibrio* species isolated from Schlöppnerbrunnen II.

2 Material and Methods

Statistical analysis and data visualization was performed in the software environment R 3.1.0 (R Core Team, 2014) using graphical packages *ggplot2* 0.9.3 (Wickham, 2009) and *lattice* 0.20-13 (Sarkar, 2008).

One fraction of this study was follow up work to a batch culture soil slurry microcosm experiment performed by Mag. Bela Hausmann (Hausmann, 2012). These anaerobic microcosms were amended with factorial variations of carbon sources (formate, acetate, lactate, propionate, butyrate and a no substrate control) with a differential amendment of sulfate (no sulfate amendment vs. sulfate amendment) at concentration parameters resembling the *in situ* conditions. Soil from Schlöppnerbunnen II was homogenized with filter sterilized Schlöppnerbrunnen II fen water and served as a growth matrix in the slurry incubations. This study aimed at investigating the response of microorganisms autochthonous in the Schlöppnerbrunnen II system under sulfate reducing conditions over a timecourse of 50 days mostly via genetic profiling. For a detailed description of experimental design of these microcosms refer to Hausmann, 2012.

2.1 Quantitative real time PCR

qPCR assays targeting the *dsrA* gene (Supplementary table 8-7) were evaluated *in silico* for specifity and coverage using a database of *dsrA* sequences (Müller et al., in preparation) and the probe match function implemented into the ARB software package (Ludwig et al., 2004). Coverage and specifity of *Acidobacteria* qPCR assays (Supplementary table 8-7) were reevaluated using the probe match function provided by the RDP database Release 10.32 (Cole et al., 2014). A description of the initial establishment of qPCR assays is provided in Steger et al., 2011. Due to changes of the qPCR setup (use of primers, chemicals and detections system) as performed here, assays were reevaluated with respect to performance parameters and specifity.
Standards for qPCR gene quantification were amplified from plasmid DNA of pre-established clone libraries via M13 primer based PCR. For acidobacterial standards, plasmid inserts were amplified from dilutions (1:10, 1:100 and 1:1000) to counteract unspecific signal amplification of the plasmid DNA. Subsequently identical PCR products from dilutions were pooled and purified with the QIAquick PCR Purification Kit (Cat. No. 28106, Qiagen, Netherlands) according to the manufacturer's instructions. The final elution volume was 50 µl. Length of purified standards was verified via agarose gelelectrophoresis. Identity of products was assessed via direct DNA sequencing (chain termination method) (Sanger et al., 1977) (microsynth AG, Switzerland), followed by querying the obtained sequence reads against the NCBI nr NT Database Release 193 (Benson et al., 2013) using BLASTn (Altschul et al., 1990). DNA concentrations used for copy number calculations were measured using the Qubit® dsDNA HS Assay (Cat. No. Q32851, life technologies, CA, USA) according to the manufacturers instructions. For absolute quantification, copy numbers were determined using Equation 1. Purified standards were diluted in Tris/EDTA 0.1 to a dilution factor of 10^{-13} and stored at −20°C. In order to assess cross specifity of qPCR assays, false positive signal amplification was evaluated by complementing the target standard with the remaining non-target group standard dilution series as controls (e.g. *Acidobacteria* SD1

assay with standards of SD2 and SD3 as non target controls (NTAC)). For standard evaluation, samples were applied as technical triplicates. A detailed description of qPCR primer pairs, employed standards, thermal cycling conditions and qPCR performance parameters is provided in supplementary material and methods section 8.1.1. DNA from microcosm experiments had been extracted previously via a cetrimonium bromide (CTAB) based Phenol/Chloroform method (Hausmann, 2012) and was ready to use for downstream qPCR analysis.

*Acidobacteria*16S rRNA gene-and *dsrA*-targeted qPCR assays were performed with a CFX96 Real–Time PCR detection system (Bio-Rad Laboratories, CA, USA) using the iQ™SYBR®Green Supermix (Bio-Rad Laboratories, CA, USA). Samples were applied as technical duplicates, while standards were applied as single copies. No template controls (NTC) were included for each run. The limit of detection (LOD) was set to be 3.3 cycles lower (one log value) than the respective quantification cycle (Cq) of the NTC (Smith and Osborn, 2009). When no signal was detected for the NTC after a complete qPCR run, the Cq value of the highest dilute standard was employed as the LOD. At the end of each run, a meltcurve analysis was performed to verify specific target amplification. Additionally, correct size of qPCR products was verified via gelelectrophoresis for each assay once. Processing of primary data was performed *in silico* with the Bio-Rad CFX Manager 3.0 (Bio-Rad Laboratories, CA, USA). Traces were normalized via the baseline subtraction option. Inhibition of qPCR (e.g. template concentration, co extracted substances) assays was assessed, using a dilution series of a DNA extract (DNA 091, microcosm propionate without sulfate, day 16 (Hausmann, 2012)) as target and *Syntrophobacter wollinii* 16S rRNA gene dilutions as standard (employing the primer pair 1389Fmix/1492R). Efficiencies and correlation coefficients were similar between STD and DNA 091 up to 5 ng of template DNA applied per reaction, which supports reaction setups as performed here.

For evaluation of cross specifity co-reactions, linear regression models were applied to resulting Cq values and corresponding log of copy numbers of standards and the respective NTAC standards. Datapoints that were clearly not within the linear part of the model were excluded from analysis, as they were supposed to be below the LOD. In order to estimate the potential contribution of unspecific amplification to Cq values (expressed as cross specifity error), the Cq value of each NTAC was calculated from their linear regression model for a copy number of 10^{-8} copies per reaction. The resulting Cq value was used to calculate the corresponding copy number from the linear model of the standard, which allowed the estimation of the introduced error under the assumption of equal copy numbers between STD and NTAC (for further details refer to the results section).

Ratios of *dsrA* gene or *Acidobacteria* 16S rRNA gene to total bacterial and archaeal 16S rRNA gene copies (BA 16S) were calculated using total 16S copy numbers provided by Mag. Bela Hausmann and used for all downstream statistical analysis.

For correlation analysis, mean *dsrA* relative abundances were compared against normalized mean sulfate concentrationsand raw anion concentrations of the respective microcosms (Hausmann, 2012). Spearman rank correlation coefficients were determined using the function *cor.test* implemented into R.

Homoscedasticity (homogeneity of variance) of treatments from acidobacterial assays was examined for each subdivision respectively via a Fligner-Killeen test (Conover et al., 1981) employing the function *fligner.test* implemented into R. Difference between treatments was examine by conducting Kruskall—Wallis one-way ANOVA (with alpha values being corrected for multiple testing by the Bonferroni method (Dunn, 1961)) using the function *kruskal* implemented into the R package *agricolae* (de Mendiburu, 2014).

In order to evaluate the predictive value of relative abundance data derived from 16S rRNA V4 region amplicon sequencing, the respective abundance values for the very same specimen for acidobacterial subdivisions 1 to 3 were correlated against the ratios obtained via qPCR analysis using Spearman rank correlation.

Equation 1(adopted from Hausmann, 2012)
Atomic mass of dsDNA was calculated using the online tool *DNA/RNA/Protein/Chemical Molecular Weight Calculator* (Copyright © 2002–2007 Chang Bioscience, Inc.). DNA sequences used for atomic mass calculations are provided in supplementary section 8.1.1. For ambiguous bases the average weight of a dNTP was used. Volume refers to the volume of template applied in one qPCR reaction.
Atomic mass constant: 1u = 1.660538921 × 10^{-27} kg.

$$copy\ number = \frac{concentration\ (ng\mu l^{-1}) \times volume\ (\mu l)}{atomic\ mass\ (u) \times atumic\ mass\ constant\ (kgu^{-1})}$$

2.2 Targeted isolation of sulfate reducing microorganisms

2.2.1 Sources of microorganisms

A soil slurry (see Section 2.2.3) containing Schlöppnerbrunnen *Desulfosporosinus* cells (DSP-SbII), enriched to a relative abundance of 4 % as determined by *Desulfosporosinus* 16S rRNA gene qPCR (Hausmann, 2012, 2014) was used as the initial source for inoculation.
Desulfosporosinus acidiphilus SJ4 (DSM no. 22704) (Alazard et al., 2010b) was obtained from the DSMZ (Deutsche Sammlung von Mikroorganismen und Zellkulturen, Braunschweig, Germany) for the purpose of cultivation and monitoring techniques optimization. A *Desulfovibrio* isolate from Schlöppnerbrunnen II (*Desulfovibrio* sp. SII13a) was provided by Mag. Bela Hausmann in order to assess the effect of acidity on growth parameters.

2.2.2 Media

D. acidiphilus was grown on DSMZ medium 1250. For the isolation procedure of DSP-SbII three different media were employed. A basal freshwater medium (pH 7.1) (FM) modified from Widdel and Bak, 1991, the DSMZ medium 1250 without fructose (pH 5.6) and a basal salts/yeast extract medium (pH 4.5) for cultivation of acidophilic sulfate reducing bacteria (aSRB medium) as described by Sen and Johnson, 1999.All media were prepared in a Widdel flask using standard sterile anoxic technique (Widdel and Bak, 1991). Stock solutions of anoxic substrates (carbon source and electron donor) and electron acceptors were made as instructed in Widdel and Bak, 1991. Substrates and electron acceptors were added to the respective basal medium prior to the inoculation step using standard anoxic technique (Widdel and Bak, 1991 and Hungate, 1969). The theoretical degree ofdissociation (α) of ionic substrates in dependence of pH, was calculated for standard condition pK_a values for the respective substance. Ionic strength and temperature were not considered in the calculation, as only minor deviations were expected (Partanen et al., 2003) and substrate concentrations were relatively high in media (5 to 10 mM). α was expressed through the Henderson-Hasselbalch equation (Supplementary table 8-8). For further information regarding anoxic cultivation working principles, as conducted here refer to Hausmann, 2012 and Widdel and Bak, 1991.

2.2.3 Isolation and growth conditions

If not stated explicitly, general imposed growth conditions for DSP-SbII enrichments were defined as stationary incubation at 14°C in the dark. Liquid cultures were incubated with a

small overpressure in the headspace (approximately 0.2 bar) to counteract diffusion of ambient oxygen into vials. For soil slurries, dialysis chambers and soil agar, autoclaved soil (121°C, 20 min) from Schlöppnerbrunnen II (core depth between 10 to 20 cm, April 2013) was used. For dialysis chambers and soil agar, fen soil was homogenized with a sieve to a particle size of 2 mm and autoclaved twice to ensure sterility. If not stated explicitly, the setup of growth environments and all downstream manipulations was performed meeting the requirements of anoxic technique. A genealogy of the enrichment setups, as well as detailed procedural description regarding the setup of isolation approaches is provided in supplementary section 8.1.2.

Soil slurries: The setup of soil slurries was already established by Mag. Bela Hausmann (Hausmann, 2012). Approximately 1 g of autoclaved soil was transferred into a Hungate tube that was subsequently flushed with the N_2/CO_2 for about 1 min. 10 ml of freshwater medium were added. Na_2SO_4 concentration was adjusted to 5 mM if not stated otherwise. For transfers of biomass and sampling, tubes were gently inverted until soil particles were fully suspended. After sedimentation 0.5 ml of the supernatant was anoxically retrieved (needle outer diameter 0.6 mm).

Pasteurization: Three approaches(Fichtel et al., 2007 and Fichtel et al., 2007b) to induce sporulation of DSP-SbII cells were set up. As a primary source of cells, active soil slurry 1A4 (measured residual 0.9 mM sulfate and 0.4 mM acetate) was used.

Exhaustion/cold stress method: 1 ml of the soil slurry enrichment was anoxically and stationary incubated at 4°C in the dark without any further amendments for the sporulation timeframe.

Resuspension method: 1 ml supernatant of the soil slurry was transferred into a Hungate tube containing only basal FM to deplete nutrients and sulfate (no sulfate could be detected via capillary electrophoresis). Incubation was performed at 14°C stationary in the dark.

Desiccation/Oxygen stress method: 1 ml of soil slurry suspension was transferred into a Hungate tube that was closed with an aluminum cap only, to permit desiccation and diffusion of oxygen.

As a fourth source of *Desulfosporosinus* spores, 2 ml of an active growing soil slurry enrichment (Sp1s) were diluted in 8 ml basal FM and directly used for pasteurization.

Spore formation was tried to be assessed via extraction and measurement of pyridine-2, 6-dicarboxylic acid (DPA) content from incubations by the method described in He et al., 2003 with Capillary Zone Electrophoresis (Beckman Coulter P/ACE™ MDQ Molecular Characterization System). Spiked DPA could be quantified in soil slurries, but indigenous DPA could not be detected via this approach.

Sporulation approaches were anoxically pasteurized after 105 days of incubation (including Sp1s) with a two factorial variation of pasteurization temperature and time for each specimen (80°C—20 min/ 90°C—20 min/ 95°C—30 min). The absence of sulfate in sporulation approaches was verified via capillary zone electrophoresis.

Pasteurized specimens were provided with basal FM (sulfate [5 mM]) and incubated stationary at 14°C in the dark.

Dialysis chamber

In order to emulate the physicochemical parameters of the soil slurry incubations, while avoiding the limitations for downstream analytical methods that arise from the soil debris, a dialysis chamber setup was designed that meets the requirements of anoxic incubations and allows growth of the target *Desulfosporosinus* population. Dialysis membrane tubing (ZelluTrans/Roth Dialysis membranes T1, Cat. No. E656.1, Carl Roth GmbH + Co. KG, Germany) was filled with approximately 2.5 cm^3 of homogenized autoclaved soil and sealed.

A flat cuboid geometry was chosen for the filled dialysis tubing (1.7 × 2 × app. 7 cm) in order to maximize its surface to volume ratio (S/V=13). Structurally intact dialysis membranes exclude the migration of microorganisms while allowing diffusion of molecules below a molecular weight cutoff of 4 to 6 kDA. The residual ambient gas atmosphere was removed from the resulting sterile soil tube. The final setup of the dialysis chamber can be specified as the dialysis soil tube being immersed in 50 ml of basal FM (Na_2SO_4 [5 mM]) in a 250 ml borosilicate flasks (GL45, Duran Group, Germany), sealed with butyl rubber stoppers to allow sampling. If not stated else, the final setup was incubated abiotically for one week before inoculation, to allow equilibration of diffusible molecules between solute fraction (later inoculated with DSP-SbII enriched biomass) and soil fraction. The headspace was provided by the N_2/CO_2 mixture at 0.2 bar. pH was determined (inoLab® pH Level 1, WTW) at the end of the preincubation period (between 7.05 and 7.00). Headspace was renewed via flushing with N_2/CO_2 for 30 min when sulfate was depleted in order to remove accumulated H_2S.

Defined media array

In order to select for DSP-SbII cells from high relative abundance enrichments via substrate preferences, the three basal media were amended with one substrate at a time (H_2/CO_2; H_2/CO_2/Na-acetate; ethanol; Na-propionate; Na-(L)-lactate, glycerol and Na-butyrate) at a concentration of 10 mM (basal FM and aSRB medium) or 5 mM (DSMZ medium 1250) each. Basal FM was intentionally left at neutral pH to ensure that SCFAs and lactic acid dominate as dissociated anions. Substrates were added from 1M anoxic stocks prepared as outlined in Widdel and Bak 1991. Entities amended with H_2/CO_2(90/10, v/v) were provided with 0.5 bar of the gas mix in the headspace of the Hungate tube.When growth started, $H_2/CO_2$was added to a final pressure of 2 bar. Tubes having H_2 as electron donor were incubated at room temperature on a shaker to increase diffusion of hydrogen into the liquid phase. Glycerol and ethanol as non ionic substrates were used specifically for acidophilic SRM, as they are considered to be physiologically beneficial at low pH (Johnson, 1998; Kolmert and Johnson, 2001; Sánchez-Andrea et al., 2013). Sulfate concentrations for the three basal media were adjusted to 5, 10 and 15 mM (DSMZ 1250, FM, aSRB) respectively. All incubations were set up in Hungate tubes with 10 ml of medium and a headspace pressure of 0.2 bar (N_2/CO_2).

Agarshake

Dilution series using the agarshake method (Widdel and Bak, 1991)were performed for two specimens highly enriched in DSP-SbII cells. Dilutions were performed down to a factor of 10^{-9}. Standard incubation conditions were applied to agarshake tubes, except that tubes were incubated upside down. After development of colonies, 12 individual colonies were picked as outline in Widdel and Bak, 1991 and transferred anoxically in basal FM containing lactate [10 mM] as a carbon source (Na_2SO_4 [10 mM]). Morphology of resulting colonies was examined using a stereomicroscope (Leica M205 C, Leica Microsystems GmbH, Germany). Morphology of the cells from a colony was examined via phase contrast microscopy (Axioplan 2 imaging microscope equipped with AxioCam HRC CCD camera, Zeiss, Oberkochen, Germany).

Soil agar

The capability of DSP-SBII cells to propagate on a solid surface support was assed via inoculation of an enriched specimen on soil agar (2 % w/v agar) petri dishes (Cat. No. 632102,Greiner bio-one, Austria). Briefly, Agar (Bacto™ Agar, Cat. No. 214010, Becton, Dickinson and Company, New Jersey, USA) was washed as described for the agarshake method, supplemented with autoclaved sieved soil and basal FM (Na_2SO_4 [5 mM]). The suspension was aerobically autoclaved at 110°C for 15 min in sealed borosilicate flasks. Plates were poured aerobically and subsequently made anoxic via transfer into an anaerobic

jar (Code: HP0011, Oxoid, Thermo Fisher Scientific, Massachusetts, USA) amended with an oxygen removal catalyst bag (Oxoid AnaeroGen, Code: AN0035,Thermo Fisher Scientific, Massachusetts, USA) and repeated renewal of the N_2 atmosphere for 10 days. The absence of oxygen within the final soil agar was verified with a needle type housing oxygen microsensor (Microx TX3/ flat broke type sensor (NTH), PreSens-Precision Sensing GmbH, Regensburg, Germany) at 5 depth sections (3, 5, 7, 9 and 11 mm) at ambient oxygen atmosphere (1007 mbar). The system was calibrated according to the manufacturers instructions. The measurement parameters were: 40 seconds of measurement at dynamic averaging (mode 4), temperature compensation enabled and measurement mode 1 sec.
Anoxic plates were inoculated from DSP-SbII enriched liquid cultures and incubated in the anoxic jar under forming gas atmosphere (N_2/H_2 = 95:5 (v/v)) with a new catalyst bag provided. Standard incubation conditions were applied.

Dilution to extinction

Dilution series were performed in Hungate tubes with basal FM using either lactate or butyrate as substrate and Na_2SO_4 or Fe(II)SO_4 as electron acceptor. Substrate concentrations and sulfate concentrations were adjusted to 10 mM. The volume of inoculated tubes was 9 ml. An overpressure of 0.2 bar (N_2/CO_2) was provided to the tubes.

Desulfovibrio pH series

Desulfovibrio sp. SII13a was analyzed in respect to its capability to grow at acidic pH with lactate as substrate. The strain has been previously shown to grow on basal FM amended with lactate [10 mM] and Na_2SO_4 [5 mM] at neutral pH (Hausmann, 2012). A growing culture was inoculated (0.5 ml) in aliquots (10 ml) of basal FM (same composition as above) into Hungate tubes with variable pH. pH was adjusted with 1M HCl to values of 7, 6.4, 6.1, 4.4, 2.4 and 1.8 for the first experiment. For the second experiment, the culture exhibiting growth at the lowest pH was used as an inoculum for a pH series of 7.1, 5.9, 5.6, 5.2, 4.5, 4.1, 3.7 and 3.4. After inoculation and at the end of exponential growth pH was measured again. Note, that at pH values below 3.86 (=pK_A of lactic acid), the major proportion of lactic acid will theoretically be constituted by its non-ionic form.
Capillary zone electrophoreris (CE) measurements were conducted for the timepoint zero, endpoint of exponential phase and mid stationary phase. Optical density at 600 nm was measured daily (M107 High Specification Visible Range,Spectronic Camspec Ltd., Leeds, UK). Fluorescence in situ hybridization (FISH) was performed for paraformaldehyde (PFA) fixed cells using the Delta495mix (Table 2-1) in combination with EUB338mix (Table 2-1) as probes. Further details are provided in section 2.2.4. Standard incubation conditions were applied.
Growth rate μ was determined from exponential growth phase turbidity measurements according to Equation 2.

Equation 2
Equation used for growth rate determination. OD denotes optical density at 600nm at timepoint 1 and 2 respectively. T denotes time (days) at the respective OD measurement points.

$$\mu = \frac{2.303(logOD_2 - logOD_1)}{(t_2 - t_1)}$$

2.2.4 Monitoring and analytical techniques

Growth monitoring and sampling

Sampling was performed using sterile single use syringes and needles that were flushed with N_2 or N_2/CO_2 gas (for details refer to Hausmann, 2012). For Hungate tubes, needle outer

diameter was 0.40 mm whereas for all other enrichment approaches sampling was performed with needles of an outer diameter of 0.60 mm. Soil slurries were gently inverted several times until full suspension was observed. After a short sedimentation time the supernatant was sampled. Dialysis chambers were gently shaken, clockwise and counterclockwise (app. 10 sec respectively) before the solute fraction was sampled. Enrichments growing in Hungate tubes were inverted several times and then sampled immediately. Samples were immediately transferred to 4°C with an aliquot being fixed for FISH analysis. Samples used for capillary electrophoresis were either analyzed directly or stored at −20°C. For FISH sampling of soil agar plates, quarter sections of sterile 0.22 µm Isopore membrane filters (GTTP01300, Merck Millipore, Darmstadt, Germany) were used to plot colonies from the plate onto the filter surface. This was done, by simply overlaying the filter section onto the soil agar region of interest, using sterile tweezers. Sampled filter sections were directly overlaid with 0.1 % (w/v) agarose solution and fixed either with PFA or ethanol. All sampling steps were performed in a vinyl anaerobic chamber (Coy Laboratory Products, Michigan, USA).
Optical density at 600 nm of enrichments growing in Hungate tubes was measured using a spectrophotometer (M107 High Specification Visible Range, Spectronic Camspec Ltd., Leeds, UK).

Capillary zone electrophoresis (CE)
Turnover of substrates (short chain fatty acids (SCFA) and lactate) and sulfate in enrichment cultures was quantified using a capillary zone electrophoresis device (Beckman Coulter P/ACE™ MDQ Molecular Characterization System, Beckman Coulter, Brea, CA, USA), equipped with a 65 cm fused silica capillary (Polymicro Technologies™) with an inner diameter of 75 µm. For quantification an external standard mixture (Na-sulfate, Na-formate, Na-acetate, Na-lactate, Na-propionate, Na-butyrate at equimolar concentrations) was used. Samples (4°C) were vortexed briefly and centrifuged at 5000 rpm for 5 min at 4°C. Supernatant was diluted by a factor of 10 in alkalization mix ([0.05 M] NaOH) to ensure proton dissociation of analytes (low K_A values of SCFAs) as the culture conditions were mainly acidic. Two internal standards were included in the alkalization mix ([5mM] Na-caproate, [5 mM] valeric acid). External standards were treated identically. Analysis was performed with the CEofix™ Anions 5 kit (Analis sa, Namur Belgium) according to the manufacturers instructions. Raw data were analyzed using 32 Karat software V 7.0 (Beckman Coulter, Brea, CA, USA) and normalized to the internal standard (caproate) to account for inter-run variability. Further methodological details are provided in Hausmann, 2012.

16S rRNA fluorescence in situ hybridization (FISH) techniques:
For quantification of target cells, standard 16S rRNA FISH (Daims et al., 2005) was performed. Specimens were either fixed in 4 % paraformaldehyde (PFA) solution (3 h at 4°C) or in absolute ethanol (99.9 % (v/v)). Fixed specimens were applied on polytetrafluoroethylene coated slides or 0.22µm Isopore membrane filters (GTTP01300, Merck Millipore, Darmstadt, Germany). In case of cells growing on a solid support (soil agar), cells were transferred onto Isoporefilters prior fixation. Fixed cells were immediately processed for downstream FISH analysis. In case of additional DNA counterstaining, 4′,6-Diamidino-2-phenylindole (DAPI) (Carl Roth GmbH + Co. KG, Germany) was employed. Fluorescence microscopy analysis was performed using a confocal laser-scanning microscope (Leica TCS SP8 (Leica, Wetzlar, Germany)). Processing and analysis of resulting images was done in DAIME 2.0 (Daims et al., 2006).

Desulfosporosinus quantitative FISH assay establishment:
Due to strong autofluorescence of soil slurry debris, that hindered downstream detection of cells, modifications from the following *prior* and *posterior* fixation treatments were evaluated in respect to reducing soil debris and extracting the cell fraction. A *prior* fixation tetrasodium-pyrophosphate (PP_i) extraction (Hahn et al., 1992), a *posterior* fixation PP_i–ultrasonication treatment (Zarda et al., 1997) and a posterior fixation homogenization method (Lücker et al., in preperation). The fixation methods were evaluated in respect to highest yield of bacterial cells and *Desulfosporosinus* cells for the very same specimen.
Catalyzed reported deposition (CARD) FISH (Pernthaler et al., 2002) was performed for one PFA–fixed soil slurry specimen, in order to assess a possible gain in overall sensitivity as compared to standard FISH for the very same specimen .
For specific staining of *Desulfosporosinus* cells, two new probes were designed *in silico* based on SILVA SSU (Quast et al., 2012) database (Release 114) (only sequences larger than 1200 bp), using the *probe design* function implemented into the Arb (Ludwig et al., 2004) software package. Probe target group coverage (proportion of the sum of true positive hits from the sum of all possible positive target group hits) and precision (proportion of the sum of true positive hitsfrom the sum of total search hits) were calculated based on the Ribosomal Database Project (Cole et al., 2014) Release 10.32, using the implemented probe match tool (default data set options, restricted search region from 600 to 700). ΔG values and hybridization efficiencies were calculated using the online tool mathFISH (Yilmaz et al., 2011). Self complementarity and hairpin formation was examined using OligoCalc (Kibbe, 2007). Candidate probes were evaluated with soil slurry specimens and log phase *D. acidiphilus* cells at formamide concentrations provided in Table 2-1.
Optimal formamide concentration for probes DSP648 (together with competitor) and S-G-Dsp-610-a-A-20 (DSP610) were evaluated via formamide seriesof log phase fixed (PFA and EtOH) *D. acidiphilus* cells. Relative abundance of DSP-SbII cells in enrichment cultures was quantified by applying the DSP assay probe set (Section 3.2.1). For further details, refer to supplementary section 8.1.3.

Table 2-1
rRNA targeted oligonucleotide probes used for (CARD)–FISH analysis. Formamide concentrations refer to those employed for analysis of biological samples. Probes employed additionally for CARD FISH experiments are specified in the remarks column. DOPE labeled FISH probes(Stoecker et al., 2010) are specified with the dye name followed by a ×2 label. A "c" as probe name prefix denotes a competitor probe. Labels for CARD FISH probes refer to the employed tyramides. For EUBmix, Delta495mix and LGCmix equimolar amounts of the underlying probes were combined.

Probe name	Sequence (5'—3')	Target Group	Formamide %	Dye	Reference	Remarks
DSP610	CTC TCA GGG TTG AGC CCT GAT C	*Desulfosporosinus*	35	Cy5	This study	
DSP648	CTCTCCTGTCCTCAAGAT	*Desulfosporosinus*, *Desulfitobacterium*, *Dehalobacter* spp.	35	Cy3	(González et al., 2006)	
cDSP648	CTCTCCTGCCCTCAAGAT	Competitor	35	—	(modified from González et al., 2006)	
DFMII1107	CTA AAT ACA GGG GTT GCG	*Desulfosporosinus* spp., *Desulfotomaculum auripigmentum*	35	Cy3	(Loy et al., 2002)	
EUB338	GCT GCC TCC CGT AGG AGT	Most *Bacteria*	35	FITC×2	(Amann et al., 1990)	CARD
EUB338 II	GCA GCC ACC CGT AGG TGT	*Planctomycetales*	35	FITC×2	(Daims et al., 1999)	CARD
EUB338 III	GCT GCC ACC CGT AGG TGT	*Verrucomicrobiales*	35	FITC×2	(Daims et al., 1999)	CARD
NON338	ACT CCT ACG GGA GGC AGC	Negative control	35	Cy3	(Wallner et al., 1993)	CARD
LGC354 A	TGG AAG ATT CCC TAC TGC	*Firmicutes*	35	Cy3	(Meier et al., 1999)	
LGC354 B	CGG AAG ATT CCC TAC TGC	*Firmicutes*	35	Cy3	(Meier et al., 1999)	
LGC354 C	CCG AAG ATT CCC TAC TGC	*Firmicutes*	35	Cy3	(Meier et al., 1999)	
HoAc1402	CTT TCG TGA TGT GAC GGG	*Acidobacteria*	10	Cy3	(Juretschko et al., 2002)	CARD
cHoAc1402	CTT TCG TGA CGT GAC GGG	Competitor	10	—	(Juretschko et al., 2002)	CARD
ALF968	GGTAAGGTTCTGCGCGTT	Most *Alphaproteobacteria*	20		(Neef, 1997)	CARD
Arch915	GTG CTC CCC CGC CAA TTCCT	*Archaea*	35	FITC×2	(Stahl and Amann, 1991)	
Delta495a	AGT TAG CCG GTG CTT CCT	Most *Deltaproteobacteria* and most *Gemmatimonadetes*	35	Cy3	(Loy et al., 2002; Lücker et al., 2007)	
Delta495b	AGT TAG CCG GCG CTT CCT	Some *Deltaproteobacteria*	35	Cy3	(Loy et al., 2002; Lücker et al., 2007)	
Delta495c	AAT TAG CCG GTG CTT CCT	Some *Deltaproteobacteria*	35	Cy3	(Loy et al., 2002; Lücker et al., 2007)	

Total cell counts, live staining and scanning electron microscopy (SEM):
For absolute cell counts in a given volume, a defined volume of EtOH fixed cells was filtered onto 0.22 µm Isopore filters. Cells were stained with SYBR® Green II RNA Gel stain (Cat. No. S-7564, life technologies, CA, USA) (3 min, 1× concentrated via dilution in Citifluor mounting solution (Citifluor Ltd., London, UK)). For each specimen cells in five fields of view were counted. Image acquisition was performed, with a confocal laser-scanning microscope (Leica TCS SP8 (Leica, Wetzlar, Germany)). Image processing and cell counting was performed in DAIME 2.0. Staining of unfixed living cells was performed by transfer of living cells into an anoxic solution of physiological saline (1 % w/v) and staining with the LIVE/DEAD® BacLight viability kit according to the manufacturers instructions. Unmounted solutions of stained cells were analyzed using the CLSM equipped with a water objective. For SEM analysis EtOH fixed cells were transferred onto Isopore filters (0.22 µm) and washed in physiological saline. Dry filters were sputtered with a gold layer (Cressington sputter coater 108). SEM analysis was performed with a FEI XL 30 microscope at the CIUS facility (University of Vienna).

DNA extraction, 16S rRNA gene PCR and DNA sequencing:
For each specimen two 1 ml aliquots of active enrichment cultures were harvested (15 000× g, 30 min, 4°C) respectively. Supernatant was removed and dry pellets were stored at −20°C for downstream processing. DNA from cell pellets was extracted using either a CTAB based Phenol/Chloroform method (Hausmann, 2012) or the PowerSoil® DNA Isolation Kit (Cat. No. 1288, MOBIO Laboratories, CA, USA) according to the manufacturers instructions. DNA concentrations were measured with a NanoDrop ND-1000 spectrophotometer (Thermo Fisher Scientific, Massachusetts, USA) and the Qubit® dsDNA HS assay. For amplification of the 16S rRNA gene the following general and *Desulfosporosinus* specific primer combinations were applied: 8F/1492R, DSP603F/1492R, 603F/821R. PCR primers and cycling parameters are provided in supplementary section 8.1.4. Size of PCR products was verified via agarose gel electrophoresis. PCR products were purified with the QIAquick PCR Purification Kit (Cat. No. 28106, Qiagen, Venlo, Netherlands), according to the manufacturers instructions. If not stated explicitly, DNA sequencing (chain termination method) was performed by microsynth AG with the following combinations of template and sequencing primers: 8F/1492R unidirectional with 8F, DSP603F/1492R bidirectional with DSP603F and 1492R.

2.2.5 Phylogenetic analysis

Unambiguous, trimmed and curated sequence FASTA files were assembled into contigs using the CAP3 assembler (Huang and Madan, 1999) implemented into Unipro UGENE 1.13 (Okonechnikov et al., 2012). 1492R primed reads were assembled into a contig with 603F reads and once with 8F reads. The two resulting contigs were then assembled into one final contig. Contigs were aligned to 16S rRNA gene sequences using the SINA (1.2.11) aligner (Pruesse et al., 2012) with the bacterial variability profile enabled. The ten nearest neighbors for each query contig were added to the database constructed for phylogenetic analysis. Furthermore all sequences matching the search query "*Desulfosporosinus*" against the SIVLA SSU database (release 117), that were larger than 1 kb, had a higher sequence quality than 90, an alignment quality bigger than 90 and a pintail quality higher than 90 were attached to the dataset. Furthermorethe sequences of*Desulfosporosinus* type strains were added. One 16S rDNA (1.5 kb) *Desulfosporosinus* contig (obtained via differential coverage binning (Albertsen et al., 2013) of a Schlöppnerbrunnen soil metagenome study (Hausmann, 2014) was included into the analysis. Sequences from Schlöppnerbrunnen *Desulfosporosinus* 16S rRNA gene clones (Pester et al., 2010) were aligned using SINA and nearest neighbors of

hits, were added to the database (13 entities). One sequence of *Desulfitobacterium metallireducens* was included as outgroup.
Multiple sequence alignment was performed with MUSCLE (Edgar, 2004) implemented into MEGA 5.2.2 (Tamura et al., 2011). The final alignments were inspected and manually curated in Mesquite 2.75 (Madison and Madison, 2011) and uncorrected dissimilarity matrices calculated.
The jModelTest 2 (Darriba et al., 2012) package was employed to test for the DNA substitution model that best fits the dataset. A General Time Reversible model with a proportion of invariable sites and a gamma-shaped distribution of rates across sites was consequently used for MrBayes 3.2.2 (Ronquist and Huelsenbeck, 2003) phylogenetic analysis. Trees were calculated once with and once without the metagenomic *Desulfosporosinus* read. The number of generations was set to 3×10^6 with a diagnostic frequency of 5000. Priors were kept at default. Average standard deviation of split frequencies at the end of analysis was 0.032 and 0.009 for the two calculations (with and without the metagenomic contig respectively). Consensus trees including posterior probabilities of splits were generated using the *sumt* command. Nexus formatted trees were visualized using the interactive Tree Of Life v2 tool (Letunic and Bork, 2011).

2.2.6 Preservation of enrichments

For long term storage of strictly anaerobic microorganisms, cells were deep frozen in liquid nitrogen (liquid phase) in soda glass capillary tubes, as described in Spring, 2006. Mid log-phase *Desulfovibrio* sp. SII13a and three DSP-SbII enrichment cultures (*Iron E-1*, *Iron E-2*, *Sodium E-2 (B)*) were anoxically harvested (8 ml *Desulfovibrio* and 3ml for*Desulfosporosinus* samples) at 4 500× g for 25 min at 14°C. Pellets were resuspended in basal FM ([10mM] Sulfate, 5 % (v/v) DMSO). Suspensions were transferred into capillaries and sealed as instructed. Proper sealed tubes were transferred into the gas phase of a liquid nitrogen tank (LS6000 Nitrogen Storage System, Taylor-Wharton International LLC, Minnetonka, MN, USA) overnight and finally submersed into the liquid phase for long-term storage.

3 Results

3.1 Quantitative PCR analysis

3.1.1 Assay evaluation

qPCR performance parameters are provided in Table 3-1. Evaluation of linear models of standards (STD) and non target controls (NTAC) suggested for only minor effects of false positive (unspecific) signal amplification throughout all assays (Figure 3-1 and Table 3-1). However when compared to the mean standard deviation of Cq values of STDs (0.102 to 0.160, equals an error percentage of 10^{-5}) it can be seen that false positive signal amplification can have ample effects (cross specifity error percentage of up to 10^{-3}). Additionally, a scenario of high copy numbers of NTACs accompanied by low copy numbers of the target group would impose a potential flaw for all examined assays.

Table 3-1
qPCR performance parameters for *dsrA* and *Acidobacteria* 16S rRNA gene (abbreviated as 16S) assays. The cross specifity error contribution is provided for the respective NTACs (indicated with brackets). Note that for the *Acidobacteria* SD2 assay only one NTAC is shown. Abbreviations: Efficiency (E), linear regression coefficient (r^2), linear dynamic range of detection (LDR)

Assay	Target	E (%)	r^2	Linear model ($f_{(x)}$)	LDR	Cross specifity error (%)
dsrA	OTU1	94.5	0.997	−3.5x+35.6	4.7×10^{8} – 4.7×10^{1}	6×10^{-5}(OTU2) 5×10^{-5}(OTU6)
dsrA	OTU2	92.3	0.999	−3.6x+36.3	6.8×10^{8} – 6.8	7×10^{-5}(OTU1) 5×10^{-3}(OTU6)
dsrA	OTU6	94.1	0.999	−3.6x+37.2	4.8×10^{8} – 4.8×10^{1}	3×10^{-3}(OTU1) 9×10^{-6}(OTU2)
16S	SD1	97.5	0.997	−3.4x + 36.3	1.1×10^{9} – 1.1	4×10^{-4}(SD2) 2×10^{-4}(SD3)
16S	SD2	95.2	0.998	−3.4x + 36.0	1.2×10^{9} – 1.2	6×10^{-5}(SD1)
16S	SD3	97.3	0.999	−3.4x + 36.8	1.1×10^{9} – 1.1	2×10^{-5}(SD1) 4×10^{-5}(SD2)

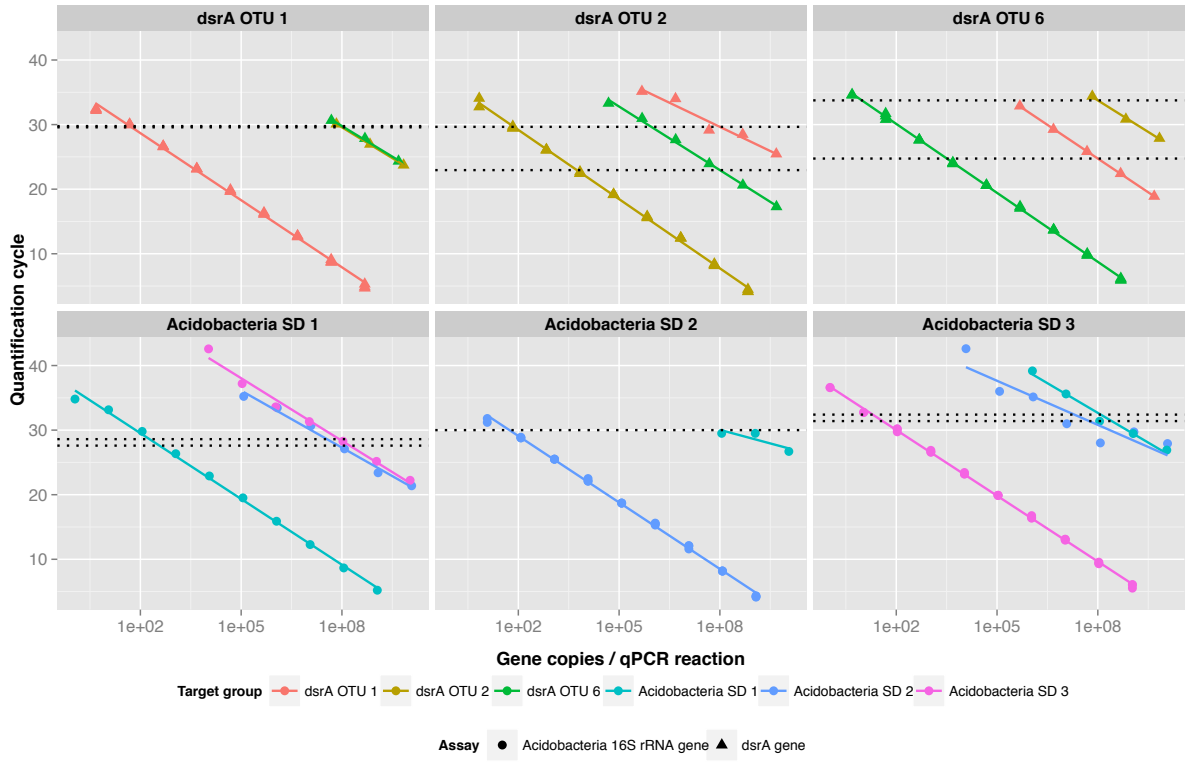

Figure 3-1
Linear models of qPCR of target group standard dilution series and the respective NTACs. Strip text denotes the performed assay setup. Horizontal dotted lines indicate Cq values of NTACs at 10^{-8} gene copies per reaction and the corresponding Cq values of the target that was used for cross specifity error estimates. Note that only SD1 was employed as NTAC in *Acidobacteria* SD2 assay evaluation.

3.1.2 Quantification of *dsrA* gene OTUs

qPCR analysis provided no conclusive evidence for a selective enrichment of the target groups through the amendment of sulfate. Mean relative abundance at timepoint zero was highest for OTU 1 followed by OTU 6 and finally OTU 2 (0.19, 0.12, and 0.07 % respectively). In the microcosms OTU 6 showed a strong decrease after 27 days down to the detection limit of the qPCR assay and was at a comparable level at timepoint 51.
OTU 1 also exhibited a similar pattern of decrease to timepoint 27 days. However a pronounced increase could be observed at timepoint 51, were some treatments exhibited similar relative abundance as compared to the timepoint zero (Figure 3-2). Similar trends could be observed at the raw *dsrA* copy number level (Supplementary Figure 8-2). The strong increase observed in the treatments of formate and propionate without sulfate can partially be attributed to a decrease in total 16S rRNA gene abundance (Supplementary Figure 8-5). Contrary, no decrease or even a small increase could be observed for lactate, no substrate and butyrate treatments without sulfate on the total 16S level when compared to the timepoint zero, which supports the assumption of *dsrA* target group increase. Of the sulfate amended treatments, the strongest positive effects on copy number levels were observed for the no substrate amendment and the butyrate treatment. Here total bacterial and archaeal (BA) 16S values were roughly constant, thus indicating an increase of the target population. However, it seems that in none of the treatments the population could recover to their initial abundance.
OTU 2 data provided no clear evidence for a selective enrichment effect before 27 days, similar as it was observed for the other target groups. In contrast to the other OTUs, this

target could maintain its level of relative abundance during the first half of the incubation period. However initial relative abundance was considerably lower as opposed to the two remaining OTUs. A consistent theme during the incubation timeframe was, that mean relative abundance was higher when no sulfate was amended. However, due to the high standard deviation between microcosm replicates, no definitive conclusion regarding the effect of sulfate can be deduced. Relative abundance peaked at timepoint 51, with a mean increase of relative abundance ranging between 0.36 (no substrate) and 0.14 (butyrate) in non-sulfate amended conditions when compared to the timepoint zero. For microcosms with sulfate added, a mean increase between 0.16 (formate) and and 0.03 (butyrate) was observed.

Raw OTU 2 *dsrA* copy number values exhibited a similar pattern of population dynamics, except for formate and acetate without sulfate addition, where total abundances equaled roughly those of the respective treatments provided with sulfate. The strong increase in relative abundance observed in no substrate and propionate without sulfate treatments, was a coherent observation and not caused by a general decrease of bacterial entities (Supplementary Figure 8-5).

Spearmann rank correlation of OTU 2 relative abundance against normalized sulfate concentrations resulted in a significant correlation ($p=0.015$, $\rho=-0.833$) for the acetate treatment only (Figure 8-6). In line with this observation a strong positive correlation ($p=0.011$, $\rho=0.857$) was observed for acetate concentrations with OTU 2 relative abundances in the respective microcosms.

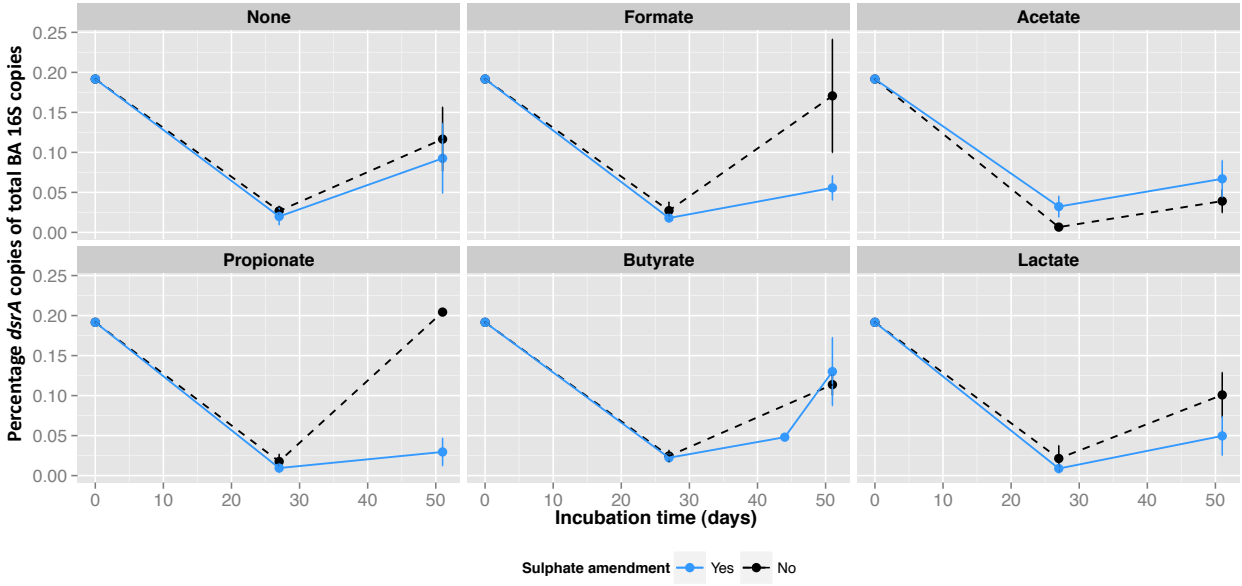

Figure 3-2
OTU 1 qPCR time series data, showing the relative percentage of target gene to total bacterial and archaeal(BA) 16S copies. Datapoints represent mean values of the microcosm triplicates for each treatment type. Error bars indicate the respective standard deviation. Note, that the timepoint zero specimen was the same for all treatments.

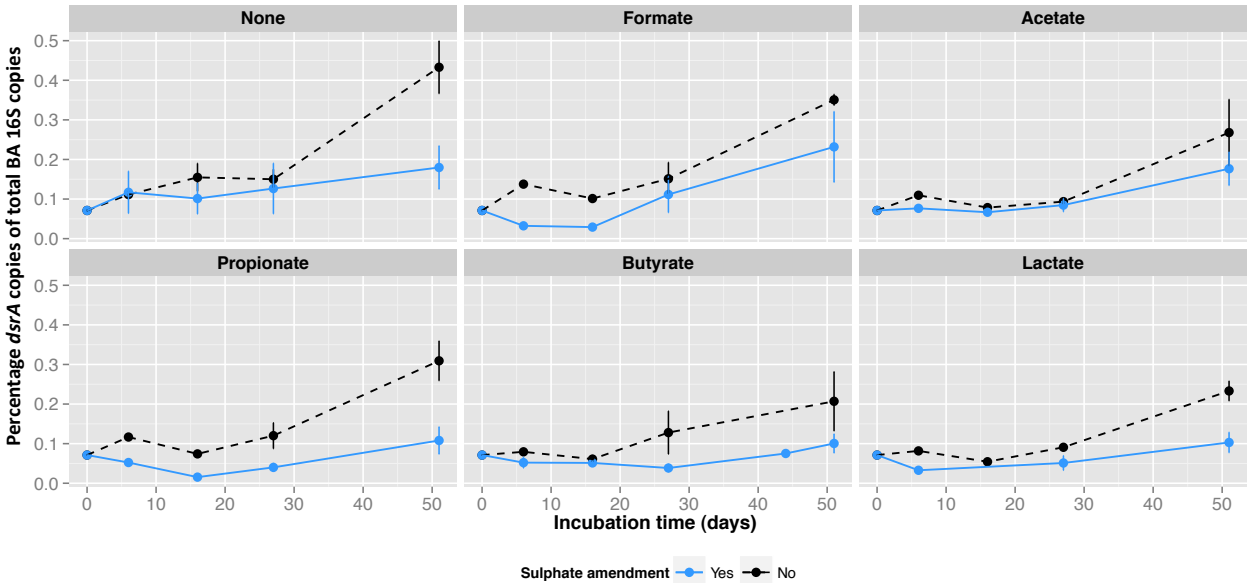

Figure 3-3
OTU 2 qPCR time series data, showing the relative percentage of target gene to total bacterial and archaeal (BA) 16S copies. Datapoints represent mean values of the microcosm triplicates for each treatment type. Error bars indicate the respective standard deviation. Note, that the timepoint zero specimen was the same for all treatments.

3.1.3 Quantification of major *acidobacterial* subdivisions

Mean copy numbers per ng of DNA at timepoint zero were highest for subdivision 2 (21 414 acidobacteria SD2 16S rRNA gene copies ng^{-1} DNA) followed by subdivision 1 (18 361 acidobacteria SD1 16S rRNA gene copies ng^{-1} DNA) and subdivision 3 (10 900 acidobacteria SD3 16S rRNA gene copies ng^{-1} DNA) exhibiting lowest values. Subdivision 2 decreased throughout all treatment combinations by up to 57 %. No selective effect of treatments could be observed. Subdivision 1 decreased up to 40 %, however in non sulfate–amended treatments the effect was less pronounced, with the butyrate treatment yielding a similar absolute abundance as the respective timepoint zero throughout triplicates. Subdivision 3 exhibited pronounced decrease of up to 45 %. In accordance with SD1 the butyrate treatment without sulfate showed comparable values as the timepoint zero (overview provided in Supplementary Figure 8-7). Mean cumulative relative abundance of total *bacterial* and *archaeal* 16S rRNA gene copies of the three subdivisions at timepoint zero was 59.7 % (21.7, 25.2 and 12.8 % for SD1, 2 and 3 respectively). Mean cumulative (SD1+SD2+SD3) relative abundances at day 51 were at approximately 60 % for non–sulfate amended microcosms and 45 % for those were sulfate was provided (Supplementary Figure 8-8).

One-way anova suggested for significant differences between treatment types only for SD1 and 3. However no clear pattern regarding selective effects of treatment type could be deduced from this analysis (Supplementary Figure 8-9). Subdivision 1 showed stable relative abundance in non–sulfate treatments (Figure 3-4), which can be partially explained by a general decrease in *bacterial* and *archaeal* 16S copy number in respect to the timepoint zero, throughout all treatments (Supplementary Figure 9-5). When sulfate was provided, a strong decrease in relative abundance could be observed. Subdivision 2 showed no significant difference between treatments. Although copy numbers decreased, an increase in relative abundance could be seen frequently regardless of treatment type. Subdivision 3 exhibited a pronounced decrease on the relative abundance level in all microcosms.

Correlation analysis of qPCR with amplicon data suggested for significant positive correlation for all three subdivisions (SD1: $p=5\times10^{-8}$, $\rho=0.79$; SD2:$p=0.012$, $\rho=0.40$; SD3:$p=4.6\times10^{-7}$, $\rho=0.73$). The correlation resembled a linear relationship and the distribution of data showed good fit to bivariate normal distributions.

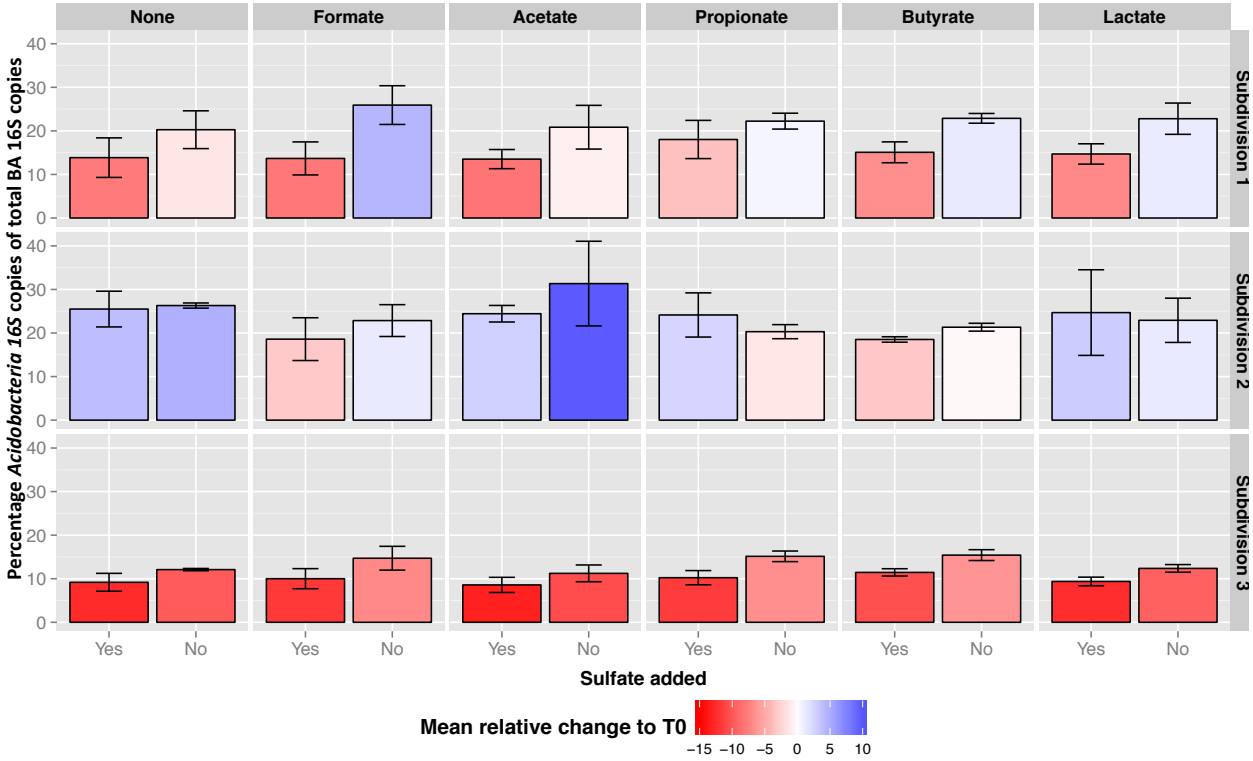

Figure 3-4
Relative abundance values of *Acidobacteria* subdivisions 1 to 3 in microcosm experiments between timepoint zero and 51 days of incubation, as determined with qPCR. Bar color indicates the mean relative change (in percentage) of microcosm replicates at timepoint 51 to the mean value of the timepoint zero. Error bars denote average standard deviation.

3.2 Cultivation and Isolation of SRM

3.2.1 Quantitative *Desulfosporosinus*FISH assay

In silico analysis indicated low specificity of probe DSP648 at the genus level. This was due to targeting also the *Desulfitobacterium* genus and partially some *Syntrophomonadaceae.* Therefore, a competitor (cDSP648) against *Syntrophomonadaceae* and a more specific probe DSP610, which does not target the *Desulfitobacterium* genus, were designed. Specifity of probe DSP610 was considerably higher when compared to DSP648. *In silico* analysis via probe match in RDP suggested, that false positive hits were mainly within the bin of unclassified *Clostridiales*. A BLAST query of entries from that cluster (exclusively EMIRGE (Miller et al., 2011) clones) indicated that sequences were affiliated to *Desulfosporosinus*. Consequently a higher precision can be expected. FISH experiments with probe DFMII1107 did not result in positive signal detection for any specimen and therefore this probe was not used in further experiments. The hierarchical probe application of DSP648, cDSP648 and DSP610 showed no false positive hit *in silico* and thus should theoretically allow for a 100 % precise detection of *Desulfosporosinus* cells (Supplementary Figure 8-11). Dissociation curve analysis (Supplementary Figure 8-12) suggested use of 35 % formamide for both probes

being simultaneously hybridized to ethanol and PFA fixed *D. acidiphilus* cells. However, this stringency implied lower signal intensity for probe DSP610.

The evaluation of cell extraction methods from soil slurries resulted in only minor improvements as compared to the standard FISH protocol. However, a combinatorial, posterior fixation treatment using PP_i extraction, bead beating and supernatant collection resulted in a considerable improvement in respect to total cell and *Desulfosporosinus* cell detection. Furthermore, a major decrease in soil debris and consequently autofluorescence was observed (Supplementary section 8.1.3). Importantly, PFA fixed specimens exhibited a major decrease of the *Desulfosporosinus* fraction detectable as compared to ethanol fixed samples. The protocol allowed for quantification of *Desulfosporosinus* cells with one technical replicate per specimen (Supplementary section 8.1.3). A qualitative comparison of CARD-FISH and conventional FISH for a soil slurry specimen extracted with this protocol did not indicate a substantial advantages of CARD-FISH for detecting total bacterial cells (double-labeled probes were employed for conventional FISH). Consequently, for quantification of the *Desulfosporosinus* population the following probe setup (DSP assay) was employed: EUBmix-FITC (double-labeled), DSP648-Cy3, cDSP648 and DSP610-Cy5 at standard concentrations.

Ethanol fixed cells of *Desulfosporosinus* growing in dialysis chambers or in defined media, could directly be used for FISH without extraction. Therefore, 10 µl of the specimen were applied per well and dried only for 5 min at 46°C, followed by 10 min at room temperature. This deviation from the standard procedure helped to reduce the formation of cell clusters and provided a more uniform distribution.

Table 3-2
*Desulfosporosinus*specific 16S rRNA targeted probes applied in the DSP-FISH assay. Note that probe DSP610 is prone to hairpin formation as indicated by *in silico* prediction. Details on the calculations of coverage and precision are provided in the material and methods section.

Probe	Coverage	Precision	Non target groups	FA %	ΔG	Hairpin Formation
DSP648	0.85	0.59	*Desulfitobacterium* (*Syntrophomonadaceae*)	35	-17.5	no
cDSP648	—	—	*Syntrophomonas*	35	-18.85	no
DSP610	0.82	0.87	Unclassified *Clostridiales*	40	-25.33	yes

3.2.2 Soil slurry enrichments and pasteurization

Soil slurries: Sulfate removal could be observed in all slurry incubations. Turnover time of the total sulfate pool varied between 25 and 98 days. The range of sulfate removal rates (SRR) as determined from linear models for the linear part of first sulfate amendments was between 0.4 and 1.5 µmol day^{-1} (Sp1s and Sp1u respectively) (Supplementary Figure 8-13). A reoccurring theme was, that initial sulfate removal was accompanied by an increase of acetate concentration (maxima between 1 and 2.4 mM) followed by nearly total depletion of acetate, while sulfate was still removed (Figure 3-5). Interestingly, a second sulfate amendment did not result in the production of acetate and exhibited ambiguous sulfate removal patterns. Median relative abundance of *Desulfosporosinus* cells peaked at app. 5 and 10 % at days 25 and 27 for Sp1u and Sp1v respectively (Figure 3-6). Here acetate concentrations were already decreasing. For Sp1u *Bacterial* cell counts correlated with *Desulfosporosinus* counts, whereas in Sp1v highest relative abundance was observed when *Bacterial* counts were still constant but the *Desulfosporosinus* counts increased (Supplementary Figure 8-14).

Pasteurization: Sulfate concentrations at timepoint zero were lower as the theoretical amount applied. Subsequently a small increase (3.5 to 4 mM) was observed followed by a strong decrease to about 1.5 mM (Supplementary Figure 8-15). Interestingly, moderate acetate concentrations (0.5 to 1 mM) were observed at day 17, which decreased afterwards, resembling the pattern observed in the soil slurries. FISH analysis at day 43 could confirm the presence of spurious *Desulfosporosinus* cells only in one specimen (1D) (Enrichment Sp1s pasteurized at 80°C for 20 min) together with other *Bacteria*. All other treatments showed bacterial signals (generally more when Sp1s was the inoculum) but no *Desulfosporosinus* cells. No enrichment could be obtained via subculturing into DSMZ medium 1250, as DSP-SbII cells were overgrown by other microorganisms. No sulfate removal was measured in this subcultures but strong gas evolution could be seen by eye. The presence of methanogenic *Archaea* could not be confirmed via FISH. No DSP-SbII cells could be detected with FISH at later timepoints.

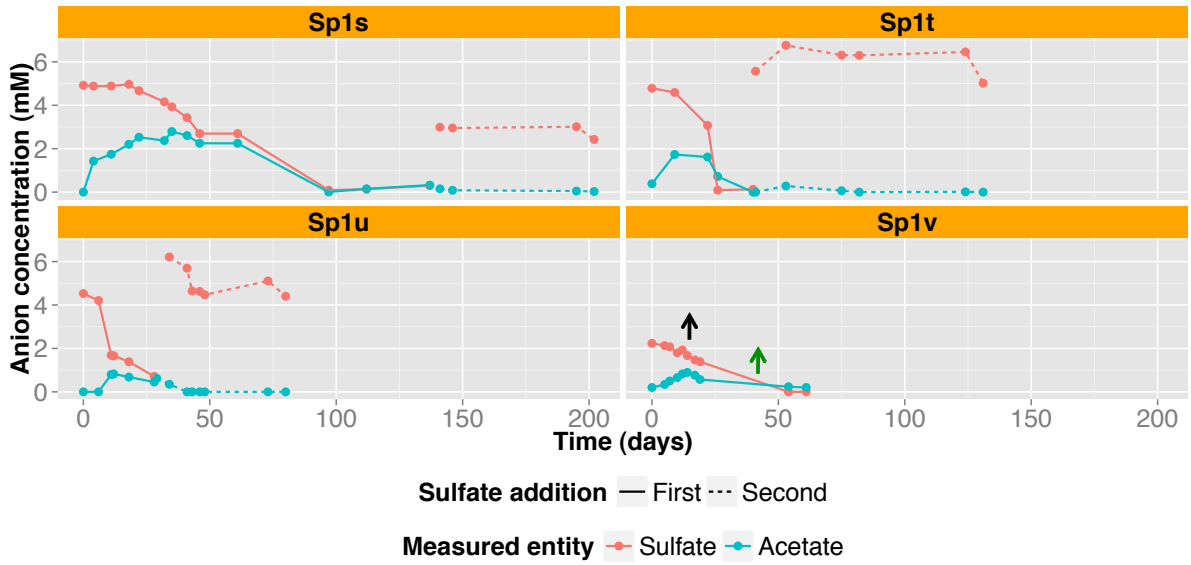

Figure 3-5
Turnover of sulfate and acetate in four generations of soil slurries. Dashed lines indicate profiles after amendment of sulfate. Black and green arrows indicate the timepoint of inoculation into dialysis chamber 1 and 3 respectively.

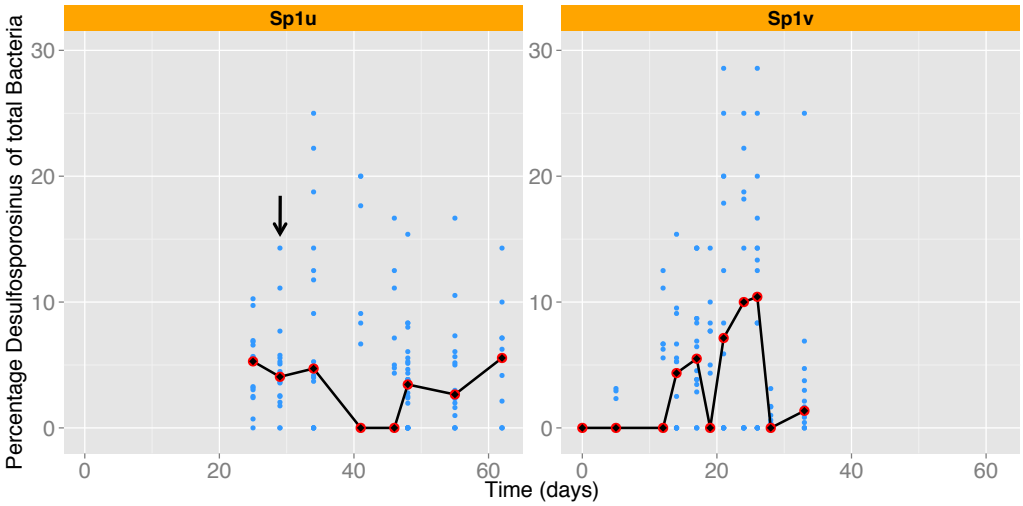

Figure 3-6
FISH quantification of *Desulfosporosinus* cells from soil slurry incubations (strip text corresponds to incubation ID) Red dots indicate median relative abundance. Blue dots indicate the relaive abundance per field of view (FOV). The arrow indicates the timepoint of the second sulfate addition.

3.2.3 Dialysis chamber enrichments

After inoculation sulfate was turned over in dialysis chambers at rates (between 1.7 and 2.9 µmol day^{-1}, 6.2 µmol day^{-1} in dialysis chamber 3), higher as compared to those of soil slurry incubations (Supplementary Figure 8-13). Only minor fluctuations of sulfate concentrations (average SD = 0.4 mM) and no acetate production was observed in a long-term (9 weeks) abiotic control. No SCFA other than acetate could be detected via capillary electrophoresis for all examined dialysis chambers. Sterile preincubations could be verified for all setups with FISH (Figure 3-8). Similar to the soil slurries, sulfate removal was accompanied by an increase in acetate production followed by its decrease (Figure 3-7). Notably DIA3 exhibited the highest sulfate removal rates and produced acetate up to a concentration of nearly 12 mM. The ratios of sulfate consumption and acetate production reflected incomplete substrate oxidation via sulfate reduction. Moreover high acetate levels were maintained throughout total consumption of sulfate. A darkening (of variable intensity) of the solute fraction and the formation of black precipitates was usually accompanied with sulfate removal. Sulfate removal led to the production of sulfide, qualitatively verified with hydrogen sulfide test stripes (Cat. No. 06728, Fluka Analytical, Sigma-Aldrich Chemie GmbH, Buchs, Switzerland).
Tracking the population dynamics of *Desulfosporosinus* cells in the chambers suggested for maximum population density in the early incubation timeframe from two to five weeks. Here relative abundance peaked with median values of up to 25 % (Figure 3-8) and maximum absolute bacterial and *Desulfosporosinus* cell counts (Supplementary Figure 8-16). Generally, acetate production was correlated with high abundance of *Desulfosporosinus*, whereas acetate consumption was accompanied by a decrease of the population.

Desulfosporosinus cells growing in dialysis chambers exhibited strong phenotypic variability in respect to morphology (Table 3-3 and Supplementary Figure 8-17). The change in morphology correlated with incubation time, with the overall proportion of the population exhibiting the same shape for a given phase. Shape parameters were calculated for cylindrical shaped cells. The percent of surface area being nutritionally available, assuming substrate support from a solid surface only, was calculated according to Equation 3. These observations were reproducible between dialysis chambers and can be characterized into three distinct phases (Table 3-4).

Initial Phases: A filamentous shape in the very first phase of growth (between 6 to 22 days), when sulfate concentrations were still at the maximum. A length of up to 270 µm (Figure 3-10) could be observed in some specimens. Living filaments did not exhibit clear indications of active motility (as indicated by live/dead staining). SEM analysis suggested for minor segmentation within a filament (Figure 3-9), whereas no indication of septa or segmentation could be found for the entire length of others (Figure 3-10). Big singular spindle formed *Desulfosporosinus* cells (length 10 µm, diameter 1.7 µm) were also detected in these early incubation phases together with shorter filaments (about 20 µm in length). At later timepoints (when sulfate removal could be detected), no filaments could be observed.
Growth phase: Typically small rod shaped cells in the growth period of maximum relative and absolute abundance (Table 3-3). This is the zone were the bulk amount of acetate is produced. Sulfate removal starts.
Stationary Phase: A clearly larger rod shaped phenotype prevails at low absolute and relative abundance. Acetate typically decreases, sulfate removal continues.

Sporulation could be observed sometimes and usually in scenarios of high abundance and minimal sulfate concentrations. Subpopulations, not committed to sporulation could continue to propagate once sulfate was available again.
Due to the exceptional parameters (high DSP-SbII abundance, prominent acetate production) of DIA3 and high enrichment in DIA4 both entities were used for further isolation attempts on defined media arrays.

Equation 3
Percentage of nutritionally available surface area for cell surface interfaces. The shape factor R (Zaritsky, 1975) was calculated according to R=l/w (l=length, w= cell diameter). The proportionality factor n (n=d/w, d=cell depth, w=cell with) was assumed to be 1 (perfect circle).

$$p_n = \frac{R}{(2+2n) \times R + 2n} \times 100$$

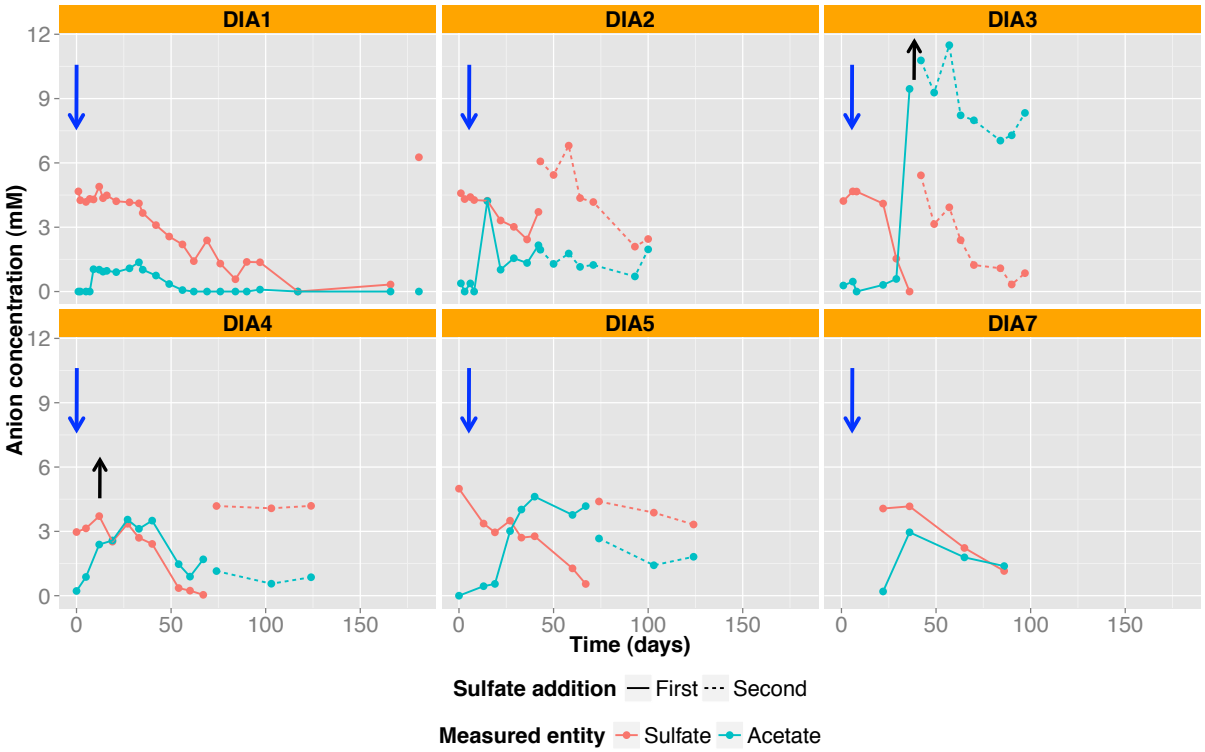

Figure 3-7
Turnover of sulfate and acetate in six generations of dialysis chambers. Dashed lines indicate profiles after the amendment of sulfate. Blue arrows indicate the timepoint of inoculation. Black arrows indicate the timepoint of subculturing into the defined media array. Note that no timepoint zero is shown for DIA7, as this entity was initially created for a metabolomics experiment where no anion turnover data are available.

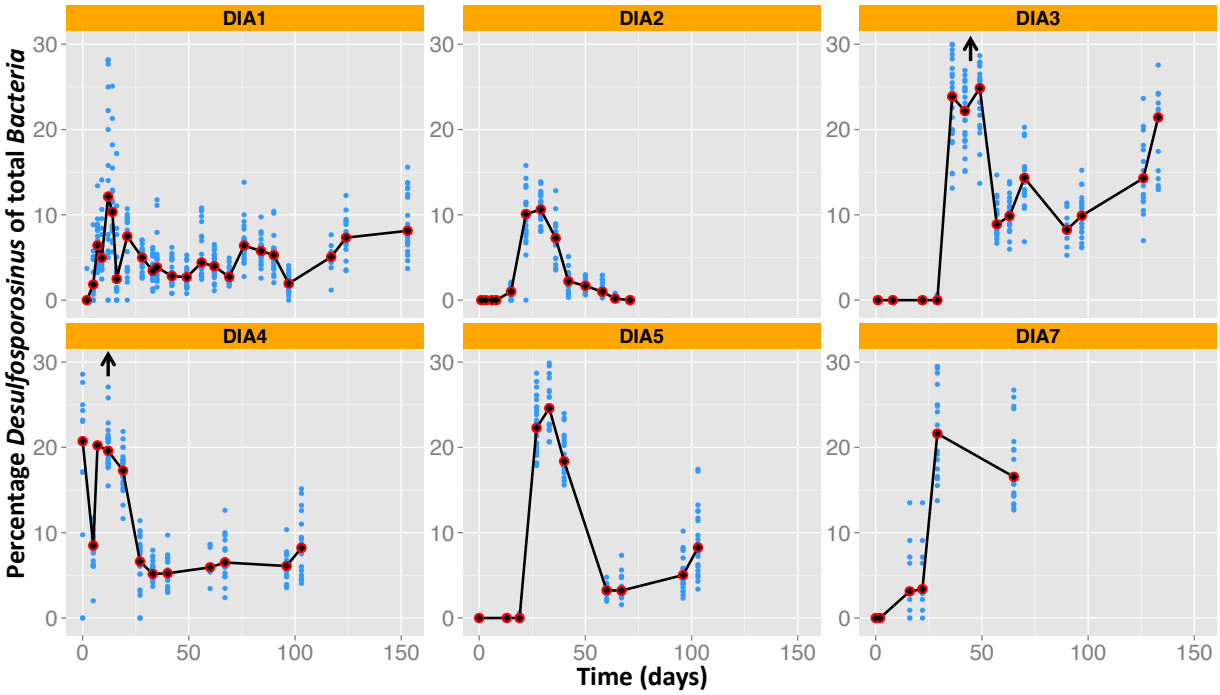

Figure 3-8
FISH quantification of *Desulfosporosinus* cells from dialysis chamber incubations (strip text corresponds to incubation ID) Red dots indicate median relative abundance. Blue dots indicate the relaive abundance per field of view (FOV). The arrow indicates the timepoint of subculturing the biomass into the define media arrays (DMA) (DIA3 into DMA series 1, DIA4 into DMA series 2). Note that chamber one and four were abiotically preincubated over night only before being inoculated.

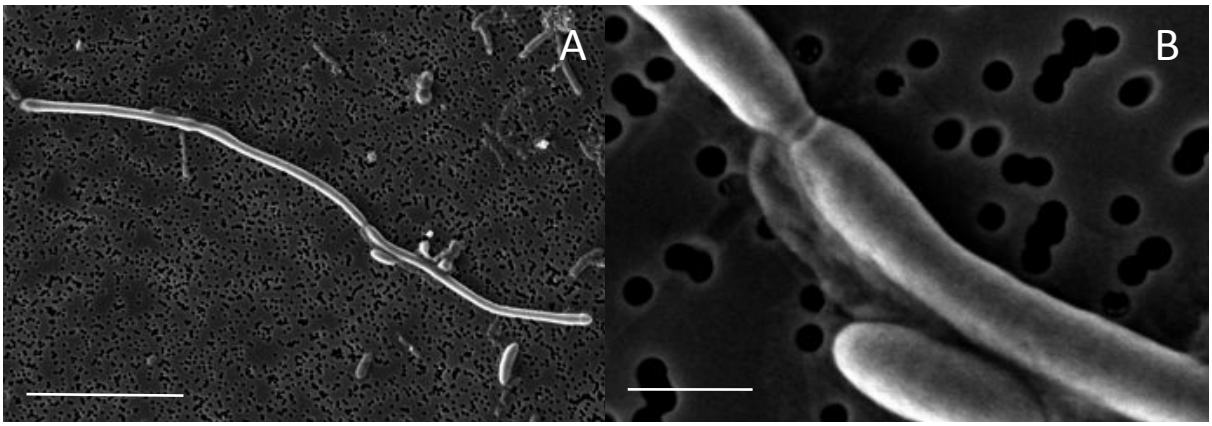

Figure 3-9
SEM images of a *Desulfosporosinus* filament growing in a dialysis chamber 1 (9 days after inoculation). Unlike in CLSM analysis filaments seem to be interspaced by septa (see magnified section in image B). Black dots are the pores of the filter. SEM analysis was performed at 12 kV acceleration voltage.
Scale bars correspond to 10 µm (Image A) and 1 µm (Image B).

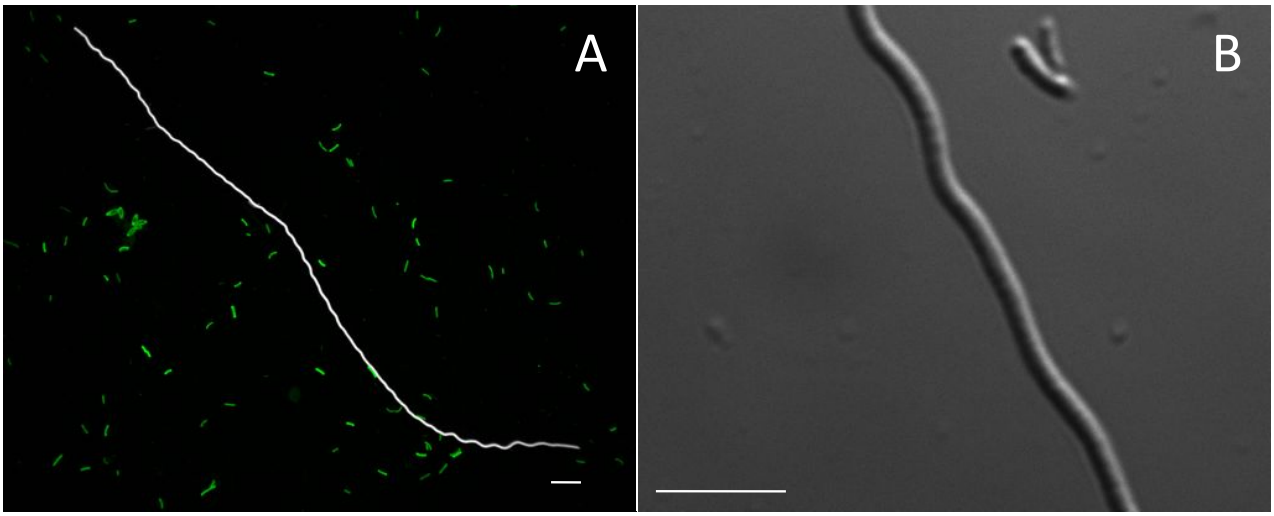

Figure 3-10
Image A: FISH analysis showing a *Desulfosporosinus* filament (white) with an approximate length of 270 µm growing in a dialysis chamber 3 (21 days after inoculation). Scale Bar: 10 µm
Image B: Magnified section of image A (differential interference contrast) of the filament. Note that no segmentation could be observed for the entire length of the filament. Scale bar: 5 µm
Desulfosporosinus cells stain in white-cyan. *Bacteria* in green. Probes: EUbmix-FITC, DSP648-Cy3, cDSP648, DSP610-Cy5

Table 3-3
Mean morphological parameters of ethanol fixed *Desulfosporosinus* cells growing in dialysis chambers. The surface to volume ratio (S/V) was calculated from mean values respectively. Cells were measured with daime 2.0. The radius of filaments was measured at terminal and intermediated position and did not exhibit reasonable variability. p_n denotes the percentage of nutritionally available surface area for cell surface interfaces. Spindle and filamentous cells correspond to the initial phase, small rods to the growth phase and big rods to the stationary phase.

Morphology	Length (µm)	Radius (µm)	Surface (µm²)	Volume (µm³)	S/V	p_n
Small rods	3.6	0.5	4.0	3.4	1.2	22.0
Big rods	6	0.7	6.6	10.4	0.6	22.4
Spindle	10	1.5	50.7	17.7	2.9	21.7
Short Filaments	82	0.45	233.1	52.2	4.5	24.9
Mean Filaments	124	0.45	351.9	78.9	4.5	24.9
Large Filaments	270	0.45	764.7	171.8	4.5	25.0

Table 3-4
Separation of morphological growth stages of the *Desulfosporosinus* population growing in dialysis chambers. Time periods are provided as days. Missing values between phases are due to missing datapoints (no sample). Note that no initial phase was observed for DIA4.

Chamber	Initial Phase	Growth Phase	Stationary Phase
DIA1	1–7	9–21	28–181
DIA3	1 – 22	29 – 42	49 – 154
DIA4	—	1 – 12	19 – 124
DIA5	1 – 19	27 –40	54 –124
DIA7	1 –16	29 – 58	65 –86

3.2.4 Soil agar

Oxygen levels allowing growth of strict anaerobes (below 2.5 % air saturation) were detected in depth sections below 3 mm. At the shallowest depth section of 1 mm, levels of about 8.5 % were measured. However, as the measurement was conducted at ambient air atmosphere, elevated oxygen levels can be attributed to diffusive effects and that plates provided an anoxic environment when incubated in the anaerobic jar (Supplementary Figure

8-18). A lawn of cells could be observed after 18 days of incubation for the very first plate entity. FISH analysis of a lawn section confirmed the presence of *Desulfosporosinus* cells amongst other *Bacteria*. Picking and streaking on agar plates resulted in growth after 10 days of incubation. Terminal streaks exhibited individual minicolonies with a diameter below 1 mm. FISH analysis of colonies from proximal position of the streak indicated a high enrichment of *Desulfosporosinus* cells (Supplementary Figure 9-19) (no quantitative statements can be made, due to the qualitative nature of the filter stamping method). Cells had a uniform cell shape with a mean length of 3.9 µm and a mean radius of 0.6 µm (resembling the small rod phenotype Table 3-3).
Subcultures could be readily maintained via streaking on plates. However, no growing culture could be obtained via transfer (using sterile anoxic needles) of individual colonies into liquid defined media (basal FM, [10 mM] lactate, [10 mM] Na-sulfate).

3.2.5 Defined Media Array and Dilution to extinction

Initial enrichment attempts on defined media were successful for two different combinations of the defined media array. Lactate in FM and butyrate in FM. The combination of H_2 /CO_2 in aSRB medium resulted in a small increase in relative abundance, however no obvious sulfate removal was detected. All other treatments either did not exhibit an increase in OD_{600} after 131 days of incubation, or no relative increase (relative abundance of inoculum of 20 to 25 %) in *Desulfosporosinus* relative abundance (Table 3-5). An overview of OD_{600}, anion turnover and FISH data is provided in supplementary section 8.3.5.
Relative abundance peaked at median levels of about 75 % around 30 to 60 (butyrate) and 20 to 30 days (lactate), in log type phase of growth (as indicated by OD_{600}). In butyrate treatments about 50 µmol of sulfate and 70 µmol of butyrate were removed with 50 to 90 days. Acetate was produced simultaneously to final levels of up to 140 µmol. Total lactate (100 µmol) was removed from incubations within about 60 days and led to the approximate equimolar production of acetate. Sulfate consumption of about 50 µmol was observed within this timeframe. Obviously, lactate was the limiting substrate for batch culture growth.

Table 3-5
Summary of growth and enrichment of substrates and media combinations used for cultivation of DSP-SbII in the defined media array. A "/" denotes no growth detected, "–"denotes bacterial growth but no growth of *Desulfosporosinus*, a "P"denotes presence of DSP-SbII but only at low abundance, "+" denotes an enrichment of *Desulfosporosinus* relative to the inoculum. Growth is defined as an increase in OD6oo, whereas DSP-SbII abundance was determined with FISH.

Substrate	aSRB	DSMZ 1250	Basal FM
H_2/CO_2	**+**	–	/
H_2/CO_2/Acetate	P	P	–
Propionate	/	/	/
Lactate	/	P	**+**
Butyrate	P	P	**+**
Ethanol	/	P	P
Glycerol	/	/	/

The first dilution to extinction experiment with lactate yielded a highly enriched *Desulfosporosinus* population in dilutions 10^{-1} and 10^{-2}(L_F_01_E-1 and L_F_01_E-2), of approximately 90 % relative abundance after 20 days of incubation. Again lactate was removed completely, resulting in the production of acetate with consumption of approximately two thirds of available sulfate. Maximum biomass yield (as indicated from OD_{600}) coincided with the timepoint of total lactate (limiting substrate) consumption. Notably, growth was observed in higher dilutions as well (10^{-3} and 10^{-5}). Here, DSP-SbII cells could not maintain a high relative abundance.

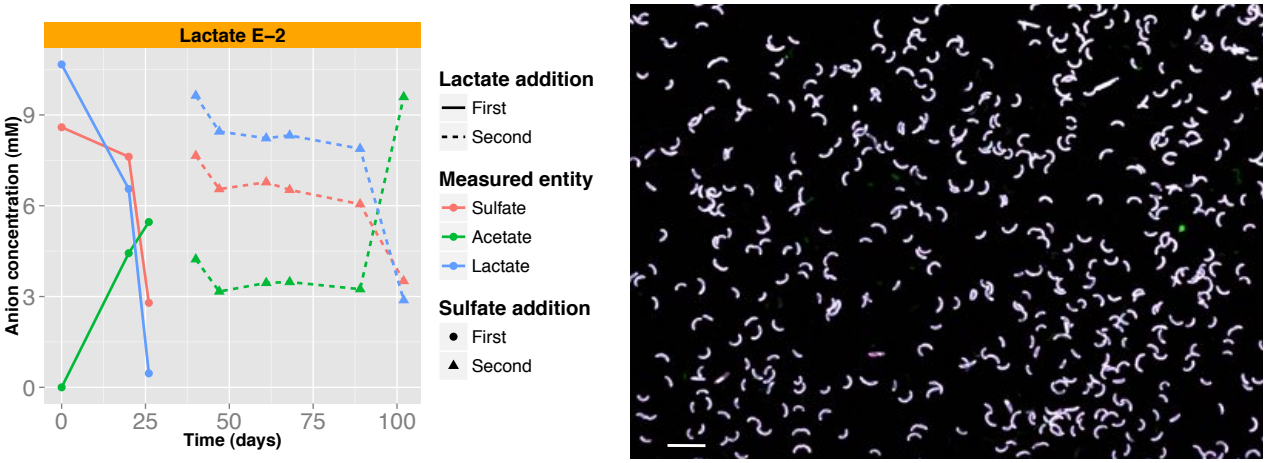

Figure 3-11
Turnover of sulfate, lactate and acetate in the 10^{-2} dilution of the first dilution series experiment. FISH analysis showing *Desulfosporosinus* cells enriched to a level of 90 % in the respective specimen. *Desulfosporosinus* cells stain in white-magenta. *Bacteria* in green. Probes: EUbmix-FITC, DSP648-Cy3, cDSP648, DSP610-Cy5. Scale bar: 10 µm

Consequently, a second generation of dilution to extinction series (2 complete series with sodiumsulfate and one series with iron(II)sulfate) was performed using the highly enriched dilutions (E-1 and E-2) as an inoculum.

Agar shake dilution series: Diluting the highly enriched culture Lactate E-1 in agarshakes, resulted in the formation of colony forming units (CFUs) down to the highest dilution (10^{-9}). No growth was observed in non-inoculated negative controls. Typically at lower dilutions a dense layer of small CFUs (<1 mm) formed in close proximity to the solid/gas interface. At higher dilutions CFUs increased in diameter towards the interface (app. 1 to 2 mm) but decreased in abundance and could be found either in vicinity to the interface or at greater depth sections (2 cm). Colonies growing in the depth had a diameter of about 2 mm. CFUs had a brownish color and a disk like shape, the cross section resembling a spindle. Microscopic analysis of unfixed colonies suggested for straight rods of an approximate length of 3 µm.
12 individual colonies from dilutions between 10^{-5} and 10^{-9} were transferred into liquid medium (basal FM with lactate and Na-sulfate). However, no single growing culture could be obtained after 55 days of incubation.

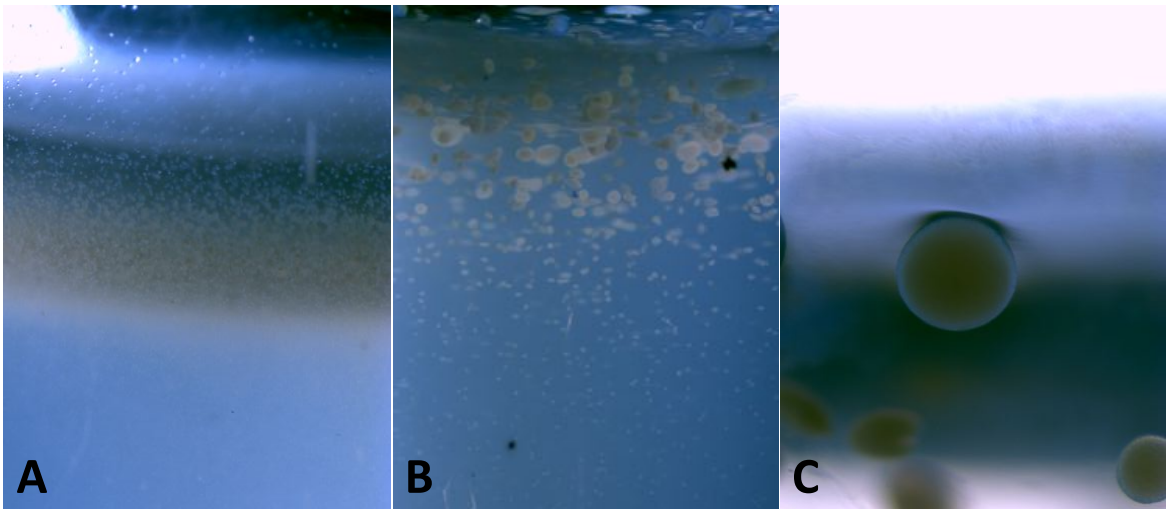

Figure 3-12
Colony forming units growing in anaerobic agar shake dilution series.
Image A: A dense lawn growing in vicinity to the surface in dilution 10^{-1}. Image B: CFUs increasing in size in dilution 10^{-5}. Magnified section of dilution 10^{-5} showing CFU growing in close proximity to the solid/gas interphase.

3.2.6 Description of candidate isolates of *Desulfosporosinus* SbII strains

From the second set of dilution to extinction series with basal FM and lactate as a substrate, five candidate high enrichments (no non target cells detectable with FISH) could be obtained (Figure 3-13).
Two enrichments derived from the two dilution series with Na–sulfate (10^{-1} and 10^{-2} dilutions respectively):Isolate Sodium *E-1 (A)* and *Sodium E-2 (B)*
Two from the dilution series with Fe_{II}Sulfate: Isolate *Iron E-1* and *Iron E-2*
A fifth enrichment was grown as a subculture of *Iron E-2* in a serum bottle: Isolate *Iron Ser*
As candidate isolates growing on Fe_{II}Sulfate derived from the same dilution series, they can likely be expected to be identical. Cells showed no active swimming motility, but a tumbling state of motion. *Iron* isolates were small straight rods, whereas *Sodium* isolates were mostly curved rods and larger as compared to *Iron* isolates.
Growth of *Iron E-1* and *Iron E-2* was observed as a consequence of strong formation of FeS precipitates after 25 days. Growth of isolates Sodium *E-1 (A)* and *Sodium E-2 (B)* started after 27 and 62 days of incubation respectively (Figure 8-25). Lactate was removed after 12 to 25 days for isolates, growing on Fe_{II}Sulfate, resulting in the production of nearly equimolar amounts of acetate. Sulfate was removed at a rate of about 2 µmol per day to about a half of the starting amount when lactate was consumed, however sulfate removal was probably limited by the availability of lactate. Similarly, half of the sulfate pool was consumed for candidate isolates growing on sodiumsulfate at a rate of about 1 µmol per day. Lactate was consumed after 55 days of incubation and yielded acetate in the corresponding amount (Figure 8-13 and Figure 8-26). The averaged stoichiometry of highly enriched specimens suggested for incomplete oxidation of lactate via reduction of sulfate. However, the production of acetate was lower than what would be expected from the theoretical reaction balance.

Equation 4
Theoretical reaction stoichiometry of incomplete oxidation of lactate via reduction of sulfate.

$$2\,CH_3\,CHOHCOO^- + SO_4^{2-} \rightarrow 2\,CH_3COO^- + 2\,HCO_3^- + HS^- + H^+$$

Equation 5
Averaged stoichiometry of sulfate and lactate consumption for highly enriched (>90 %) *Desulfosporosinus* specimens. Reaction balances were calculated from linear regression analysis of binary comparisons of turnover rates over enriched specimens (lactate removal rates~sulfate removal rates, lactate removal rates~acetate production rates). Note that from the reaction products only acetate was measured. The other reaction products either result from the theoretical balance (carbonate, sulfide and protons) or represent the missing molecular fractions of carbon, hydrogen and oxygen.

$$1.7CH_3CHOHCOO^- + SO_4^{2-} \rightarrow 1.5CH_3COO^- + 1.5HCO_3^- + HS^- + H^+ + 2.1C + 0.5H + 1.6O$$

Cell specific sulfate reduction rates (csSRR) were estimated for three isolates based on total cell counts of one timepoint corresponding to endpoint of lactate turnover. No further timepoint was quantified due to time constraints. Sulfate reduction rates were determined from the linear models shown in Figure 3-14. Mean absolute cell counts (cells per incubation volume (10 ml)) were 4.6×10^8, 2.2×10^8 and 1.3×10^8 for *Iron E-1*, *Iron E-2*and *Sodium E-1 (A)* respectively. The estimated csSRR was 5, 12 and 7 fmol cell^{-1} day^{-1}for *Iron E-1*, *Iron E-2* and *Sodium E-1 (A)* respectively.

DNA sequencing of 16S rRNA gene PCR products, amplified directly from genomic DNA extracts of the five candidate enrichments, resulted in unambiguous trace files both for the 1492R/8F and the DSP603F/1492R PCR products, which supports the highly enriched status of the specimens. Analysis of uncorrected distances of the alignment of *Desulfosporosinus* DNA sequences (Supplementary Figure 8-27) indicated for high intraspecific similarity of *Iron* and *Sodium* isolates (below 0.1 % distance). However interspecific dissimilarity was reasonably high at a level of 3%. Distance to the clones of Schlöppnerbrunnen II (SbII)(Pester et al., 2010) was smaller than 2 %, with *Sodium* isolates showing more similarity. A 16S rRNA gene from a SbII metagenome (Hausmann, 2014) was highly similar to the SbII clones and exhibited a dissimilarity of 2.2 and 2.7 % to the *Sodium* and *Iron* isolates respectively(Supplementary Figure 9-28). The minimum observed dissimilarity to type strains was observed with *D. lacus* (3.2 %) and *D. meridiei* (1.9%) for the *Sodium* and *Iron* enrichments respectively. Phylogenetic analysis suggested for a placement of all five candidate isolates into a cluster together with all Schlöppnerbrunnen II clones and *D. lacus* as the only represented type strain (Figure 3-15). The cluster had a high posterior probability support of 0.96. Notably, *Iron* and *Sodium* isolates formed stable clusters within this clade (posterior probability of 1), with the *Sodium* cluster branching at deeper levels.

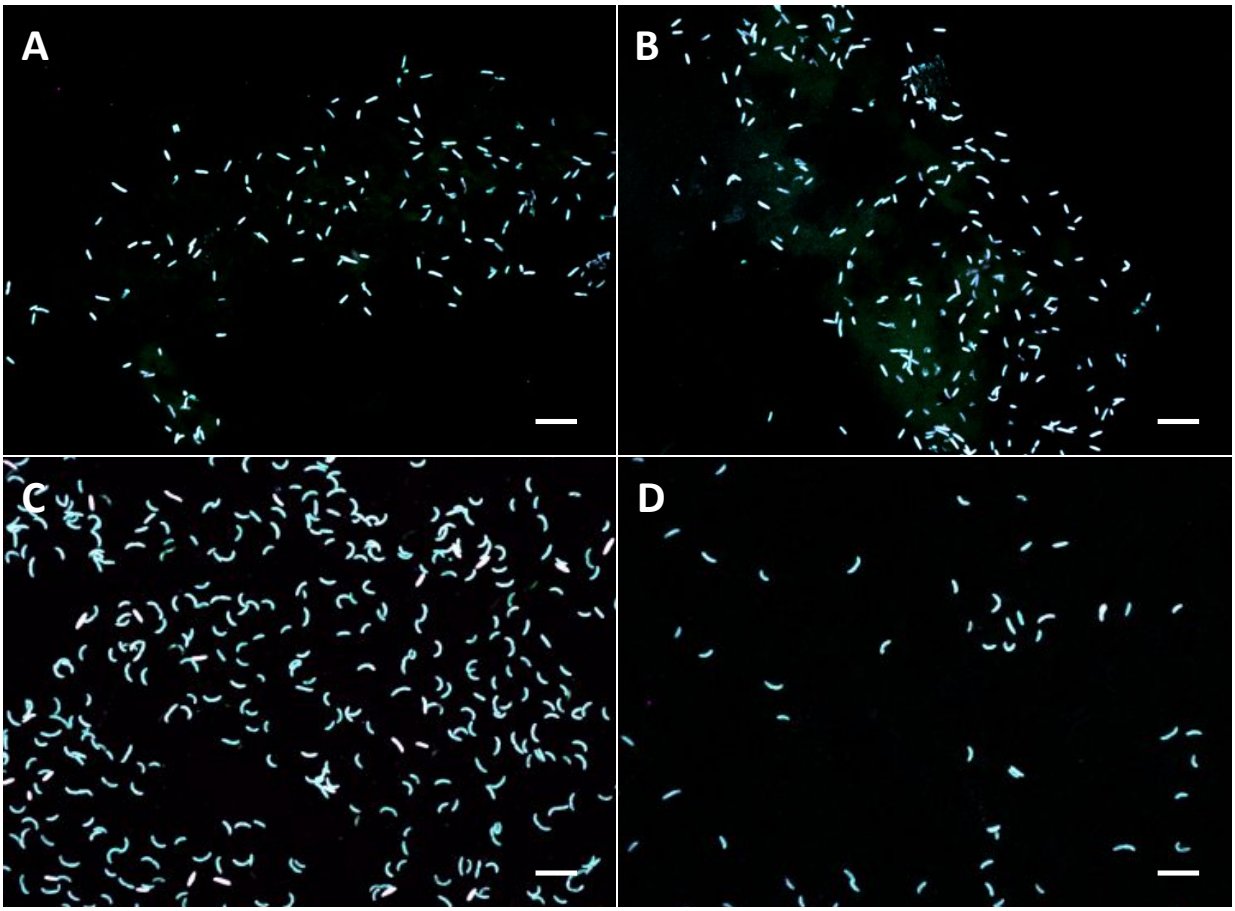

Figure 3-13
FISH analysis of highly enriched cultures from dilution to extinction experiments. Image A: Isolate *Iron E-1,* Image B: *Iron E-2,* Image C: *Sodium E-1 (A), Image D: Sodium E-2 (B)*
Desulfosporosinus cells stain in white-cyan. Probes: EUbmix-FITC, DSP648-Cy3, cDSP648, DSP610-Cy5. The greenish cell in image C is an artifact of unequal staining (all three probes had bound however). *Iron E-1* and *Iron E-2* were DAPI stained as well. An extensive autofluorescent background of FeS precipitates caused the diminished signal quality in Image A and B. Scale bar: 10 µm

Table 3-6
Morphological dimensions of DSP SbII candidate isolates. Length and diameter are given as mean values with average standard deviation. The incubation timepoint for morphology determination (same images as in Figure 3-13) is provided in the timepoint column (refer to supplementary Figure 8-26 for the respective anion turnover data)

Isolate	Length (µm)	Diameter (µm)	Morphology	Timepoint (days)
Iron E-1	2.8 (±0.7)	0.7 (±0.3)	Straight rods	26
Iron E-2	2.8 (±0.6)	0.7 (±0.3)	Straight rods	26
Sodium E-1 (A)	3.9 (±0.7)	1.3 (±1.0)	Curved and straight rods	39
Sodium E-2 (B)	4.2 (±0.6)	1.2 (±0.6)	Curved and straight rods	74

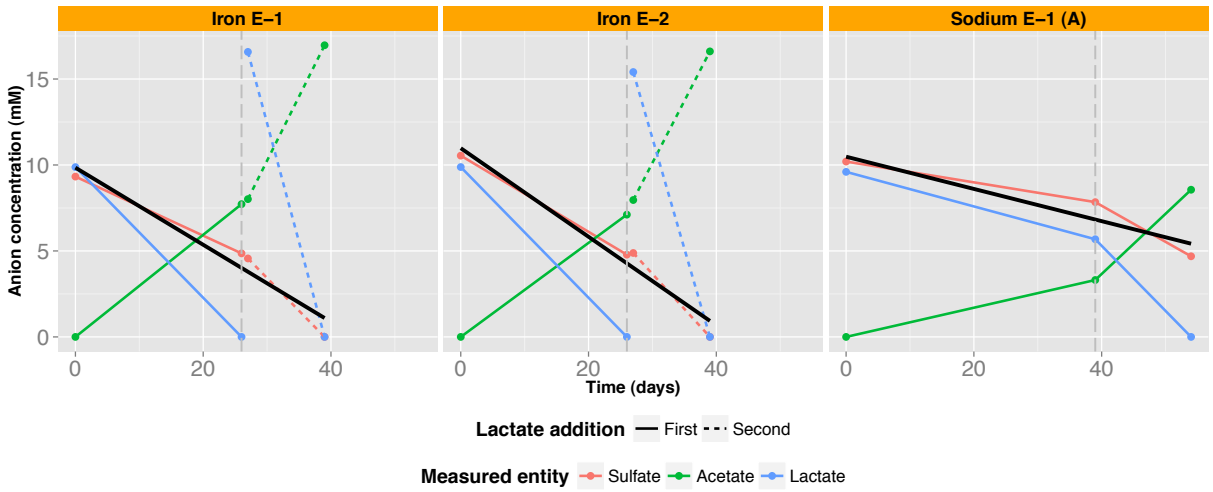

Figure 3-14
Turnover data of sulfate, lactate and acetate in three of the four candidate DSP-SbII isolates. Linear models used to calculate overall sulfate removal rates are shown as solid lines. The grey vertical dashed line denotes the singular timepoint for determination of absolute cell counts.

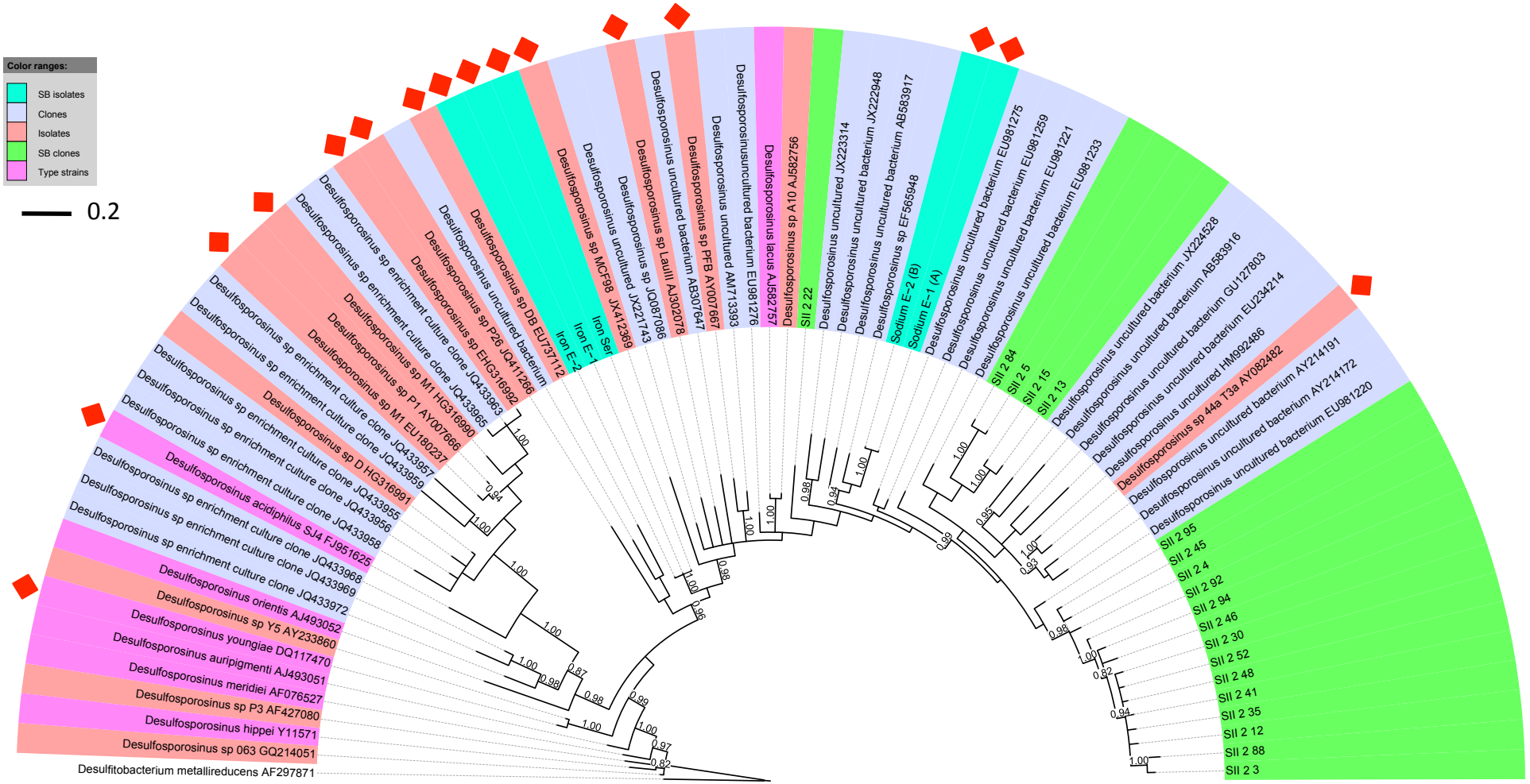

Figure 3-15
MrBayes tree showing the phylogentic affiliation of the novel DSP-SbII candidate isolates (turquoise) to type strains of *Desulfosporosinus* (pink). Furthermore other not validately described, environmental *Desulfosporosinus* isolates (orange) are shown. Environmental clone sequences are shown in light blue. Clones from Schlöppnerbrunnen II are shown in green. *Desulfitobacterium metallireducens* was used as an outgroup (white). The last segment of the label ID denotes the GenBank accession number. Red diamonds mark type strains and environmental isolates that were either isolated under acidic conditions or derived from an acidic environment. Posterior probability values higher than 0.8 are provided for the respective branches.

3.2.7 *Desulfovibrio* sp. SII13a, pH series

pH values increased upon inoculation with the *Desulfovibrio* specimen. Bacterial growth was positively associated with a decrease in proton concentration for about one order of magnitude (supplementary Figure 8-31 and Figure 8-32). The duration of the lag phase increased with decreasing starting pH values, whereas generally higher growth rates (μ) were observed at higher pH values (Figure 3-16). Highest growth rates were observed at neutral pH were the HCO_3^-/CO_2 buffer system was still intact. No growth was detected below a pH of 5.3.

The beginning of stationary phase coincided with total consumption of lactate (app. 100 μmol) and app. 50 μmol of sulfate (supplementary Figure 8-31). Acetate was produced at amounts corresponding to the oxidation of lactate. A prolonged lag phase was observed as a consequence of decreasing pH, with longer lag times in the second series (inoculated from the lowest pH incubation exhibiting growth of series 1)

Detailed OD_{600} data are provided in supplementary Figure 8-32.

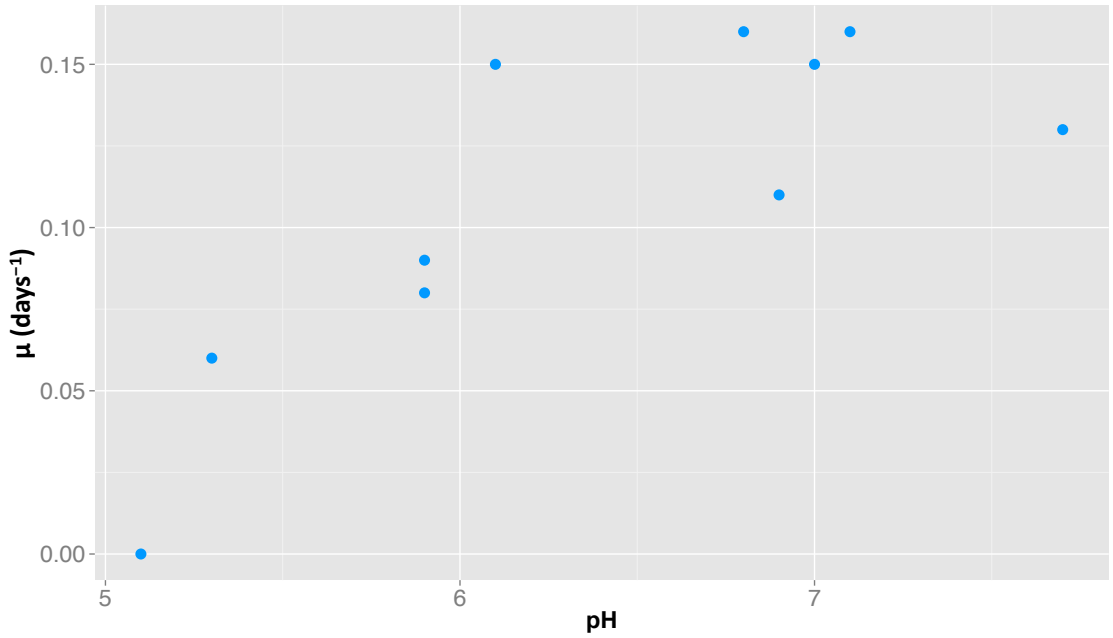

Figure 3-16
Dependency of growth rates (μ) of *Desulfovibrio* sp. SII13a on pH as determine from OD_{600} measurements. The pH value from the timepoint of inoculation was used here.

4 Discussion

4.1 qPCR

4.1.1 The physiological identity of *dsrAB* core OTUs remains elusive

From the data shown above, no clear statement regarding the physiology of the three *dsrA* OTUs can be made. The imposed conditions were obviously unsuitable to enrich for either OTU1 or OTU6, as none of them could even sustain at an equal abundance level compared to the timepoint zero. The observed distribution profile at timepoint zero with OTU1 (0.19 %) being the most abundant group, followed by OTU6 (0.12 %) and finally OTU2 (0.07 %), is in stark contrast to previous *in situ* qPCR profiles where OTU2 (1.16 %) dominated followed by OTU1 (0.77 %) and OTU6 (0.04 %) (Steger et al., 2011). The intraspecific variation in relative abundance for a given OTU between the studies might partially be attributed to spatiotemporal variability at the sampling sites. Furthermore it has to be mentioned, that different primer sets were employed between studies, to assess the total bacterial and archaeal abundance (1389F vs. 1389Fmix as used here). Moreover qPCR data can be highly biased by for instance the employed detection system, quantification method (Brankatschk et al., 2012) and DNA extraction chemistry towards certain taxa. Thus a direct comparison with previous studies, using other protocols is not valid.
Importantly, OTU2 could sustain at its initial relative abundance and even showed a small increase in some of the sulfate-amended microcosms (e.g. no substrate amendment and formate amendment). Although higher relative abundances were observed in non–sulfate amended microcosms, this does not imply that these SRM are not capable of dissimilatory sulfate reduction. Absolute copy numbers were highly variable throughout the treatments and do not allow for a clear separation based on the sulfate variable. The decreased relative abundance of OTU2 when compared to non–sulfate–amendments can of course be caused by growth of competing SRM that are better adapted to the imposed sulfate amounts. Furthermore SRM are amongst the metabolically most versatile groups of organisms and can make use of a variety of electron acceptors other then sulfate (Rabus et al., 2006).
The possibility of these genes being not functionally relevant for the respective organism is known for certain *dsrAB* carrying species and would be another way to describe the lack of response seen here (Imachi et al., 2006). Tackling the response of the metagenomic totality of *dsrA* or *dsrB* genes in the microcosm experiments described here via next generation amplicon sequencing would definitely provide further evidence on the response of the SRM community. The observation of clearly lower abundance values already for the timepoint zero and a shift in composition of OTU1, 2 and 6 as compared to those of earlier studies, suggests for a potential flaw, as samples are not comparable. This highlights the relevance of seasonal and annual variability of SRM communities and abiotic factors, which are well described for this model fen (Küsel et al., 2008).

An intriguing question is, to which extend the microcosm setup is suitable for the enrichment of SRM or acidophilic SRM (aSRM) in particular. Loy et al., 2004 reported on the occurrence of SRM and in particular the novel *dsrAB* OTUs in the Schlöppnerbrunnen II (SbII) system. So far these results were all confirmed by incubation independent *in situ* assessments of *dsrAB* diversity (Schmalenberger et al., 2007b; Steger et al., 2011) in SbII and other pristine wetland microbial communities (Castro et al., 2002; He et al., 2010).

No positive selective response of these particular OTUs to incubation conditions was so far described in the literature. Batch microcosm soil slurry studies using SbII soil and solute fractions and provision of SCFAs (Pester et al., 2010,Hausmann, 2012) under acidic sulfate reducing conditions reported on the enrichment of *Desulfosporosinus SbII*. There is growing evidence that *Desulfosporosinus* representatives from various sources might be well adapted to acidic conditions (Figure 3-15) although definitive evidence of SCFAs utilization of *Desulfosporosinus* species in acidic SbII soil slurries is not available. Hypothetically, the primary substrates used here and in previous studies batch incubations might impose toxic effects for the reason of decreased dissociation at the imposed pH of about 4 (for details refer to section 4.2 and 0). The partial increase of OTU2 in sulfate-amended microcosms without substrate would be a line of evidence pointing towards other, yet untested substrates. SRM are heterogeneous when it comes to electron donor metabolism (Rabus et al., 2006), a chemical dissolution of iron coupled to oxidation of the resulting H_2 species might be a possible metabolic pathway which would not be detected in this experimental setup (Muyzer and Stams, 2008).

Tackling the physiological capabilities of these OTUs is not straightforward to accomplish without associated genetic information and directly linked chemical parameters. An increase of sulfate amendments and use of other (non ionic) substrate in targeted experiments aiming to investigate the response of these elusive OTUs would be one strategy. A more straightforward approach via the acquisition of genomic metadata or even taxonomic marker genes for each specific *dsrAB* taxon could potentially provide useful insight into physiological properties too. Cloning of metagenomic soil DNA into high capacity vectors and screening for *dsrAB* inserts could serve as a highly promising method.

4.1.2 *Acidobacteria* can sustain a high relative abundance in anoxic microcosms

Several lines of evidence describe the phylum of *Acidobacteria* as the major taxonomic group found in the Schlöppnerbrunnen II system (Hausmann, 2014; Steger et al., 2011) and in *in vitro* studies (Pester et al., 2010). The results presented here confirm their prevalence in unmodified SbII soil and are in accordance with V4 amplicon data obtained for the very same specimens (Hausmann, 2014). Due to the significant positive correlation between amplicon and qPCR data it may further be speculated that at least for certain highly abundant groups the sequencing technology might be adequate to generate hypothesis regarding the abundance distribution of taxa. However, this assumption is only valid for this particular case and relates only to the reciprocal abundance of specific samples. If the relative abundance (of total microbes) estimates of either of the two methods is biased cannot be deduced from this analysis. Furthermore, numerous factors (both systemic and technical) can infer distortions on amplicon data and thus a different statement might be deduced for other taxonomic targets, using the very same methodology (Amend et al., 2010; Gomez-Alvarez et al., 2009).

Acidobacteria seem to be stably integrated into carbon degradation in the fen system and identification and functional assessment of major active groups clearly represents a missing piece in microbial research in this habitat. Although the data here cannot report on a selective effect of the treatments or a definite enrichment for any of the three investigated subdivisions (SD), a strong tolerance to anoxia could be observed. Obviously, the incubation time of 51 days cumulated in a negative effect. On the other side, decay of SD1 and SD2 was less pronounced as for total *Bacteria* and *Archaea*. In particular, non-sulfate amended treatments were less detrimental and allowed for a more or less stable culture. Summarizing these findings, it seems that *Acidobacteria* in the soil slurries did not stringently rely on the availability of oxygen as an electron acceptor for metabolizing and maintaining their

population level. Furthermore, growth at intermediate timepoints can of course not be excluded, as it would be for prolonged incubation time.

Acidobacteria are typical core constituents in wetland ecosystems all over the world (Hartman et al., 2008; Kanokratana et al., 2011) and are described as typical degraders of polymeric substances such as humic acids, polysaccharides and also simple sugars (Ward et al., 2009). Use of cultivation based techniques allowed for the successful isolation of *Acidobacteria* from acidic wetland systems, highlighting the capability of these organisms to be well adapted to the acidic conditions(Kulichevskaya et al., 2010; Pankratov and Dedysh, 2010a). Evidence is growing for *Acidobacteria* as a coherent taxonomic group, being diverse in respect to energy generation and respiration. While many isolates are described as aerobes, isolates being capable of fermentation or respiration using alternative electron acceptors such as Fe(III), Mn(IV), fumerate or 2,6-anthraquinone disulfonate (Coates et al., 1999; Pankratov and Dedysh, 2010a) are also known. Strict anaerobic growth could also be demonstrated for *Telmatobacter bradus* (SD1) and *Acidobacterium capsulatum* (SD1) (Pankratov et al., 2012). Their dominance in Schlöppnerbrunnen soil and the recognized function as being key players in complex carbon degradation in wetland ecosystems emphasizes research focusing on this taxon. Eventually even cultivation-based techniques under anoxic conditions can provide promising insights.

4.2 Enrichment and cultivation of novel *Desulfosporosinus* SbII species

Biochemical considerations

A common theme of all enrichment attempts was reduction of sulfate and production of acetate resembling the incomplete substrate oxidation type, characteristic for *Desulfosporosinus* species (Spring and Rosenzweig, 2006). In contrast to the defined media array, where the electron donor was known, the respective identity could not be verified for soil slurries and the dialysis chambers. Except for the produced acetate, SCFAs and lactate could never be identified via CE measurements (not even in long term abiotic controls). A previous study of SbII soil reported typically low concentrations of candidate electron donors such as lactate and acetate (maximum measured: 80 and 100 µmol g^{-1}(wet soil weight) respectively). Translating these concentrations to the approximate applied amount of soil per dialysis chamber (2 g wet weight) would yield 0.16 µmol of available lactate per dialysis chamber, which is in stark contrast to the observed quantities of sulfate consumption and acetate production (acetate amounts varied between 75 and 600 µmol). Consequently, the possibility of SCFAs or lactate being directly provided as substrates via diffusion from soil into the solute fraction seems to be unlikely, as it cannot explain the overall turnover rates. The usage of high molecular weight substances such as extracellular DNA, or humic acids can be excluded, as these substances are far above the molecular weight cutoff of the dialysis tubing.

A hypothetical way of substrate provision would be an upstream metabolic process catalyzed by another functional guild of microbes such as fermentative or Fe(III) reducing microorganisms (FRM). Importantly, FRM have been demonstrated to play a fundamental role for carbon degradation in the Schlöppnerbrunnen II system, accounting up to 71.6 % of anaerobic carbon mineralization (Küsel et al., 2008). Interestingly, anoxic microcosm incubations demonstrated high Fe(III) reduction rates within the first seven days of incubation followed by its stagnation but starting with the depletion of sulfate (Küsel et al., 2008). Thus in a hypothetical scenario in a dialysis chamber, FRM could act as a mediator of initial carbon breakdown via Fe(III) reduction and provide the substrates for *Desulfosporosinus* species. In line with this theory would be the pronounced lag phase

(app. 25 days) before reasonable sulfate reduction could be observed in these setups. Utilization of the insoluble Fe(III) pool within the dialysis tubing might be mediated through redox shuttles such or bacterial nanowires (Weber et al., 2006), resulting in soluble Fe(II) formation , which could than penetrate the membrane (Alewell et al., 2008). This would be in line with the observation of black precipitate formation within active dialysis chambers. Furthermore acetate is also a typical product of FRM (Weber et al., 2006) which could partially explain elevated acetate levels, while sulfate still was not reduced.

Certain *Desulfosporosinus (*e.g. *D. lacus)* strains are also capable of Fe(III) reduction coupled to the oxidation of various substrates such as glucose or lactate which yields acetate. Acetate itself seems to be tightly and directly coupled to the growth dynamics of the *Desulfosporosinus* population in dialysis chambers. Product inhibition of growth, due to accumulation of a metabolic product is a common observation in microbial processes (e.g. alcohol fermentation (Aiba et al., 1968)) and can even lead to "negative" growth (Chmiel and Sonnleitner, 2011). The toxic effect of acetate for SRB at low pH is well documented and mainly ascribed to unhindered passive membrane passage of protonated, unpolar acetate species into the cytoplasm were they cause a depolarization of the proton gradient upon dissociation(Baronofsky et al., 1984; Gemmell and Knowles, 2000). A successful example of sulfate reduction at acidic pH using a co–culture approach was described by Kimura and Johnson, 2004. Using a continuous culture of *Desulfosporosinus M1* and acetotrophic *Acidocella PFBC,* they were able to demonstrate growth and sulfate reduction of *D. M1* only in the presence of *A. PFBC,* which efficiently removed the produced acetate, thereby promoting growth of *D. M1*. Importantly, an *Acidocella sp*. was also co-enriched with *Desulfosporosinus* in the heavy fractions of a SIP Study of Schlöppnerbrunnen II soil (Pester et al., 2010), which can point towards a beneficial symbiotic relation.

Consequently, the steep drop of acetate concentrations after peaking at maximum *Desulfosporosinus* abundance might be attributed to the activity of an acetotrophic community. However, counterintuitively absolute DSP-SbII abundance decreased in accordance with acetate levels, which does not favor the theory of product inhibition. Furthermore, due to the circumneutral pH of the incubation the toxic effect of acetic acid is most likely less pronounced (Supplementary table 8-8). The rise of acetoclastic methanogens, which can make use of these elevated levels, seems also plausible. Another explanation of the rapid initial growth phase followed by a pronounced decay could be substrate limitation due to rapid consumption of the increasing *Desulfosporosinus* population and by limiting supply by the unknown providing entity.

An advantageous approach for revealing the interaction of *Desulfosporosinus* SbII with the biogeochemical parameters and microbial unknowns it faces in its natural environment, could be assessing this very first phase of incubation, by tracing the flow of carbon and electron acceptors namely Fe(III) and sulfate at a high resolution. Eventually, this would provide useful insights into the elusive identity of the primary substrate. Here, the very narrow specifity of the capillary electrophoresis system clearly missed a wide range of carbon sources (carbohydrates, aromatic compounds, alcohols…) known to be utilized by *Desulfosporosinus* representatives (Alazard et al., 2010a; Lee et al., 2009; Liu et al., 2004).

Population dynamics and pleomorphy of Desulfosporosinus

Knowledge of the limiting substrate could provide further insights into the life strategy of *Desulfosporosinus SbII* in the fen ecosystem and allow for an explanation of the early and rapid peak of DSP abundance followed by its decrease. A r-strategy of life was speculated for *Desulfosporosinus* in the Schlöppnerbrunnen II system, that makes use of temporal elevated sulfate levels (Pester et al., 2010).
Assuming that sulfate is the limiting compound in the fen system or in dialysis chambers here, a high K_s value (low affinity of *Desulfosporosinus* cells to sulfate) can be expected. Thus, under the following rationale separating r- and K-strategists(Chmiel and Sonnleitner, 2011);

$\mu_{max,u} \leq \mu_{max,DSP}$ BUT $K_{s,u} \leq K_{s,DSP}$

(Where μ_{max} denotes the maximum specific growth rate and K_s the affinity constant to the substrate, u representing the unknown population and DSP the *Desulfosporosinus* population) *Desulfosporosinus sp.* would be defined as r strategist, as maximum growth was observed at highest sulfate concentrations in dialysis chambers. Thus, it could efficiently propagate due to its high specific growth rate and not its high affinity to the substrate. This could provide a theory for its decrease at lower sulfate concentrations, as SRM having a lower K_s value could be favored here. However, if sulfate can be regarded as the limiting compound, both in the fen and the dialysis chamber is not known.
Contrary, it is also plausible that the unknown substrate is the limiting compound, as it would be expected from the stoichiometry of incomplete substrate oxidation with sulfate. Additionally, sulfate amounts were clearly not limited in dialysis chambers. A scenario of instant consumption of produced substrate due to the high affinity (low K_s) of *Desulfosporosinus* cells would favor growth of a K-strategist according to the following rationale:

$\mu_{max,DSP} \leq \mu_{max,u}$ BUT $K_{s,DSP} \leq K_{s,u}$.

The generally low dilution rates (long incubation times) imposed throughout all incubations (Supplementary Figure 8-1) could also support the idea of a K- type strategy. As a consequence from the limited data presented here no definite statement regarding a r or K strategy of live can be made at this point. Accordingly, defining the identity and turnover of the used substrate would allow getting useful insights into the population dynamics and growth parameters (μ_{max} and K_s) of *Desulfosporosinus* SbII. Furthermore,it is required to reveal the presence and identity of competing and mutualistic microorganisms for the substrate, products or sulfate. A tempting experimental design would be to study the interplay of, for instance, the a dominant *Desulfosporosinus* enrichment and its contaminant counterpart as it was observed in the first generation of dilution series in a continuous culture setup. Theoretically, one could determine the life strategy of *Desulfosporosinus* via adjustment of the dilution rate in the system and perform mixed population experiments in a continuous mode setup.

A phenomenon that could possibly be linked to life strategy and biochemical regimes could be the postulated phenotypic plasticity of *Desulfosporosinus* species growing in dialysis chambers. As outlined above, depending on the incubation stage, different cell morphologies could be observed in dialysis chambers that are beyond the expected variance for a quasi fixed cell morphology (Koch, 1966). Two different rationales for this observation seem plausible.
First, different *Desulfosporosinus* strains might be dominant at different stages – a hypothesis that is also supported by the observed difference in 16S rRNA sequence identity of the

candidate isolates. However, filamentation was not detected in any of the defined media incubations.
Second, the observation might be attributed to a pleomorphic life strategy as an adaption to environmental effectors.
An often neglected point in microbiology is the sheer diversity of bacterial shapes and the morphological plasticity one single genotype can exhibit in response to changes in its environment (Young, 2006). This variability implies functional relevance, as a change in shape is known to be an active process (Justice et al., 2008) and might even result in exotic modes of energy generation, allowing for the generation of electric energy potentials along biogeochemical gradients (Pfeffer et al., 2012).
Members of the genus *Desulfosporosinus* are described as sausage shaped (slightly curved to straight) rods that occasionally (2 cases) can form filaments (Spring and Rosenzweig, 2006). However, size reported in literature for a single filament is 15 µm in length (Vos et al., 2011), which is in stark contrast to the maximal length observed here (up to 270 µm). Other representatives of SRM known to form a filamentous shape are rarely found and include only the genus *Desulfonema* (Fukui et al., 1999; Widdel et al., 1983). However, in contrast to *Desulfonema,* where filaments are constituted of individual cells, *Desulfosporosinus* filaments did exhibit septa formation only occasionally. Thus, the filamentous phenotype described here can be speculated to be a continuous mode of cell growth without septa formation (Justice et al., 2008).
The reported size of *Bacteria* and *Archaea* ranges from midget *Pelagibacter ubique* with an estimated volume of 0.01 μm^3 (Rappé et al., 2002) to true giants like *Epulopiscium fishelsoni* with up to 600 µm in length an 80 µm in diameter (Angert et al., 1993). Similarly here, cells of *Desulfosporosinus* were observed, that varied in volume over two orders of magnitude, which raises the question of the causal origin. The major factor limiting cell size and dimensions is regarded to be imposed by diffusive constraints (Koch, 1996). A flat shaped filamentous morphology is speculated to be beneficial in substrate limited environments as it maximizes the surface to volume ratio of the cell and thereby should allow for increased uptake of the limiting compound (Schulz and Jørgensen, 2001). Furthermore, filamentous phenotypes have been shown to be induceable virulence factors in uropathogenic *E. coli* (Justice et al., 2006), mediated and being reversed in *Burkholderia pseudomallei* via effector molecules such as beta lactam antibiotics (Chen et al., 2005), or being related to nutrient limitation and surface maximization on solid surfaces in *Pseudomonas aeruginosa* biofilms (Steinberger et al., 2002). On the other extreme, small rods as observed here in growth phase, might have advantages in nutrient limited environments without stratification were facilitated dispersal due to decreased size promotes access to the substrate (Young, 2006).
The hypothesized pleomorphy in dialysis chambers might consequently be approached via different theoretical conceptions, for me the most reasonable here would be that of a diffusion limited cell (Schulz and Jørgensen, 2001). The concept states, that a cell can either be limited by diffusion of the substrate with concentrations approaching zero at the cells surface due to efficient uptake mechanisms (presumably low K_s value), or uptake limited when substrate influx can not be compensated by assimilation.
Thus, in a low substrate environment it can be advantageous of being diffusion limited. The maximum surface to volume ratio of filamentous forms could provide *Desulfosporosinus* cells with means to efficiently monopolize a substrate diffusing through the dialysis membrane in the very first incubation stage. This is exemplified by the efficiency of uptake (or specific metabolic rate) for a given substrate of a diffusion limited cell, that is proposed to be directly

proportional to ambient concentration of the substrate and indirectly proportional to cell radius according to Koch, 1990 and Schulz and Jørgensen, 2001.

Where

$E=(3D/R^2)\times C_\infty$

(E=Efficiency, D=Diffusion constant of the substrate, R=cell radius, C_∞ = Substrate concentration in the bulk solution).
Consequently, the decrease in cell diameter, as it is observed for the filaments would increase the efficiency. Furthermore the increase in surface would allow a big percentage of the cell surface to be in contact with the surface of the membrane, as indicated by maximum p_n values (percentage of nutritionally available surface area) for this morphology (Table 3-3). Hypothetically if bulk substrate concentrations are still low in dialysis chambers but the solute solid fractions are equilibrated this could decrease the effectiveness of the high S/V ratio of filaments and favor a small rod phenotype, whereas at high substrate concentration (C_∞) the need for the "streamlined" cell would become diminished allowing rise of the bigger phenotype. Additionally the big rods could possibly be less prone to influx of inhibitory products that accumulate in their surrounding.

Another theory based on the Monod growth equation ($\mu=\mu_{max}\times(S/S+K_s)$, where μ=specific growth rate, μ_{max}=maximum specific growth rate, S=substrate concentration, K_s=affinity constant) (Monod, 1949), explaining the dominance of filamentous bacteria in mixed microbial assemblages was proposed by Chudoba et al., 1973. They observed that for the scenario of S beeing much higher than K_s, μ is controlled mainly by μ_{max} (r–strategist), whereas if S is much smaller than K_s, μ is controlled by K_s (K–strategist). Two component systems of an r– and a K– strategist can exhibit an idealized growth model as depicted in Figure 4-1 and Chudoba and colleagues argued based on their observation, that filamentous bacteria characteristically exhibit the K type of growth.

Summarizing these ideas up, a pleomorphic lifestyle of a K-strategist *Desulfosporosinus* growing in dialysis chambers in response to changing substrate regimes would be a fascinating explanation for the observations described. Moreover, a K-type strategy of life would be in line with the observation of SRM outcompeting methanogens for substrates at elevated sulfate concentrations due to higher substrate affinity (lower K_s)(Kristjansson and Schönheit, 1983; Lovley and Klug, 1983). Furthermore, determination whether the systems limiting compound is the substrate (carbon source) or sulfate is a key question. Experimental assessment of this hypothesis will not be straightforward as the identity of the substrate is unknown and this plasticity could not be observed in defined media so far. Reproducing this "behavior" in pure and mixed culture experiments followed by attempts to stimulate a given morphology by a factorial but constant modification of substrate concentration in a continuous culture setup can serve as the first step experiments to elucidate these phenomena in detail.

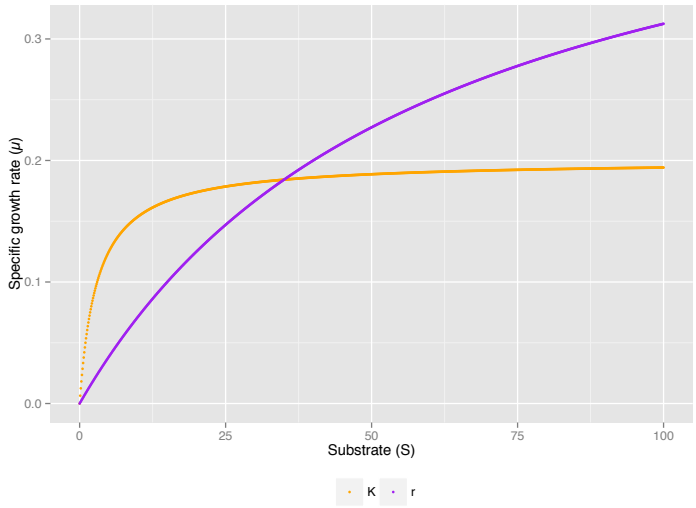

Figure 4-1
Simulated growth rates (based on Monod equation) for a two-component system of entity K (K_s=3, μ_{max}=0.2) and entity r (K_s=60, μ_{max}=0.5). Modified from (Chudoba et al., 1973).

Desulfosporosinus Iron and Sodium enrichments as candidate isolates

Evidence of FISH and phylogenetic analysis indicate that two different candidate isolates of novel *Desulfosporosinus* representatives could be obtained via dilution to extinction experiments. Raw 16S rRNA gene sequence dissimilarities to validately described *Desulfosporosinus* species as well as interspecific distances between *Iron* and *Sodium* isolates were above the propose minimum threshold of 98.65 % for species delineation (Kim et al., 2014). The observed difference between the candidate isolates is in line with observation of *Desulfosporosinus* 16S rRNA gene clone diversity determined in the previous SIP study of Schlöppnerbrunnen II soil (Pester et al., 2010).

An intriguing question would be, if the selective factor causing the separated enrichments of the two candidate isolates can be solely attributed to the differential amendment of sodiumsulfate and ironsulfate. Kumar et al., 2014 recently reported on a selective response of *Desulfosporosinus lacus* related bacteria in batch culture experiments were Fe(II) was provided in addition to sulfate and glycerol at low pH, accompanied by makinawite (FeS) formation. Interestingly, no response of *Desulfosporosinus* representatives could be observed without the amendment of iron particles. Due to the similar observations made here (e.g. presumably FeS formation, high similarity of candidate isolates to *D. lacus*) it seems compelling that iron exerts an important biogeochemical function and selects for a specific ecotype of *Desulfosporosinus*. A possibility would be the attenuation of the inhibitory effect of H_2S exerted at neutral pH for certain SRB (O'Flaherty et al., 1998; Okabe et al., 1995). H_2S toxicity can be ascribed to membrane transmittance of non dissociated entities (Colleran et al., 1995). Hypothetically, a scavenging mechanism based on FeS formation, which thus would divert the reaction equilibrium of H_2S dissociation towards the fully dissociated S^{2-} anion could be possible. On the contrary other SRM tolerate sulfide concentrations up to 10 mM (Rabus et al., 2006).

A crucial factor still to be verified is the purity of candidate isolates, which was so far only confirmed via 16S rRNA FISH and 16S rRNA gene sequencing of PCR products. At its best a purity of 99 % can be postulated based on the detection limit of FISH (Daims et al., 2005) and neglecting methodological biases that can cause false negative predictions for both PCR and FISH. Restriction digests of cloned 16S rRNA gene PCR

products could provide with a more sensitive approach to assess purity (Clement et al., 1998). The threat of a dormant contaminant can of course not be excluded. As a consequence, acquiring a clonal population with another iteration of the agarshake method, the soil agar combined with picking of mini colonies with a dissection microscope (Davis et al., 2011) or an overlay technique (Sen and Johnson, 1999) streaks seem imperative.

A first glimpse at the characteristic metabolic features would classify the isolates as incomplete substrate oxidizing SRB, that produce acetate according to a type I production mode(Gaden, 2000). The first stoichiometric estimates provided above are for sure heavily biased, however the non equimolar relationship between lactate consumption and acetate production is probably due to carbon loss in the process of growth and assimilation, as lactate was the single organic carbon source in the medium.

One of the hallmark features proposed for the rare biosphere member *Desulfosporosinus* representatives of Schlöppnerbrunnen II is the proposed capability to transform considerable amounts of carbon based on their estimated cell specific sulfate reduction rates (csSRR)(Pester et al., 2010). The csSRRs as estimated here are far below the proposed ones and within the average range reported for pure cultures under optimized conditions (Detmers et al., 2001). On the other side they are far above the maximum proposed csSRR for marine sediments of 0.1 fmol per cell per day (Bowles et al., 2014) and still can account for a substantial amount for SRR in the Schlöppnerbrunnen II system as it was already proposed (Pester et al., 2010).It has to be emphasized that a proper assessment of substrate usage of the candidate isolates remains to be done as the values provided here are heavily biased and would not be acceptable for a model. Ruther they can be used as a first orientation for subsequent proper assessment. Cell density was determined at a timepoint close to stationary growth, whereas growth rates were averaged across t_0 and t_{end} of incubations, which most likely underestimates the actual removal rates (no knowledge of lag phase and no real timepoint for sulfate approaching zero). Furthermore sulfate removal must be treated as a function of cell growth (exponential). Thus the provided values of csSRR are for sure underestimates.

To get an understanding of the metabolic profile of *Desulfosporosinus* SbII isolates, K_s and μ_{max} would have to be acquired in two sets of experiments where the limiting substrate is either constituted by sulfate or lactate (and thus treating it as substrate in the model). csSRR in exponential growth could then be assessed as it was describe by Detmers et al., 2001, which would allow a direct comparison against respective values, or as substrate consumption rates based on the Monod model of growth for a batch culture as described in Chmiel and Sonnleitner 2011 ($r_s=-(1/Y_{X/S})\times r_x$; r_s= substrate consumption rate, $Y_{X/S}$=Yield coefficient, r_x= cell production). In both cases sulfate would have to constitute the limiting substrate, as it wase performed here for the candidate isolates.

Assessing these parameters and extrapolating or even define them in more *in situ* like scenarios (e.g. a co-culture experiments with *Acidocella* strain PFBC (Jones et al., 2013)) will provide useful insights into the potential contribution of this rare biosphere member in modulating the carbon flow in these key ecosystems, potentially affecting global climate regimes. Moreover assessment of growth in acidic environments will eventually reveal their applicability for bioremediation processes and biotechnological applications.

4.3 pH dependent growth of *Desulfovibrio* sp. SII13a

Although there is ample evidence for SRM living in acidic environments (Johnson, 1995, 1998; Sánchez-Andrea et al., 2013), reports on truly acidophilic SRM (aSRM) isolates are scarce (Alazard et al., 2010b; Küsel et al., 2001; Mori et al., 2003). The lack of cultured aSRM is found to be attributed to the frequent use of organic acids as primary substrate in isolation efforts, which can impose toxic effects (Sánchez-Andrea et al., 2013). Within the genus *Desulfovibrio*, *D. bastinii* is found to be a moderately aSRM with a pH–growth optimum of 5.8 to 6.2.

Based on the data presented here, *Desulfovibrio* sp. SII13a cannot be defined as acidophilic. The maximum growth rates were centered at neutral pH, with only a minor decrease at a pH of 6. No growth could be observed at values below 5.2 which can be attributed to the decreased percentage of dissociation of lactate (< 95.6 % dissociated) and importantly the produced acetate (< 73.4 % dissociated) and thus depolarization of the cell membrane proton gradient (Supplementary table 8-8). A pH series experiment using glycerol as a substrate instead of lactate did not result in growth at any pH (data not shown).
The decrease in proton concentration by almost one order of magnitude was clearly linked to growth (Supplementary Figure 8-31). This effect is unwanted in the determination of growth rates as a function of pH (which should be the independent variable) and could for instance be avoided by the use of an appropriate buffering systems (e.g. Sörensen's citrate buffer (Alazard et al., 2010a)) or use of alginic acid to adjust pH (Pankratov and Dedysh, 2010b) without increasing ionic strength, as this factor can also be detrimental for certain microbes.
The changes in pH upon growth can be interpreted as a consequence of a proton-anion symport transport mechanism for sulfate, as it was proposed for *D. desulfuricans* (Cypionka, 1987), which thus increases extracellular pH. Another rationale would be due to overall changes in ratios of weak acids being present in the solute fraction. Upon total assimilation of lactate (pK_A= 3.9) and sulfate (presumably as sulfuric acid via the symport mechanism) equimolar amounts of acetate (pK_A=4.8) and H_2S (pK_{A1}=7.0) are produced, which can act as bases and thereby reduce proton concentrations.

Consequently, the isolate *Desulfovibrio* sp. SII13a might be regarded as being tolerant to mild acidic conditions, but not as an acidophilic SRM. This is however not contradictory to the parameters it can encounter in the its original fen habitat, as pH values here are found to be seasonally variable and peaking with values up to 6 (Küsel et al., 2008). It might therefore be an autochthonous member of the SRM community in this particular wetland, eventually being favored at conditions of higher pH.

5 References

Aiba, S., Shoda, M., and Nagatani, M. (1968). Kinetics of product inhibition in alcohol fermentation. Biotechnol. Bioeng. *10*, 845–864.

Alazard, D., Joseph, M., Battaglia-Brunet, F., Cayol, J.-L., and Ollivier, B. (2010a). Desulfosporosinus acidiphilus sp. nov.: a moderately acidophilic sulfate-reducing bacterium isolated from acid mining drainage sediments. Extremophiles *14*, 305–312.

Albertsen, M., Hugenholtz, P., Skarshewski, A., Nielsen, K.L., Tyson, G.W., and Nielsen, P.H. (2013). Genome sequences of rare, uncultured bacteria obtained by differential coverage binning of multiple metagenomes. Nat. Biotechnol. *31*, 533–538.

Alewell, C., Paul, S., Lischeid, G., and Storck, F.R. (2008). Co-regulation of redox processes in freshwater wetlands as a function of organic matter availability? Sci. Total Environ. *404*, 335–342.

Allègre, C., Manhès, G., and Lewin, É. (2001). Chemical composition of the Earth and the volatility control on planetary genetics. Earth Planet. Sci. Lett. *185*, 49–69.

Altschul, S.F., Gish, W., Miller, W., Myers, E.W., and Lipman, D.J. (1990). Basic local alignment search tool. J. Mol. Biol. *215*, 403–410.

Amann, R.I., Binder, B.J., Olson, R.J., Chisholm, S.W., Devereux, R., and Stahl, D.A. (1990). Combination of 16S rRNA-targeted oligonucleotide probes with flow cytometry for analyzing mixed microbial populations. Appl. Environ. Microbiol. *56*, 1919–1925.

Amend, A.S., Seifert, K.A., and Bruns, T.D. (2010). Quantifying microbial communities with 454 pyrosequencing: does read abundance count? Mol. Ecol. *19*, 5555–5565.

Angert, E.R., Clements, K.D., and Pace, N.R. (1993). The largest bacterium. Nature *362*, 239–241.

Ayers, G.P., and Cainey, J.M. (2007). The CLAW hypothesis: a review of the major developments. Environ. Chem. *4*, 366–374.

Baronofsky, J.J., Schreurs, W.J.A., and Kashket, E.R. (1984). Uncoupling by Acetic Acid Limits Growth of and Acetogenesis by Clostridium thermoaceticum. Appl. Environ. Microbiol. *48*, 1134–1139.

Benson, D.A., Cavanaugh, M., Clark, K., Karsch-Mizrachi, I., Lipman, D.J., Ostell, J., and Sayers, E.W. (2013). GenBank. Nucleic Acids Res. *41*, D36–D42.

Bertel, D., Peck, J., Quick, T.J., and Senko, J.M. (2012). Iron Transformations Induced by an Acid-Tolerant Desulfosporosinus Species. Appl. Environ. Microbiol. *78*, 81–88.

Blodau, C., Mayer, B., Peiffer, S., and Moore, T.R. (2007). Support for an anaerobic sulfur cycle in two Canadian peatland soils. J. Geophys. Res. Biogeosciences *112*, G02004.

Boetius, A., Ravenschlag, K., Schubert, C.J., Rickert, D., Widdel, F., Gieseke, A., Amann, R., Jørgensen, B.B., Witte, U., and Pfannkuche, O. (2000). A marine microbial consortium apparently mediating anaerobic oxidation of methane. Nature *407*, 623–626.

Bowles, M.W., Mogollón, J.M., Kasten, S., Zabel, M., and Hinrichs, K.-U. (2014). Global rates of marine sulfate reduction and implications for sub–sea-floor metabolic activities. Science *344*, 889–891.

Brankatschk, R., Bodenhausen, N., Zeyer, J., and Bürgmann, H. (2012). Efficiency of real-time qPCR depends on the template: a simple absolute quantification method correcting for qPCR efficiency variations in microbial community samples. Appl. Environ. Microbiol. AEM.07878–11.

Castro, H., Reddy, K.R., and Ogram, A. (2002). Composition and Function of Sulfate-Reducing Prokaryotes in Eutrophic and Pristine Areas of the Florida Everglades. Appl. Environ. Microbiol. *68*, 6129–6137.

Chen, K., Sun, G.W., Chua, K.L., and Gan, Y.-H. (2005). Modified Virulence of Antibiotic-Induced Burkholderia pseudomallei Filaments. Antimicrob. Agents Chemother. *49*, 1002–1009.

Chen, S., Wang, L., and Deng, Z. (2010). Twenty years hunting for sulfur in DNA. Protein Cell *1*, 14–21.

Chmiel, H., and Sonnleitner, B. (2011). Bioprozesstechnik (Spektrum Akademischer Verlag).

Chudoba, J., Grau, P., and Ottová, V. (1973). Control of activated-sludge filamentous bulking–II. Selection of microorganisms by means of a selector. Water Res. *7*, 1389–1406.

Clement, B.G., Kehl, L.E., DeBord, K.L., and Kitts, C.L. (1998). Terminal restriction fragment patterns (TRFPs), a rapid, PCR-based method for the comparison of complex bacterial communities. J. Microbiol. Methods *31*, 135–142.

Coates, J.D., Ellis, D.J., Gaw, C.V., and Lovley, D.R. (1999). Geothrix fermentans gen. nov., sp. nov., a novel Fe(III)-reducing bacterium from a hydrocarbon-contaminated aquifer. Int. J. Syst. Evol. Microbiol. *49*, 1615–1622.

Cole, J.R., Wang, Q., Fish, J.A., Chai, B., McGarrell, D.M., Sun, Y., Brown, C.T., Porras-Alfaro, A., Kuske, C.R., and Tiedje, J.M. (2014). Ribosomal Database Project: data and tools for high throughput rRNA analysis. Nucleic Acids Res. *42*, D633–D642.

Colleran, E., Finnegan, S., and Lens, P. (1995). Anaerobic treatment of sulphate-containing waste streams. Antonie Van Leeuwenhoek *67*, 29–46.

Conover, W.J., Johnson, M.E., and Johnson, M.M. (1981). A Comparative Study of Tests for Homogeneity of Variances, with Applications to the Outer Continental Shelf Bidding Data. Technometrics *23*, 351–361.

Cypionka, H. (1987). Uptake of sulfate, sulfite and thiosulfate by proton-anion symport in Desulfovibrio desulfuricans. Arch. Microbiol. *148*, 144–149.

Daims, H., Brühl, A., Amann, R., Schleifer, K.-H., and Wagner, M. (1999). The Domain-specific Probe EUB338 is Insufficient for the Detection of all Bacteria: Development and Evaluation of a more Comprehensive Probe Set. Syst. Appl. Microbiol. *22*, 434–444.

Daims, H., Stoeker, K., and Wagner, M. (2005). Fluorescence in situ hybridization for the detection of prokaryotes.

Daims, H., Lücker, S., and Wagner, M. (2006). daime, a novel image analysis program for microbial ecology and biofilm research. Environ. Microbiol. *8*, 200–213.

Dalsgaard, T., and Bak, F. (1994). Nitrate Reduction in a Sulfate-Reducing Bacterium, Desulfovibrio desulfuricans, Isolated from Rice Paddy Soil: Sulfide Inhibition, Kinetics, and Regulation. Appl. Environ. Microbiol. *60*, 291–297.

Darriba, D., Taboada, G.L., Doallo, R., and Posada, D. (2012). jModelTest 2: more models, new heuristics and parallel computing. Nat. Methods *9*, 772–772.

Davis, K.E.R., Sangwan, P., and Janssen, P.H. (2011). Acidobacteria, Rubrobacteridae and Chloroflexi are abundant among very slow-growing and mini-colony-forming soil bacteria. Environ. Microbiol. *13*, 798–805.

Detmers, J., Brüchert, V., Habicht, K.S., and Kuever, J. (2001). Diversity of Sulfur Isotope Fractionations by Sulfate-Reducing Prokaryotes. Appl. Environ. Microbiol. *67*, 888–894.

Dunn, O.J. (1961). Multiple Comparisons among Means. J. Am. Stat. Assoc. *56*, 52–64.

Edgar, R.C. (2004). MUSCLE: multiple sequence alignment with high accuracy and high throughput. Nucleic Acids Res. *32*, 1792–1797.

Fichtel, J., Köster, J., Rullkötter, J., and Sass, H. (2007a). Spore dipicolinic acid contents used for estimating the number of endospores in sediments. FEMS Microbiol. Ecol. *61*, 522–532.

Fichtel, J., Köster, J., Scholz-Böttcher, B., Sass, H., and Rullkötter, J. (2007b). A highly sensitive HPLC method for determination of nanomolar concentrations of dipicolinic acid, a characteristic constituent of bacterial endospores. J. Microbiol. Methods *70*, 319–327.

Frolking, S., Roulet, N., and Fuglestvedt, J. (2006). How northern peatlands influence the Earth's radiative budget: Sustained methane emission versus sustained carbon sequestration. J. Geophys. Res. Biogeosciences *111*, G01008.

Fuhrman, J.A. (2009). Microbial community structure and its functional implications. Nature *459*, 193–199.

Fukui, Teske, Assmus, Muyzer, and Widdel (1999). Physiology, phylogenetic relationships, and ecology of filamentous sulfate-reducing bacteria (genus desulfonema). Arch. Microbiol. *172*, 193–203.

Gaden, E.L. (2000). Fermentation process kinetics. Biotechnol. Bioeng. *67*, 629–635.

Gauci, V., Matthews, E., Dise, N., Walter, B., Koch, D., Granberg, G., and Vile, M. (2004). Sulfur

pollution suppression of the wetland methane source in the 20th and 21st centuries. Proc. Natl. Acad. Sci. U. S. A. *101*, 12583–12587.

Gemmell, R.T., and Knowles, C.J. (2000). Utilisation of aliphatic compounds by acidophilic heterotrophic bacteria. The potential for bioremediation of acidic wastewaters contaminated with toxic organic compounds and heavy metals. FEMS Microbiol. Lett. *192*, 185–190.

Gomez-Alvarez, V., Teal, T.K., and Schmidt, T.M. (2009). Systematic artifacts in metagenomes from complex microbial communities. ISME J. *3*, 1314–1317.

Hahn, D., Amann, R.I., Ludwig, W., Akkermans, A.D.L., and Schleifer, K.-H. (1992). Detection of micro-organisms in soil after in situ hybridization with rRNA-targeted, fluorescently labelled oligonucleotides. J. Gen. Microbiol. *138*, 879–887.

Hallberg, K.B., and Johnson, D.B. (2005). Microbiology of a wetland ecosystem constructed to remediate mine drainage from a heavy metal mine. Sci. Total Environ. *338*, 53–66.

Hartman, W.H., Richardson, C.J., Vilgalys, R., and Bruland, G.L. (2008). Environmental and anthropogenic controls over bacterial communities in wetland soils. Proc. Natl. Acad. Sci. *105*, 17842–17847.

Hausmann, B. (2012). Substrate utilisation of sulfate-reducing microorganisms in a peatland.pdf (University of Vienna).

Hausmann, B. (2014).

He, J., Luo, X., Chen, S., Cao, L., Sun, M., and Yu, Z. (2003). Determination of spore concentration in Bacillus thuringiensis through the analysis of dipicolinate by capillary zone electrophoresis. J. Chromatogr. A *994*, 207–212.

He, J.-Z., Liu, X.-Z., Zheng, Y., Shen, J.-P., and Zhang, L.-M. (2010). Dynamics of sulfate reduction and sulfate-reducing prokaryotes in anaerobic paddy soil amended with rice straw. Biol. Fertil. Soils *46*, 283–291.

Henstra, A.M., Dijkema, C., and Stams, A.J.M. (2007). Archaeoglobus fulgidus couples CO oxidation to sulfate reduction and acetogenesis with transient formate accumulation. Environ. Microbiol. *9*, 1836–1841.

Huang, X., and Madan, A. (1999). CAP3: A DNA Sequence Assembly Program. Genome Res. *9*, 868–877.

Huddleston, J., Ranade, S., Malig, M., Antonacci, F., Chaisson, M., Hon, L., Sudmant, P.H., Graves, T.A., Alkan, C., Dennis, M.Y., et al. (2014). Reconstructing complex regions of genomes using long-read sequencing technology. Genome Res. gr.168450.113.

Hungate, R.E. (1969). A roll tube method for cultivation of strict anaerobes. METHODS Microbiol. Vol. 3B *3*, 117.

Imachi, H., Sekiguchi, Y., Kamagata, Y., Loy, A., Qiu, Y.-L., Hugenholtz, P., Kimura, N., Wagner, M., Ohashi, A., and Harada, H. (2006). Non-sulfate-reducing, syntrophic bacteria

affiliated with desulfotomaculum cluster I are widely distributed in methanogenic environments. Appl. Environ. Microbiol. *72*, 2080–2091.

Johnson, D.B. (1995). Selective solid media for isolating and enumerating acidophilic bacteria. J. Microbiol. Methods *23*, 205–218.

Johnson, D.B. (1998). Biodiversity and ecology of acidophilic microorganisms. FEMS Microbiol. Ecol. *27*, 307–317.

Jones, R.M., Hedrich, S., and Johnson, D.B. (2013). Acidocella aromatica sp. nov.: an acidophilic heterotrophic alphaproteobacterium with unusual phenotypic traits. Extrem. Life Extreme Cond. *17*, 841–850.

Jørgensen, B.B. (1982). Mineralization of organic matter in the sea bed—the role of sulphate reduction. Nature *296*, 643–645.

Jørgensen, B.B., and Kasten, S. (2006). Sulfur Cycling and Methane Oxidation. In Marine Geochemistry, P.D.H.D. Schulz, and D.M. Zabel, eds. (Springer Berlin Heidelberg), pp. 271–309.

Juretschko, S., Timmermann, G., Schmid, M., Schleifer, K.-H., Pommerening-Röser, A., Koops, H.-P., and Wagner, M. (1998). Combined Molecular and Conventional Analyses of Nitrifying Bacterium Diversity in Activated Sludge: Nitrosococcus mobilis and Nitrospira-Like Bacteria as Dominant Populations. Appl. Environ. Microbiol. *64*, 3042–3051.

Juretschko, S., Loy, A., Lehner, A., and Wagner, M. (2002). The Microbial Community Composition of a Nitrifying-Denitrifying Activated Sludge from an Industrial Sewage Treatment Plant Analyzed by the Full-Cycle rRNA Approach. Syst. Appl. Microbiol. *25*, 84–99.

Justice, S.S., Hunstad, D.A., Seed, P.C., and Hultgren, S.J. (2006). Filamentation by Escherichia coli subverts innate defenses during urinary tract infection. Proc. Natl. Acad. Sci. U. S. A. *103*, 19884–19889.

Justice, S.S., Hunstad, D.A., Cegelski, L., and Hultgren, S.J. (2008). Morphological plasticity as a bacterial survival strategy. Nat. Rev. Microbiol. *6*, 162–168.

Kanokratana, P., Uengwetwanit, T., Rattanachomsri, U., Bunterngsook, B., Nimchua, T., Tangphatsornruang, S., Plengvidhya, V., Champreda, V., and Eurwilaichitr, L. (2011). Insights into the Phylogeny and Metabolic Potential of a Primary Tropical Peat Swamp Forest Microbial Community by Metagenomic Analysis. Microb. Ecol. *61*, 518–528.

Karnachuk, O.V., Gerasimchuk, A.L., Banks, D., Frengstad, B., Stykon, G.A., Tikhonova, Z.L., Kaksonen, A., Puhakka, J., Yanenko, A.S., and Pimenov, N.V. (2009). Bacteria of the sulfur cycle in the sediments of gold mine tailings, Kuznetsk Basin, Russia. Microbiology *78*, 483–491.

Kendall, M.M., Liu, Y., and Boone, D.R. (2006). Butyrate- and propionate-degrading syntrophs from permanently cold marine sediments in Skan Bay, Alaska, and description of Algorimarina butyrica gen. nov., sp. nov. FEMS Microbiol. Lett. *262*, 107–114.

Kibbe, W.A. (2007). OligoCalc: an online oligonucleotide properties calculator. Nucleic Acids Res. *35*, W43–W46.

Kim, M., Oh, H.-S., Park, S.-C., and Chun, J. (2014). Towards a taxonomic coherence between average nucleotide identity and 16S rRNA gene sequence similarity for species demarcation of prokaryotes. Int. J. Syst. Evol. Microbiol. *64*, 346–351.

Kimura, S., and Johnson, D.B. (2004). Sulfate reduction at low pH by a defined mixed culture of acidophilic bacteria (CRC Press).

Klüpfel, L., Piepenbrock, A., Kappler, A., and Sander, M. (2014). Humic substances as fully regenerable electron acceptors in recurrently anoxic environments. Nat. Geosci. *7*, 195–200.

Kniemeyer, O., Musat, F., Sievert, S.M., Knittel, K., Wilkes, H., Blumenberg, M., Michaelis, W., Classen, A., Bolm, C., Joye, S.B., et al. (2007). Anaerobic oxidation of short-chain hydrocarbons by marine sulphate-reducing bacteria. Nature *449*, 898–901.

Knorr, K.-H., and Blodau, C. (2009). Impact of experimental drought and rewetting on redox transformations and methanogenesis in mesocosms of a northern fen soil. Soil Biol. Biochem. *41*, 1187–1198.

Koch, A.L. (1966). Distribution of Cell Size in Growing Cultures of Bacteria and the Applicability of the Collins-Richmond Principle. J. Gen. Microbiol. *45*, 409–417.

Koch, A.L. (1990). Diffusion The Crucial Process in Many Aspects of the Biology of Bacteria. In Advances in Microbial Ecology, K.C. Marshall, ed. (Springer US), pp. 37–70.

Koch, A.L. (1996). WHAT SIZE SHOULD A BACTERIUM BE? A Question of Scale. Annu. Rev. Microbiol. *50*, 317–348.

Kolmert, Å., and Johnson, D.B. (2001). Remediation of acidic waste waters using immobilised, acidophilic sulfate-reducing bacteria. J. Chem. Technol. Biotechnol. *76*, 836–843.

Kristjansson, J.K., and Schönheit, P. (1983). Why Do Sulfate-Reducing Bacteria Outcompete Methanogenic Bacteria for Substrates? Oecologia *60*, 264–266.

Kulichevskaya, I.S., Suzina, N.E., Liesack, W., and Dedysh, S.N. (2010). Bryobacter aggregatus gen. nov., sp. nov., a peat-inhabiting, aerobic chemo-organotroph from subdivision 3 of the Acidobacteria. Int. J. Syst. Evol. Microbiol. *60*, 301–306.

Kumar, N., Omoregie, E.O., Rose, J., Masion, A., Lloyd, J.R., Diels, L., and Bastiaens, L. Inhibition of sulfate reducing bacteria in aquifer sediment by iron nanoparticles. Water Res.

Küsel, K., Roth, U., Trinkwalter, T., and Peiffer, S. (2001). Effect of pH on the anaerobic microbial cycling of sulfur in mining-impacted freshwater lake sediments. Environ. Exp. Bot. *46*, 213–223.

Küsel, K., Blöthe, M., Schulz, D., Reiche, M., and Drake, H.L. (2008). Microbial reduction of iron and porewater biogeochemistry in acidic peatlands. Biogeosciences Discuss. *5*, 2165–2196.

Lee, Y.-J., Romanek, C.S., and Wiegel, J. (2009). Desulfosporosinus youngiae sp. nov., a spore-forming, sulfate-reducing bacterium isolated from a constructed wetland treating acid mine

drainage. Int. J. Syst. Evol. Microbiol. *59*, 2743–2746.

Letunic, I., and Bork, P. (2011). Interactive Tree Of Life v2: online annotation and display of phylogenetic trees made easy. Nucleic Acids Res. *39*, W475–W478.

Limpens, J., Berendse, F., Blodau, C., Canadell, J.G., Freeman, C., Holden, J., Roulet, N., Rydin, H., and Schaepman-Strub, G. (2008). Peatlands and the carbon cycle: from local processes to global implications – a synthesis. Biogeosciences *5*, 1475–1491.

Liu, A., Garcia-Dominguez, E., Rhine, E.., and Young, L.. (2004). A novel arsenate respiring isolate that can utilize aromatic substrates. FEMS Microbiol. Ecol. *48*, 323–332.

Lovley, D.R., and Klug, M.J. (1983). Sulfate Reducers Can Outcompete Methanogens at Freshwater Sulfate Concentrations. Appl. Environ. Microbiol. *45*, 187–192.

Loy, A., Lehner, A., Lee, N., Adamczyk, J., Meier, H., Ernst, J., Schleifer, K.-H., and Wagner, M. (2002). Oligonucleotide Microarray for 16S rRNA Gene-Based Detection of All Recognized Lineages of Sulfate-Reducing Prokaryotes in the Environment. Appl. Environ. Microbiol. *68*, 5064–5081.

Loy, A., Küsel, K., Lehner, A., Drake, H.L., and Wagner, M. (2004). Microarray and Functional Gene Analyses of Sulfate-Reducing Prokaryotes in Low-Sulfate, Acidic Fens Reveal Cooccurrence of Recognized Genera and Novel Lineages. Appl. Environ. Microbiol. *70*, 6998–7009.

Lücker, S., Schwarz, J., Gruber-Dorninger, C., Spiek, E., Wagner, M., and Daims, H. (in preperation). Nitrotoga-like bacteria are previously unrecognized key nitrite oxidizers in full-scale wastewater treatment plants.

Lücker, S., Steger, D., Kjeldsen, K.U., MacGregor, B.J., Wagner, M., and Loy, A. (2007). Improved 16S rRNA-targeted probe set for analysis of sulfate-reducing bacteria by fluorescence in situ hybridization. J. Microbiol. Methods *69*, 523–528.

Ludwig, W., Strunk, O., Westram, R., Richter, L., Meier, H., Yadhukumar, Buchner, A., Lai, T., Steppi, S., Jobb, G., et al. (2004). ARB: a software environment for sequence data. Nucleic Acids Res. *32*, 1363–1371.

Madison, W.P., and Madison, D.R. (2011). Mesquite: a modular system for evolutionary analysis.

Mayeux, B., Fardeau, M.-L., Bartoli-Joseph, M., Casalot, L., Vinsot, A., and Labat, M. (2013). Desulfosporosinus burensis sp. nov., a spore-forming, mesophilic, sulfate-reducing bacterium isolated from a deep clay environment. Int. J. Syst. Evol. Microbiol. *63*, 593–598.

Meier, H., Amann, R., Ludwig, W., and Schleifer, K.H. (1999). Specific oligonucleotide probes for in situ detection of a major group of gram-positive bacteria with low DNA G + C content. Syst. Appl. Microbiol. *22*, 186–196.

De Mendiburu, F. (2014). A statistical analysis tool for agricultural research. National Engineering University, Lima Peru.

Miller, C.S., Baker, B.J., Thomas, B.C., Singer, S.W., and Banfield, J.F. (2011). EMIRGE: reconstruction of full-length ribosomal genes from microbial community short read sequencing data. Genome Biol. *12*, R44.

Monod, J. (1949). The Growth of Bacterial Cultures. Annu. Rev. Microbiol. *3*, 371–394.

Moraru, C., Lam, P., Fuchs, B.M., Kuypers, M.M.M., and Amann, R. (2010). GeneFISH – an in situ technique for linking gene presence and cell identity in environmental microorganisms. Environ. Microbiol. *12*, 3057–3073.

Mori, K., Kim, H., Kakegawa, T., and Hanada, S. (2003). A novel lineage of sulfate-reducing microorganisms: Thermodesulfobiaceae fam. nov., Thermodesulfobium narugense, gen. nov., sp. nov., a new thermophilic isolate from a hot spring. Extrem. Life Extreme Cond. *7*, 283–290.

Müller, A., Kjeldsen, K.U., Rattei, T., Pester, M., and Loy, A. (in preparation). Classifying the phylogenetic and environmental diversity of DsrAB-type dissimilatory (bi)sulfite reductases.

Musat, F., Galushko, A., Jacob, J., Widdel, F., Kube, M., Reinhardt, R., Wilkes, H., Schink, B., and Rabus, R. (2009). Anaerobic degradation of naphthalene and 2-methylnaphthalene by strains of marine sulfate-reducing bacteria. Environ. Microbiol. *11*, 209–219.

Muyzer, G., and Stams, A.J.M. (2008). The ecology and biotechnology of sulphate-reducing bacteria. Nat. Rev. Microbiol. *6*, 441–454.

Newman, D.K., Kennedy, E.K., Coates, J.D., Ahmann, D., Ellis, D.J., Lovley, D.R., and Morel, F.M.M. (1997). Dissimilatory arsenate and sulfate reduction in Desulfotomaculum auripigmentum sp. nov. Arch. Microbiol. *168*, 380–388.

Nielsen, L.P., Risgaard-Petersen, N., Fossing, H., Christensen, P.B., and Sayama, M. (2010). Electric currents couple spatially separated biogeochemical processes in marine sediment. Nature *463*, 1071–1074.

O'Flaherty, V., Mahony, T., O'Kennedy, R., and Colleran, E. (1998). Effect of pH on growth kinetics and sulphide toxicity thresholds of a range of methanogenic, syntrophic and sulphate-reducing bacteria. Process Biochem. *33*, 555–569.

Oduro, H., Alstyne, K.L.V., and Farquhar, J. (2012). Sulfur isotope variability of oceanic DMSP generation and its contributions to marine biogenic sulfur emissions. Proc. Natl. Acad. Sci. 201117691.

Okabe, S., Nielsen, P.H., Jones, W.L., and Characklis, W.G. (1995). Sulfide product inhibition of Desulfovibrio desulfuricans in batch and continuous cultures. Water Res. *29*, 571–578.

Okonechnikov, K., Golosova, O., and Fursov, M. (2012). Unipro UGENE: a unified bioinformatics toolkit. Bioinformatics bts091.

Pankratov, T.A., and Dedysh, S.N. (2010a). Granulicella paludicola gen. nov., sp. nov., Granulicella pectinivorans sp. nov., Granulicella aggregans sp. nov. and Granulicella rosea sp. nov., acidophilic, polymer-degrading acidobacteria from Sphagnum peat bogs. Int. J. Syst. Evol. Microbiol. *60*, 2951–2959.

Pankratov, T.A., Kirsanova, L.A., Kaparullina, E.N., Kevbrin, V.V., and Dedysh, S.N. (2012). Telmatobacter bradus gen. nov., sp. nov., a cellulolytic facultative anaerobe from subdivision 1 of the Acidobacteria, and emended description of Acidobacterium capsulatum Kishimoto et al. 1991. Int. J. Syst. Evol. Microbiol. *62*, 430–437.

Park, H.S., Lin, S., and Voordouw, G. (2008). Ferric iron reduction by Desulfovibrio vulgaris Hildenborough wild type and energy metabolism mutants. Antonie Van Leeuwenhoek *93*, 79–85.

Partanen, J.I., Juusola, P.M., and Minkkinen, P.O. (2003). Determination of stoichiometric dissociation constants of lactic acid in aqueous salt solutions at 291.15 and at 298.15 K. Fluid Phase Equilibria *204*, 245–266.

Paul, S., Küsel, K., and Alewell, C. (2006). Reduction processes in forest wetlands: Tracking down heterogeneity of source/sink functions with a combination of methods. Soil Biol. Biochem. *38*, 1028–1039.

Pernthaler, A., Pernthaler, J., and Amann, R. (2002). Fluorescence In Situ Hybridization and Catalyzed Reporter Deposition for the Identification of Marine Bacteria. Appl. Environ. Microbiol. *68*, 3094–3101.

Pester, M., Bittner, N., Deevong, P., Wagner, M., and Loy, A. (2010). A "rare biosphere" microorganism contributes to sulfate reduction in a peatland. ISME J. *4*, 1591–1602.

Pester, M., Knorr, K.-H., and Loy, A. (2012). Sulfate-reducing microorganisms in wetlands – fameless actors in carbon cycling and climate change. Front. Terr. Microbiol. *3*, 72.

Pfeffer, C., Larsen, S., Song, J., Dong, M., Besenbacher, F., Meyer, R.L., Kjeldsen, K.U., Schreiber, L., Gorby, Y.A., El-Naggar, M.Y., et al. (2012). Filamentous bacteria transport electrons over centimetre distances. Nature *491*, 218–221.

Plugge, C.M., Zhang, W., Scholten, J.C.M., and Stams, A.J.M. (2011). Metabolic Flexibility of Sulfate-Reducing Bacteria. Front. Microbiol. *2*.

Pruesse, E., Peplies, J., and Glöckner, F.O. (2012). SINA: Accurate high-throughput multiple sequence alignment of ribosomal RNA genes. Bioinformatics *28*, 1823–1829.

Quast, C., Pruesse, E., Yilmaz, P., Gerken, J., Schweer, T., Yarza, P., Peplies, J., and Glockner, F.O. (2012). The SILVA ribosomal RNA gene database project: improved data processing and web-based tools. Nucleic Acids Res. *41*, D590–D596.

R Core Team (2014). R: A Language and Environment for Statistical Computing.

Rabus, Hansen, Theo A, and Widdel, F. (2006). Dissimilatory Sulfate- and Sulfur-Reducing Prokaryotes (New York, NY: Springer New York).

Ramamoorthy, S., Sass, H., Langner, H., Schumann, P., Kroppenstedt, R.M., Spring, S., Overmann, J., and Rosenzweig, R.F. (2006). Desulfosporosinus lacus sp. nov., a sulfate-reducing bacterium isolated from pristine freshwater lake sediments. Int. J. Syst. Evol. Microbiol. *56*, 2729–2736.

Rappé, M.S., Connon, S.A., Vergin, K.L., and Giovannoni, S.J. (2002). Cultivation of the ubiquitous SAR11 marine bacterioplankton clade. Nature *418*, 630–633.

Robertson, W.J., Bowman, J.P., Franzmann, P.D., and Mee, B.J. (2001). Desulfosporosinus meridiei sp. nov., a spore-forming sulfate-reducing bacterium isolated from gasolene-contaminated groundwater. Int. J. Syst. Evol. Microbiol. *51*, 133–140.

Ronquist, F., and Huelsenbeck, J.P. (2003). MrBayes 3: Bayesian phylogenetic inference under mixed models. Bioinformatics *19*, 1572–1574.

Sánchez-Andrea, I., Stams, A.J.M., Amils, R., and Sanz, J.L. (2013). Enrichment and isolation of acidophilic sulfate-reducing bacteria from Tinto River sediments. Environ. Microbiol. Rep. n/a–n/a.

Sanger, F., Nicklen, S., and Coulson, A.R. (1977). DNA sequencing with chain-terminating inhibitors. Proc. Natl. Acad. Sci. U. S. A. *74*, 5463–5467.

Sarkar, D. (2008). Lattice: Multivariate Data Visualization with R (Springer New York).

Schlesner, H. (1994). The Development of Media Suitable for the Microorganisms Morphologically Resembling Planctomyces spp., Pirellula spp., and other Planctomycetales from Various Aquatic Habitats Using Dilute Media. Syst. Appl. Microbiol. *17*, 135–145.

Schmalenberger, A., Drake, H.L., and Küsel, K. (2007a). High unique diversity of sulfate-reducing prokaryotes characterized in a depth gradient in an acidic fen. Environ. Microbiol. *9*, 1317–1328.

Schulz, H.N., and Jørgensen, B.B. (2001). Big Bacteria. Annu. Rev. Microbiol. *55*, 105–137.

Sen, A.M., and Johnson, B. (1999). Acidophilic sulphate-reducing bacteria: candidates for bioremediation of acid mine drainage. In Process Metallurgy, R. Amils and A. Ballester, ed. (Elsevier), pp. 709–718.

Senko, J.M., Zhang, G., McDonough, J.T., Bruns, M.A., and Burgos, W.D. (2009). Metal Reduction at Low pH by a Desulfosporosinus species: Implications for the Biological Treatment of Acidic Mine Drainage. Geomicrobiol. J. *26*, 71–82.

Sievert, S., Kiene, R., and Schulz-Vogt, H. (2007). The Sulfur Cycle. Oceanography *20*, 117–123.

Smith, C.J., and Osborn, A.M. (2009). Advantages and limitations of quantitative PCR (Q-PCR)-based approaches in microbial ecology. FEMS Microbiol. Ecol. *67*, 6–20.

Sogin, M.L., Morrison, H.G., Huber, J.A., Welch, D.M., Huse, S.M., Neal, P.R., Arrieta, J.M., and Herndl, G.J. (2006). Microbial diversity in the deep sea and the underexplored "rare biosphere."Proc. Natl. Acad. Sci. *103*, 12115–12120.

Sousa, D.Z., Smidt, H., Alves, M.M., and Stams, A.J.M. (2007). Syntrophomonas zehnderi sp. nov., an anaerobe that degrades long-chain fatty acids in co-culture with Methanobacterium formicicum. Int. J. Syst. Evol. Microbiol. *57*, 609–615.

Spring, S. (2006). Preservation of Thermophilic Microorganisms. METHODS Microbiol. *38*.

Spring, S., and Rosenzweig, F. (2006). The Genera Desulfitobacterium and Desulfosporosinus:Taxonomy (New York, NY: Springer US).

Stackebrandt, E., Sproer, C., Rainey, F.A., Burghardt, J., Päuker, O., and Hippe, H. (1997). Phylogenetic Analysis of the Genus Desulfotomaculum: Evidence for the Misclassification of Desulfotomaculum guttoideum and Description of Desulfotomaculum orientis as Desulfosporosinus orientis gen. nov., comb. nov. Int. J. Syst. Bacteriol. *47*, 1134–1139.

Steger, D. (2010). Community structure and distribution of functional microbial groups within two complex environments. University of Vienna.

Steger, D., Wentrup, C., Braunegger, C., Deevong, P., Hofer, M., Richter, A., Baranyi, C., Pester, M., Wagner, M., and Loy, A. (2011). Microorganisms with Novel Dissimilatory (Bi)Sulfite Reductase Genes Are Widespread and Part of the Core Microbiota in Low-Sulfate Peatlands. Appl. Environ. Microbiol. *77*, 1231–1242.

Steinberger, R.E., Allen, A.R., Hansa, H.G., and Holden, P.A. (2002). Elongation correlates with nutrient deprivation in Pseudomonas aeruginosa-unsaturates biofilms. Microb. Ecol. *43*, 416–423.

Stoecker, K., Dorninger, C., Daims, H., and Wagner, M. (2010). Double Labeling of Oligonucleotide Probes for Fluorescence In Situ Hybridization (DOPE-FISH) Improves Signal Intensity and Increases rRNA Accessibility. Appl. Environ. Microbiol. *76*, 922–926.

Tamura, K., Peterson, D., Peterson, N., Stecher, G., Nei, M., and Kumar, S. (2011). MEGA5: Molecular Evolutionary Genetics Analysis Using Maximum Likelihood, Evolutionary Distance, and Maximum Parsimony Methods. Mol. Biol. Evol. *28*, 2731–2739.

Vairavamurthy Murthy A., Orr Wilson L., and Manowitz Bernard (1995). Geochemical Transformations of Sedimentary Sulfur: An Introduction. In Geochemical Transformations of Sedimentary Sulfur, (American Chemical Society), pp. 1–14.

Vatsurina, A., Badrutdinova, D., Schumann, P., Spring, S., and Vainshtein, M. (2008). Desulfosporosinus hippei sp. nov., a mesophilic sulfate-reducing bacterium isolated from permafrost. Int. J. Syst. Evol. Microbiol. *58*, 1228–1232.

Vos, P., Garrity, G., Jones, D., Krieg, N.R., Ludwig, W., Rainey, F.A., Schleifer, K.-H., and Whitman, W.B. (2011). Bergey's Manual of Systematic Bacteriology: Volume 3: The Firmicutes (Springer).

Wächtershäuser, G. (1990). Evolution of the first metabolic cycles. Proc. Natl. Acad. Sci. *87*, 200–204.

Wagner, M., Roger, A.J., Flax, J.L., Brusseau, G.A., and Stahl, D.A. (1998). Phylogeny of Dissimilatory Sulfite Reductases Supports an Early Origin of Sulfate Respiration. J. Bacteriol. *180*, 2975–2982.

Wagner, M., Loy, A., Klein, M., Lee, N., Ramsing, N.B., Stahl, D.A., and Friedrich, M.W. (2005). Functional marker genes for identification of sulfate-reducing prokaryotes. Methods Enzymol.

397, 469–489.

Wallner, G., Amann, R., and Beisker, W. (1993). Optimizing fluorescent in situ hybridization with rRNA-targeted oligonucleotide probes for flow cytometric identification of microorganisms. Cytometry *14*, 136–143.

Ward, N.L., Challacombe, J.F., Janssen, P.H., Henrissat, B., Coutinho, P.M., Wu, M., Xie, G., Haft, D.H., Sait, M., Badger, J., et al. (2009). Three Genomes from the Phylum Acidobacteria Provide Insight into the Lifestyles of These Microorganisms in Soils. Appl. Environ. Microbiol. *75*, 2046–2056.

Weber, K.A., Achenbach, L.A., and Coates, J.D. (2006). Microorganisms pumping iron: anaerobic microbial iron oxidation and reduction. Nat. Rev. Microbiol. *4*, 752–764.

Wickham, H. (2009). ggplot2: elegant graphics for data analysis (Springer New York).

Widdel, F., and Bak, F. (1991). Gram-Negative Mesophilic Sulfate-Reducing Bacteria (Springer New York).

Widdel, F., Kohring, G.-W., and Mayer, F. (1983). Studies on dissimilatory sulfate-reducing bacteria that decompose fatty acids. Arch. Microbiol. *134*, 286–294.

Wieder, R.K., Yavitt, J.B., and Lang, G.E. (1990). Methane production and sulfate reduction in two Appalachian peatlands. Biogeochemistry *10*, 81–104.

Wuebbles, D.J., and Hayhoe, K. (2002). Atmospheric methane and global change. Earth-Sci. Rev. *57*, 177–210.

Yilmaz, L.S., Parnerkar, S., and Noguera, D.R. (2011). mathFISH, a Web Tool That Uses Thermodynamics-Based Mathematical Models for In Silico Evaluation of Oligonucleotide Probes for Fluorescence In Situ Hybridization. Appl. Environ. Microbiol. *77*, 1118–1122.

Young, K.D. (2006). The Selective Value of Bacterial Shape. Microbiol. Mol. Biol. Rev. *70*, 660–703.

Zarda, B., Hahn, D., Chatzinotas, A., Schönhuber, W., Neef, A., Amann, R.I., and Zeyer, J. (1997). Analysis of bacterial community structure in bulk soil by in situ hybridization. Arch. Microbiol. *168*, 185–192.

Zaritsky, A. (1975). On dimensional determination of rod-shaped bacteria. J. Theor. Biol. *54*, 243–248.

Zhou, X., He, X., Liang, J., Li, A., Xu, T., Kieser, T., Helmann, J.D., and Deng, Z. (2005). A novel DNA modification by sulphur. Mol. Microbiol. *57*, 1428–1438.

6 Abstract

Wetland ecosystems can act as important vectors directing global climate via sequestration of recalcitrant carbon. On the opposite many of these environments have been demonstrated to emit substantial quantities (10 to 20 % of the total global emission) of the greenhouse gas methane. Microorganisms are major components catalyzing the degradation of organic matter in wetland ecosystems. In the past decade, evidence accumulated that dissimilatory sulfate reducing microorganisms (SRM) constitute an important functional building block in anoxic freshwater ecosystems

Assessments of SRM in the acidic fen peatland Schlöppnerbrunnen (Bavaria, Germany), by employing 16S rRNA and dissimilatory (bi)sulfite reductase (*dsrAB*) gene sequence information, suggested for a yet undiscovered diversity of this guild *in situ*. In particular, 53 *dsrAB* species level operational taxonomic units (OTUs) had been proposed with OTU1 and 2 accounting for 1 to 2 % of the total bacterial abundance in the system. These core taxa potentially exert an influential function on the anoxic degradation of carbon in the peatland, however their physiological profile is not known so far. Using stable isotope DNA probing a previous study proposed only a low abundance (0.006 % of the total microbial community) rare biosphere *Bacterium* associated with the genus *Desulfosporosinus*to to actively respire sulfate in anoxic soil slurry incubations of Schlöppnerbrunnen soil at rates of 341 fmol per cell per day. As a consequence, this novel *Desulfosporosinus* species could be a key player in the trophic chain of wetlands.

This work describes the assessment of the response in gene abundance of three *dsrAB* OTUs (1, 2 and 6) to anoxic conditions in soil slurry incubations from Schlöppnerbrunnen II soil in a factorial variation of carbon source and sulfate amendments for a time period of 51 days via qPCRquantification of the respective genes. In addition the change in abundance of acidobacterial subdivisions 1, 2 and 3, which constitute also a dominant fraction of the autochthonous fen microbial community was investigated in these incubations.
Second, a targeted enrichment strategy for the novel *Desulfosporosinus* species, using culture dependent techniques in combination with a specific screening assay, based on 16S rRNA gene fluorescence in situ hybridization (FISH) and a constrained metabolic profiling based on capillary electrophoresis is described.

OTUs 1, 2 and 6 exhibited no clear positive response to any of the substrate variations. While OTU1 and 6 showed a decrease in abundance for the incubation time, OTU 2 could maintain its population density and in some cases exhibited an increase in abundance towards the end of the incubation. No clear distinction between sulfate amended and non-amended microcosms could be drawn, although a trend towards higher abundance could be observed in non-amended entities. Analysis of the acidobacterial community could confirm the previous findings of their dominance in this type of ecosystem and also suggested for a high tolerancein situations of prolonged anoxia.

Using a series of different enrichment strategies, it was possible to enrich for *Desulfosporosinus* cells using either butyrate or lactate as carbon source under anoxic conditions, with sulfate being the only electron acceptor available. Two novel candidate isolates could be acquired that could represent novel species representatives within the genus *Desulfosporosinus* based on 16S rRNA sequence dissimilarity to type strains. Both isolates were able to incompletely oxidize lactate and were probably separated during enrichment attempts via a differential amendment of either sodium or ironsulfate. A K-type

of growth is proposed for the novel isolates based on substrate utilization profiles and the observed pleomorphic lifestyle.

7 Zusammenfassung

Feuchtgebiete als Ökosysteme nehmen eine Schlüsselposition in der Regulierung des globalen Klimas ein und stellen essentielle Speicher von rekalzitrantem Kohlestoff dar. Es wird davon ausgegangen, dass sie zwischen 10 und 20 % zur totalen globalen Methanemission beitragen. Mikroorganismen sind Schlüsselentitäten im Abbau von organischem Material in diesem System und ihre Interaktion mit den vorherrschenden biogeochemischen Regime determiniert das Schicksal der enthaltenen Kohlenstoffverbindungen. Im Laufe des letzten Jahrzehntes wurden vermehrt Indizien für die direkte Einbindung von Sulfat reduzierenden Mikroorganismen (SRM), als katalytische Einheiten in anoxischen Abbauprozessen in Feuchtgbieten gefunden.
Durch die Informationenaus 16S rRNA und dissimillatorischer (Bi)Sulfit Reductase (*dsrAB)* Gensequenz Unterschieden wurde es möglich, die nicht kultivierbare Fraktion von SRM in einem saurem Flachmoor – Torfland System (Schlöppnerbrunnen, Bayern, Deutschland) molekularbiologisch zu untersuchen. Dadurch konnte eine, bis - dato unbekannte Biodiversität dieser funktionellen Gilde *in situ* aufgezeigt werden.
53 *dsrAB* Spezies level "operational taxonomic units" (OTUs) wurden postuliert, von denen OTU1 und 2 zwischen ein bis zwei Prozent der totalen bakteriellen und archaeellen Abundanz darstellen. Diese OTUs könnten, ob ihrer hohen Abundanz, eine Schlüsselrolle im anoxischen Abbau von Kohlenstoff in diesem Torfland-Ökosystem einnehmen. Eine definitive physiologische Klassifizierung konnte bislang jedoch nicht erreicht werden.
Die Applikation von "stable isotope DNA probing" in einer vorangegangenen Studie konnte nur ein wenig abundantes (0.006 % der totalen mikrobiellen Gemeinschaft) "rare biosphere" Bakterium, welches dem Genus *Desulfosporosinus* zugehörig ist, als aktiven Sulfat Veratmer in anoxischen Boden – Schlamm Inkubationen vom Schlöppnerbrunnen Standort identifizieren. Aufgrund der extrapolierten hohen zellspezifischen Sulfatreduktionsrate von 341 fmol pro Zelle pro Tag, könnte diese neue *Desulfosporosinus* Spezies eine Schlüsselposition im Nahrungsnetz von Feuchtgebieten einnehmen.
Die hier vorgestellte Arbeit beschreibt die Analyse der Anwort (in Dimensionen von relativen Gen Abundanzen) von drei *dsrAB* OTUs (1, 2 und 6) auf anoxische Bedingungen in Boden – Schlamm Inkubationen von Schlöppnerbrunnen II Boden in einer faktoriellen Variation von Kohlenstoffquellen und Sulfatzugaben über einen Zeitraum von 51 Tagen mittels qPCR Quantifizierung der jeweiligen Gene. Zusätzlich wurde die Häufigkeit von drei taxonomischen Subeinheiten der Acidobakterien (1, 2 und 3), welche die häufigste bakterielle Gruppe der autochthonen mikrobiellen Gemeinschaft des Flachmoors darstellt, im identischen Inkubationssetup untersucht.
Weiters, wird eine eine gezielte Anreicherungsstrategie für die neue *Desulfosporosinus* Spezies, basierend auf kultivierungsabhängigen Techniken in Verbindung mit einem spezifischen Screening Verfahren mittels 16S rRNA gene Fluoreszenz *In Situ* Hybridisierung und einer eingeschränkten metabolischen Charakterisierung anhand von Kapillarelektrophorese beschrieben.
OTUs 1, 2 und 6 zeigten keine eindeutige positive Antwort auf die auferlegten Substrat – Sulfate Regime. Im Gegensatz zu OTU1 und 6, welche eine konsistente Verminderung der Abundanz für den Inkubationszeitraum aufwiesen, konnte OTU 2 seine anfängliche

Populationsdichte in manchen Szenarios aufrechterhalten, beziehungsweise gegen Ende der Inkubation sogar erhöhen. Ein offensichichtlicher Unterschied zwischen Sulfatinkubationen und jenen ohne Sulfat konnte nicht beobachtet werden. Die Analyse der acidobakteriellen Populationsdynamik konnte vorherige Indizien einer dominaten Acidobakterien Fraktion in diesen Ökosystem untermauern und suggeriert deren hohe Toleranz für anhaltende anoxische Bedingungen im Torfboden.
Durch eine Reihe verschiedener Kultivierungsstrategien war es möglich, *Desulfosporosinus* Zellen in definierten Medien mit Butyrat oder Laktat als Kohlenstoffquelle und Sulfat als alleinigen Elektronenakzeptor anzureichern. Zwei neue Kandidaten-Isolate konnten dadurch erhalten werden, welche basierend auf 16S rRNA DNA Sequenzunterschieden zu den bislang gültig beschrieben *Desulfosporosinus* Vertretern, neue Arten innerhalb dieser Gattung darstellen könnten. Beide Isolate zeigten Muster einer unvollständigen Oxidation von Laktat mittels Sulfat und wurden vermutlich während den Anreicherungen aufgrund einer getrennten Zugabe von Natrium - beziehungsweise Eisensulfat selektiert. Für diese neuen Isolate wird ein K–Typ des Wachstums, basierend auf Substratverwendungsmustern und der beobachteten Pleomorphie postuliert.

Acknowledgements

First and foremost I would like to thank Bela Hausmann for his guidance and constant supervision. He always discussed and outlined the next steps for experiments with me, analyzed the results very thoroughly and motivated me when it was necessary. Bela introduced me into the world of science, spent numerous hours proofreading and discussing my presentations and always took care for a good spirit with his sense of humor. I am really grateful for the time spending together with such a dedicated scientist and the numerous techniques he introduced me to.

Second, I'd like to express my gratitude to our group PI, Alexander Loy for giving me the chance and the trust to do my masterthesis in this project at DOME, which I always wanted to do. Thank you especially for discussing results together and for the valuable and honest feedback on my work. Also a thank you to Michael Pester our project leader for his encouragement.
I also want to thank Alexander Galushko, who shared his profound expertise in cultivation techniques and microbial physiology with me, which was a grate honor for me. He always had paid attention to my questions and helped me whenever I asked.

A big thank you to all DOME members especially my Master student friends. I wouldn't have managed to enjoy this time as much without the "free association dialogs" at the patio, swallowing exorbitant amounts of coffee, satisfying my urges for sausages, incorporating some Budweiser beer and smoking cigarettes to calm down together.

Of course I thank my parents. For accepting each of my decisions, for their trust and for their support which made me experience my time at university without pressure.

Finally I want to thank my girlfriend Daniela. For accepting the long time being physically separated, for her motivation, and for the experiences we shared together. Thank you also for all the help in my studies, for keeping me on track and being with me for all of those years.

8 Supplementary

8.1 Supplementary material and methods

8.1.1 qPCR

Supplementary table 8-1
Reaction mixture per one reaction of *Acidobacteria* targeted qPCR assays. DNA concentration applies to biological samples not for qPCR standards. For no template controls PCR grade water was used instead of template DNA.

Component	Manufacturer	Volume (µl)	Concentration in final reaction volume
2× iQ™ SYBR® Green Supermix	Bio-Rad Laboratories	12.5	1×
Primer Forward	Thermo Scientific	0.25	1 µM
Primer Reverse	Thermo Scientific	0.25	1 µM
Template DNA	—	10	0.1 ngµl^{-1}
PCR grade water	Fresnius	2	—

Supplementary table 8-2
Reaction mixture per reaction of *dsrA* targeted qPCR assays. DNA concentration applies to biological samples not for qPCR standards. For no template controls PCR grade water was used instead of template DNA. Note that for qPCR assays of day 27 the reaction was scaled to a volume of 50 µl.

Component	Manufacturer	Volume (µl)	Concentration in final reaction volume
2× iQ™ SYBR® Green Supermix	Bio-Rad Laboratories	12.5	1×
Primer Forward	Thermo Scientific	0.125	0.250 µM
Primer Reverse	Thermo Scientific	0.125	0.250 µM
Template DNA	—	10	0.1 ngµl^{-1}
PCR grade water	Fresnius	2.25	—

Supplementary table 8-3
Reaction mixture per reaction for M13 PCR.
Primer sequences: M13 F: GTA AAA CGA CGG CCA G / M13 R: CAG GAA ACA GCT ATG AC

Component	Manufacturer	Volume (µl)	Concentration in final reaction volume
10× Taq Buffer with KCL	Thermo Scientific	10	1×
dNTP Mix, 2mM each	Thermo Scientific	10	0.2 mM
MgCl2	Thermo Scientific	8	2 mM
BSA	Thermo Scientific	0.5	0.1 mg ml^{-1}
M13 forward	Thermo Scientific	2	1 µM
M13 reverse	Thermo Scientific	2	1 µM
Taq DNA Polymerase (recombinant)	Thermo Scientific	0.5	0.025 U µl^{-1}
Template DNA	—	2.5	—
PCR grade water	Fresnius	64.5	—

Supplementary table 8-4
Thermal cycling protocol of *Acidobacteria* qPCR assays. Primer annealing temperatures are given for Subdivision 1/ 2 and 3 respectively.

Step	Temperature (°C)	Time (min)	Iterations	Notes
Initial denaturation	94	3:00	1×	
Denaturation	94	0:40		
Annealing	68.5/ 62.5/ 69	0:40	45 ×	
Elongation	72	0:40		
Denaturation	94	1:00	1×	
Cool down	55	1:00	1×	
Melt Curve Analysis	55 – 95	0:10	80 ×	Meltcurve analysis (+0.5 °C increments)

Supplementary table 8-5
Thermal cycling protocol of *dsrA* qPCR assays

Step	Temperature (°C)	Time (min)	Iterations	Notes
Initial denaturation	95	5:00	1×	
Denaturation	95	0:40		
Annealing	64	0:30	45 ×	
Elongation	72	0:40		
Denaturation	95	1:00	1×	
Cool down	55	1:00	1×	
Melt Curve Analysis	55 – 95	0:10	80 ×	Meltcurve analysis (+0.5 °C increments)

Supplementary table 8-6
Thermal cycling protocol for M13 PCR reactions used for amplifying qPCR standards from plasmid DNA.

Step	Temperature (°C)	Time (min)	Iterations
Initial denaturation	95	3:00	1×
Denaturation	95	0:30	
Annealing	60	0:30	35 ×
Elongation	72	1:45	
Final Elongation	72	10:00	1×
Final Hold	12	∞	

Supplementary table 8-7
Primer and clones used for 16S rRNA gene *Acidobacteria* and *dsrA* gene qPCR assays.

Primer	Sequence (5' – 3')	Length (bp)	Target Gene	Target Group	Primer Reference	Template used for as standard (Accesion no.)	Internal clone ID	Vector
DsrA243Fa DsrA561Ra	CAC CAC CAC CGA TGA ACT ATA GGC CTT BAC YGC GGC C	18 19	*dsrA*	OTU 1	(Steger et al., 2011)	AY167473	dsrSbI-59	pCR®– XL-TOPO®
DsrA243Fb DsrA561Rb	CAC GAC CAC CGA TCA GCT GTA CTT GGT CAS TTC GGC C	18 19	*dsrA*	OTU 2	(Steger et al., 2011)	AY167467	dsrSbII-3	pCR®– XL-TOPO®
DsrA216F DsrA561Re	CUC AAC GGG AGA CAU CGU U ATA GGC TTT GAC CGC TGC C	19 19	*dsrA*	OTU 6	(Steger et al., 2011)	AY167466	dsrSbI-54	pCR®– XL-TOPO®
Acid303Fa Acid657R	GCG CAC GGM CAC ACT GGA ATT CCA CKC ACC TCT CCC AY	18 19	16S rRNA	*Acidobacteria* Subdivision 1	(Steger et al., 2011)	—	p4k3f	pCR®– XL-TOPO®
Acid702Fa Acid805R	AGA TAT CTG CAG GAA CAY CC CTG ATS GTT TAG GGC TAG	20 18	16S rRNA	*Acidobacteria* Subdivision 2	(Steger et al., 2011)	—	p4k4f	pCR®– XL-TOPO®
Acid306F Acid493R	CAC GGC CAC ACT GGC AC AGT TAG CCG CAG CTK CTT CT	18 20	16S rRNA	*Acidobacteria* Subdivision 3	(Steger et al., 2011)	—	p2k11f	pCR®– XL-TOPO®
1389Fmix 1492R	TG YAC ACA CCG CCC GT GGY TAC CTT GTT ACG ACT T	16 16	16S rRNA	*Bacteria* and *Archaea*	(Loy et al., 2002)	—	*Syntrophobacter wolinii* 16S rRNA gene	—

Supplementary table 8-8
Theoretical relative percentage of dissociated short chain fatty acids and lactate (A^-)at a given pH value, as calculated from the theoretical alpha value. pH values provided here were either imposed in the "*Desulfovibrio* pH range" experiment or in the three basal media for the "*Desulfosporosinus* defined media array" experiment. pH values are highlighte in bold numbers. Underlined values for pH 4.5 , 5.6 and 7.1 correspond to the aSRB, DSMZ 1250 and freshwater medium respectively.

Substance	pKA	pH												
		1.8	**2.4**	**3.4**	**4.1**	**4.4**	***4.5***	**5.2**	***5.6***	**5.9**	**6.1**	**6.4**	**7**	***7.1***
Acetatic acid	4.76	0.1	0.4	4.2	18.0	30.4	*35.5*	73.4	*87.4*	93.2	95.6	97.8	99.4	*99.5*
Propionic acid	4.88	0.1	0.3	3.2	14.2	24.9	*29.4*	67.6	*84.0*	91.3	94.3	97.1	99.2	*99.4*
Lactic acid	3.86	0.9	3.4	25.7	63.5	77.6	*81.4*	95.6	*98.2*	99.1	99.4	99.7	99.9	*99.9*
Butyric acid	4.82	0.1	0.4	3.7	16.0	27.5	*32.4*	70.6	*85.8*	92.3	95.0	97.4	99.3	*99.5*

For calculation of % dissociation into A^- for a particular SCFA, the Henderson - Hasselbalch equation in combination with the standard pK_a of the particular acid was used to calculate the degree of dissociation ($[A^-]/[HA]$) α according to Supplementary equation 8-1. α can be expressed as change (x) in the reaction equilibrium assuming equimolar distributions (0.5/0.5) of $[A^-]$ and [HA] Supplementary equation 8-2. Transformation of Supplementary equation 8-2 to x yields the percentage of A^- in solution (0.5 + x)×100 (Supplementary equation 8-3)

Supplementary equation 8-1

$$\propto = \frac{[A^-]}{[HA]} = 10^{pH-pK_a}$$

Supplementary equation 8-2

$$\propto = \frac{0.5 + x}{0.5 - x}$$

Supplementary equation 8-3

$$\%A^- = \left(\frac{0.5 \propto -0.5}{1+\propto} + 0.5\right) \times 100$$

8.1.2 Isolation and growth conditions

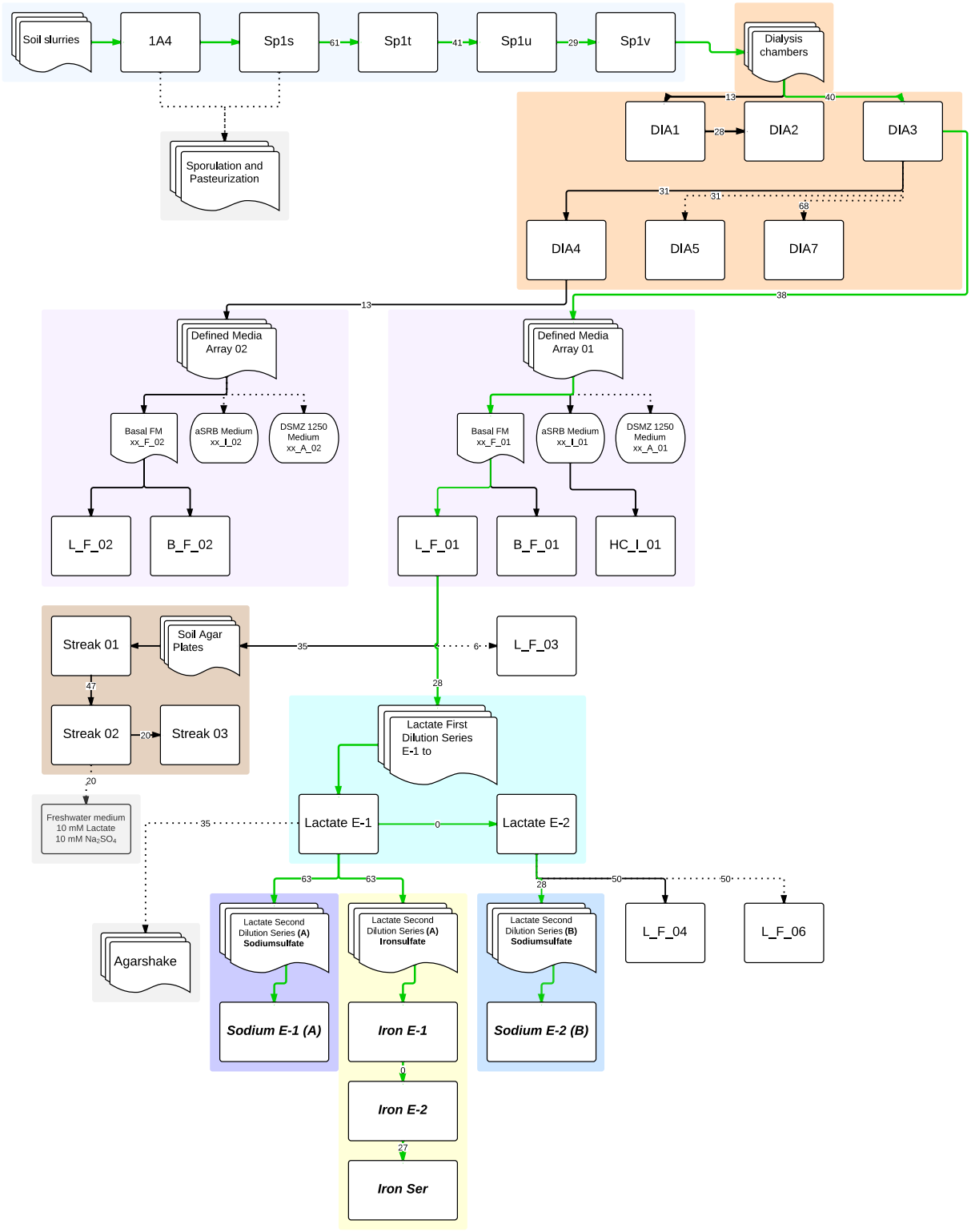

Figure 8-1

Genealogy of enrichments targeting the *Desulfosporosinus* population from Schlöppnerbrunnen II. Boxes indicate individual cultivation entities. Folders indicate experimental approaches. Arrows indicate the direction of subcultivation. Green solid lines indicate the paths that led to the candidate isolates. Solid black lines indicate an enrichment of *Desulfosporosinus* against the background of bacterial cells. Dashed lines indicate growth of *Desulfosporosinus* cells, but no enrichment. Note, that for the defined media array only subselections of media substrate combinations that exhibited reasonable growth of the target are shown. Numbers within lines indicate incubation time of the inoculum.

Pasteurization workflow:
All steps described were performed in Hungate tubes, using sterile anoxic technique. For all setups basal FM was used. After pasteurization basal FM with a sulfate concentration of 5 mM was amended to the vials.
Prior pasteurization steps:
The soil crust, resulting from the desiccation approach was suspended in basal FM and supplemented with four glass plating beads. The sealed tube was subsequently vortexed until a coarse suspension had formed. 8 ml of basal FM were added to the exhaustion approach vial and to 2 ml of Sp1s soil slurry respectively. The vial of the resuspension approach was already incubated in volume of 10 ml basal FM. For each of the subsequent treatment-specimen combination, approximately 1 g of autoclaved soil was added to a Hungate tube together with 2.2 ml of the respective spore specimen. Tubes were sealed anoxically.
Pasteurization:
Pasteurization was performed in a water bath at the conditions provided in Supplementary table 8-9. Special care was taken, that the entire tube was submersed in the water phase.
Posterior pasteurization steps:
Tubes were imposed to three iterations of short vacuum followed by flushing with N_2/CO_2 gas. Final pressure was adjusted to approximately 0.2 bar. When tubes were at room temperature 10 ml of the final FM were added respectively, gently inverted and sampled for capillary electrophoresis.

Dialysis chambers:
Dialysis tubing was cut to a length of 15 cm and autoclaved in 50 ml of milli-Q water for 10 min at 121 °C. The tubing was directly processed after autoclaving. A pair of autoclaved cotton wool threads wrapped in aluminum foil was used to seal dialysis tubing at the ends (double overhand knot-using two sterile forceps). The setup of dialysis chambers as described here, takes one week of time, until they are ready to be inoculated.
It is advisable to train the procedure (making knots with tweezers, avoiding contamination, making proper seals) in advance. All manipulations of dialysis tubings were performed in single use sterile petri dishes (Cat. No. 632102, Greiner bio-one, Austria), maintaining standard microbial sterile procedures.
Approximately 3 ml of sieved (2 mm particle size), twice autoclaved moist soil were transferred with a sterile spatula into the barrel of a 3 ml syringe (Cat. No. 4616025 V, B.Braun Omnifix® Luer Lock) having the plunger removed. Subsequently the plunger was attached again to the rest of the syringe. The dialysis tubing was sealed at one end and pulled over the syringe. Soil was pressed into the sealed tubing, taking care that the tubing was filled to capacity at the sealed end. Subsequently the syringe was removed and the soil fraction was rolled towards the opposite end (leaving 5 cm from the open end) using a sterile drigalski spatula to increase the surface of the soil fraction interacting with the membrane (approximate dimensions: 1.7×0.2×7 cm). Next, the open end was closed, taking care that the seal was made outside the part of the tubing were soil was present.
Final soil tubings were UV irradiated at both sides for 10 min respectively (laminar flow). Next, tubings were transferred into sterile 250 ml borosilicate bottles (Schott-Duran GL45) and sealed with butyl rubber stoppers. Oxygen was removed from the sealed bottle via ten iterations of vaccumization and flushing with N_2/CO_2. Special care was taken to keep the vacuumization period short (app. 30 sec) to avoid bursting of the sealed dialysis tubing inside the chamber. Finally 0.5 bar of the gas mix were applied to the chamber to allow diffusion of remaining oxygen into the headspace over night.

The next day the total headspace had to be renewed with the N_2/CO_2 mix and 50 ml of basal FM (Na_2SO_4 [5mM]) were added. A final equilibration period of 6 days was specified for each dialysis chamber unless stated contrary. Sterility of each setup was verified before inoculation via FISH (DSP probe set + DAPI). Inoculation volumes were either 0.2 ml or 0.5 ml .
Furthermore one abiotic control (DIA 8) was maintained for a period of 2 month to assess the effect of abiotic sulfate turnover and available molecular entities in the solute fraction as well as the possibility of contamination from slow growing microorganisms.
Dialysis chambers were incubated stationary at 14°C in the dark.

Agarshake dilution series:
300 ml of milli-Q water were added to 3.3 g agar (Bacto™ Agar, Cat. No. 214010, Becton, Dickinson and Company, New Jersey) in a 500 ml erlenmeyer flask, containing a magnetic stir bar. The suspension was stirred for 10 min at RT. After sedimentation of the agar fraction (app. 10min) the supernatant was decanted and 300 ml milli-Q water were added again. This process was performed for four iterations. The final suspension was filtered and dried for 1h, using the vacuum pump. The dried agar was transferred into an Erlenmeyer flask and supplemented with milli-Q water to a total weight of 103.3 g (agar + water). Agar was molten to homogeneity at 130°C (temperature of heating plate) under constant stiring. Afterwards agar was kept stirring at 90 °C (water bath). 3 ml aliquots of agar were dispensed into Hungate tubes provided with a 3 ml and 9 ml mark on the outside of the vial. Tubes were sealed aerobically with butyl rubber stoppers while agar was still hot and transferred at 4°C, to allow rapid solidification in a horizontal position. Subsequently the headspace was exchanged, by three iterations of vacuum and N_2/CO_2 flushing. Tubes were then left at vacuum and autoclaved. While still hot, tubes were subsequently transferred to a 50°C water bath.
6 ml of prewarmed (50°C) basal FM (lactate and sulfate [10 mM] respectively) were added to each tube (using a sterile dispenser setup) to achieve a final agar concentration of 1 % (w/v). Tubes were kept at 50°C for inoculation. For inoculation, 1 ml of enrichment culture (LF01-E1 and LF01-E3) were added to the first liquid agarshake tube with a syringe (needle OD= 0.90 mm). Subsequently dilution series were performed to a factor of 10^{-9}. After solidification tubes were incubated upside down at 14°C stationary in the dark. Three tubes were incubated without inocula to verify sterility throughput the process.

Soil Agar Plates:
Agarose concentrations were adjusted to 2 % as soil agar plates exhibited decreased gelling strength in combination with the soil. Too low pH (4.5 as in aSRB medium) did exclude gelling of the agarose. Consequently only the basal FM was found to be suitable. The anaerobic jar was cleaned with ethanol (80 % v/v) and UV irradiated over night.
The protocol here refers to 150 ml of total final volume of soil agar. 3.3 g agar (Bacto™ Agar, Cat. No. 214010, Becton, Dickinson and Company, New Jersey) were washed as outlined in the agarshake method section. The final wet weight of the agar was 34.3 g. 24 g of twice autoclaved sieved soil (typical water content = 80 %) and 99.5 ml of medium were added. Sulfate concentration was adjusted to 5 mM with 1M anoxic Na_2SO_4. The mixture was autoclaved at 110°C for 15 min in 500 ml borosilicate bottles (Schott-Duran GL45) and subsequently poured in petri dishes (Cat. No. 632102, Greiner bio-one, Austria) in the laminar flow. Solidified plates were transferred into the anaerobic jar, that was flushed with N_2 gas at timepoint zero, after 3 days and after 7 days. Tubing with autoclaved cotton wool was attached to the inlet valve of the jar to exclude contamination via flushing. At

timepoint zero a catalyst sachet was added. For the oxygen removal timeframe, plates were incubated at 14°C in the dark. 100 µl and 20 µl of liquid enrichment cultures were inoculated onto the plate and streaked with sterile single use streaking loops in the anaerobic tent. Plates were sealed with parafilm and incubated in the anerobic jar under N_2/H_2 atmosphere (95:5 (v/v)) with a new catalyst bag. Two plates were incubated without inoculum for the entire incubation period. The anaerobic jar was incubated at standard incubation conditions.

Supplementary table 8-9
Specimens used for pasteurization experiments and the respective treatment combinations summarized by ID.

Specimen	Temperature (°C)	Time (min)	ID
Resuspension	80	20	1A
	90	20	2A
	95	30	3A
Desiccation	80	20	1B
	90	20	2B
	95	30	3B
Exhaustion at 4 °C	80	20	1C
	90	20	2C
	95	30	3C
Sp1s	80	20	1D
	90	20	2D
	95	30	3D

8.1.3 Desulfosporosinus quantitative FISH

Extraction protocols:
For comparison of extraction protocols either an unfixed or fixed (PFA and EtOH) enrichment culture from soil slurry Sp1s (identical timepoint) was used. Samples were taken of the enrichment from the coarse supernatant fraction, after one minute of homogenization (repeated inverting of tube). The concentration of the pyrophosphate (PP_i) solution was always at 1 % (w/v).

Supernatant pyrophosphate extraction (modified from Hahn et al., 1992):
1. Sample 200 µl of the unfixed homogenized supernatant and combine it with 2 ml PP_i solution in 15 ml conical centrifuge tube (Greiner bio-one, Austria).
2. Vortex at maximum intensity for 10 sec
3. Allow for 2 min of particle sedimentation on ice.
4. Collect supernatant and re-extract the remaining soil pellet in 2 ml PP_i solution (same parameters as in steps 2 and 3)
5. Combine supernatants and centrifuge them at 5 000× g for 15 min at 4°C.
6. Carefully aspirate the supernatant and resuspend the pellet in 200 µl of ice-cold 1×PBS (by means of a pipette).
7. Fix in either PFA or Ethanol

Ultrasonication pyrophosphate extraction (modified from (Zarda et al., 1997))
1. Ethanol and PFA fixed specimens were diluted 1:5 and 1:20 in PP_i solution (V_{tot}=0.5 and 1 ml respectively) and kept on ice.
2. Diluted specimens were extracted via ultrasonication on ice. Three iterations for 10 sec in pulse modus at the lowest power value.

3. The extracts were directly used for FISH analysis.

Bead beating (modified from(Lücker et al., in preperation))
Remove the silica sand fraction from a DNA extraction Fast Prep™ Lysis Matrix A Tube (MP Biomedicals) and rinse the ceramic bead and tube in sterile water to remove remaining silica sand.

1. Add 100 µl of 1×PBS to tubes containing the ceramic bead.
2. Add 100 µl of Ethanol or PFA fixed specimen.
3. Bead beat tubes in a horizontal position for 12 min on a vortex (MO BIO Vortex Adapter) at maximum intensity.
4. Transfer the suspension in a new 1.5 ml reaction tube and centrifuge at 10 000× g for 10 min at 4°C
5. Aspirate supernatant and suspend pellet in 200 µl of 1×PBS and centrifuge at 10 000× g for 5 min at 4°C.
6. Aspirate supernatant and resuspend the final pellet 200 µl of 1×PBS/ ethanol (1:1)

Combinatorial treatment used for soil slurry FISH in this study

1. Vortex ethanol fixed specimens at maximum intensity (app. 5 sec)
2. Diluted 20 µl of the specimen in 180 µl of PP_i (1% w/v) solution
3. Horizontally vortex for 12 min at room temperature in DNA lysis matrix tube A (MP Biomedicals)(containing only the ceramic bead)
4. Transfer the total solution into a 0.5 ml tube and spin down at 2 000× g for 10 sec at room temperature
5. Avoiding the pellet, take of the supernatant and transfer into 1.5 ml round bottom tube (do not use 2 ml tubes)
6. Centrifuge at 18 000× g for 10 min at room temperature
7. Discard the supernatant and resuspend the pellet in 20 µl Ethanol/PBS (1:1 (v/v))
8. For FISH on glass slides, apply 5 µl of the specimen onto the well

Quantification and image processing:
The establishment of cell quantification was performed with an ethanol fixed specimen from soil slurry Sp1s. Cells were extracted with the combinatorial extraction protocol described in the results section here.
For quantification of bacterial cells and abundance of *Desulfosporosinus* cells, 25 images (221.35/221.35 µm physical length) per well and specimen were acquired at predefined random positions covering a square of maximum area in respect to the slide well. Normal distribution and homoscedasticity for *bacterial* counts and *Desulfosporsinus* counts per field of view could be observed when 25 images were acquired (as confirmed by Shapiro–Wilk and Levene Test respectively). No significant difference in relative abundance of *Desulfosporosinus* cells between three wells containing the very same sample could be detected with one-way ANOVA. Consequently for the purpose of quantification of relative abundance of *Desulfosporosinus* cells, 25 images of only one well per specimen were acquired.
Cells were quantified in DAIME after removing artifacts.

FISH on Filters was modified from a protocol provided by PhD Stephanie Eichhorst (Division of Microbial Ecology (University of Vienna).

A. Fixation of Isopore 0.22 µm GTTP filters
    1. Embed samples in 0.1 % agarose as described earlier.
    2. Fixation is performed in 50mm diameter petridishes.
    3. For fixation place on quarter of a Rotilabo-Rundfilter(Cat. No. AP58.1, Carl-Roth, Germany) or any other glass filter into a petridish and soak with ~350 µl of 4 % PFA or 96 % EtOH depending on the specimen.
    4. Place the GTTP section on top of the filter, taking care that the inoculum is facing upwards (advisable to make a note at the filter edge with a pencil)
    5. Seal petridish with parafilm and fix for 4 h at 4°C.
    6. Wash fixative away via placing the GTTP section into a new petridish containing 3 ml of sterile destilled water. Wash for 30 min at room temperature.
    7. Repeat step 7 using new water.
    8. Dry fixed sections in a petri dish containing paper towel (~5min).

B. Hybridzation →avoid light!
    1. Apply fixed sections onto glass slide, the area around it is enclosed using a liquid repellent pen. (Daido Sangyo Co- Ltd. Tokyo, Japan, Liquid Blocker Super PAP Pen)
    2. Prepare 1 ml of hybridization buffer of desired stringency
    3. Add 27 µl of hybridzation buffer and 3 µl of each probes working solution (5 pmolμl^{-1}). Final concentration of probes (0.45 pmolμl^{-1}). Mix gently via pipetting.
    4. Transfer the slide into a 50 ml conical centrifuge tube, containing paper towel soaked with the remaining hybridization buffer.
    5. Transfer tube into hybridization oven at 46°C for 90 min.
    6. In the meantime prepare washing buffer (50 ml) and pre-warm it in a water bath at 48°C.
    7. After hybridization, transfer the filters into washing buffer using sterile tweezers, and wash for 15 min at 48°C.
    8. After washing transfer sections into a petridish containg 50 ml of ice-cold milliQ water for 10 sec.
    9. Air-dry sections in a petry dish containing paper towel in the dark for 5 min at room temperature.
    10. Mount sections on glass slides using Citifluor. Take care that the entire section is mounted (4 µl per section is minimum). Better to also place a droplet on top of coverslip.
    11. Seal coverslip and slide with nail polish.

8.1.4 Enrichment cultures PCR screening

Supplementary table -8-10
16S rRNA gene targeted primers used for enrichment screenings.

Primer	Sequence (5'— 3')	Target Group	Reference
8F	AGA GTT TGA TYM TGG CTC	Most *Bacteria*	(Juretschko et al., 1998)
1492R	GGY TAC CTT GTT ACG ACT T	Most *Bacteria* and *Archaea*	(Loy et al., 2002)
DSP603F	TGT GAA AGA TCA GGG CTC A	*Desulfosporosinus*	(Pester et al., 2010)
DSP821R	CCT CTA CAC CTA GCA CTC	*Desulfosporosinus*	(Pester et al., 2010)

Supplementary table 8-11
Thermal cycling conditions for general and *Desulfosporosinus* targeted 16SrRNA gene PCR. PCR cycles were initialized by 5 min of denaturation followed by 40 cycles at the parameters below and a final elongation step at 72°C for 10 min. Reaction setup is identical (except for primers) as for M13 PCR (reaction volume of 50 µl) Supplementary table 8-3

Primer pair	Denaturation	Annealing	Elongation
8F/1492R	94°C/ 30 sec	56°C/ 30 sec	72°C/ 90 sec
603F/1492R	94°C/ 40 sec	64°C/ 30 sec	72°C/ 60 sec
DSP603F/DSP821R	94°C/ 40 sec	64°C/ 30 sec	72°C/ 40 sec

8.2 Supplementary results

8.2.1 qPCR *dsrA*

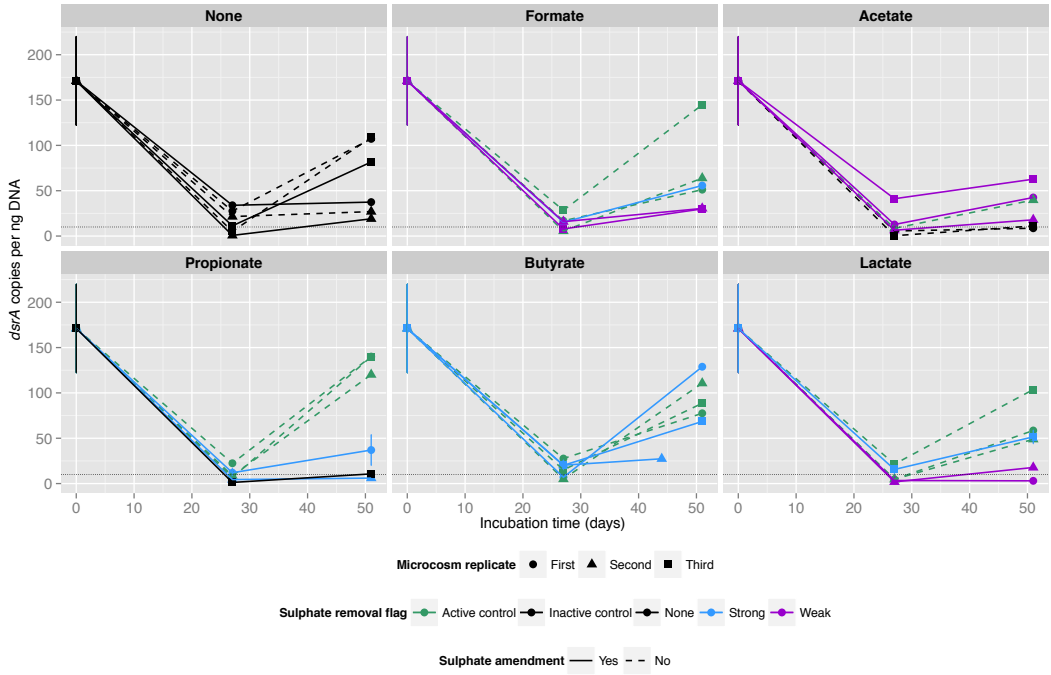

Figure 8-2
qPCR data for copy numbers of *dsrA* OTU1 for indivdual microcosms. Active control refers to micocosms without sulfate amended but rapid turnover of the indigenous sulfate pool. The horizontal dotted line marks the detection limit.

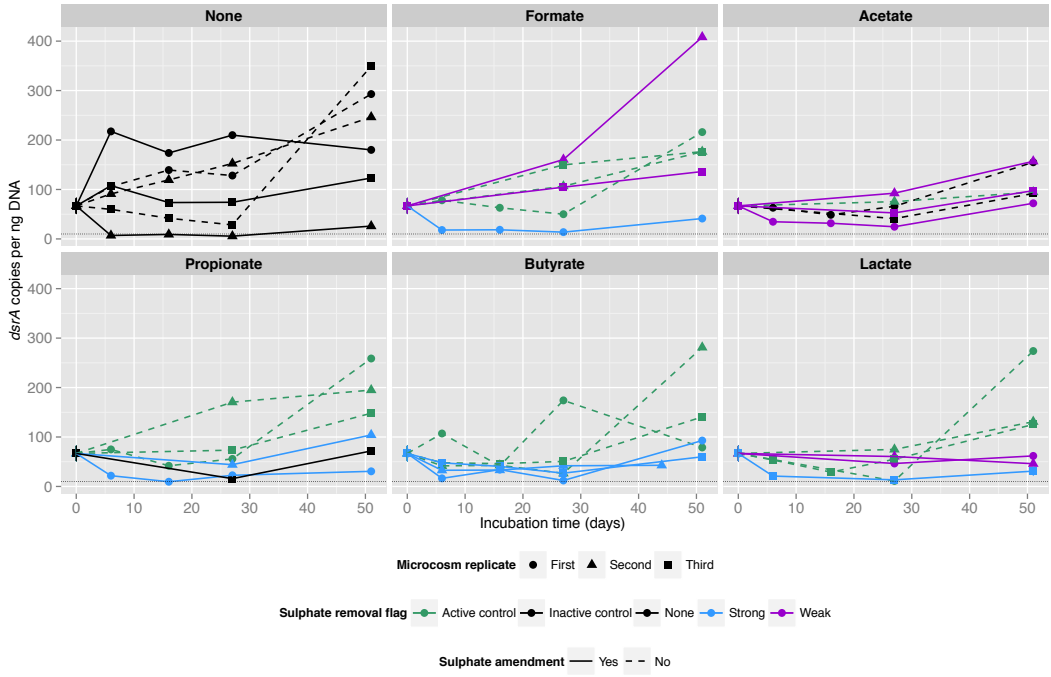

Figure 8-3
qPCR data for copy numbers of *dsrA* OTU2 for indivdual microcosms. Active control refers to micocosms without sulfate amended but rapid turnover of the indigenous sulfate pool. The horizontal dotted line marks the detection limit.

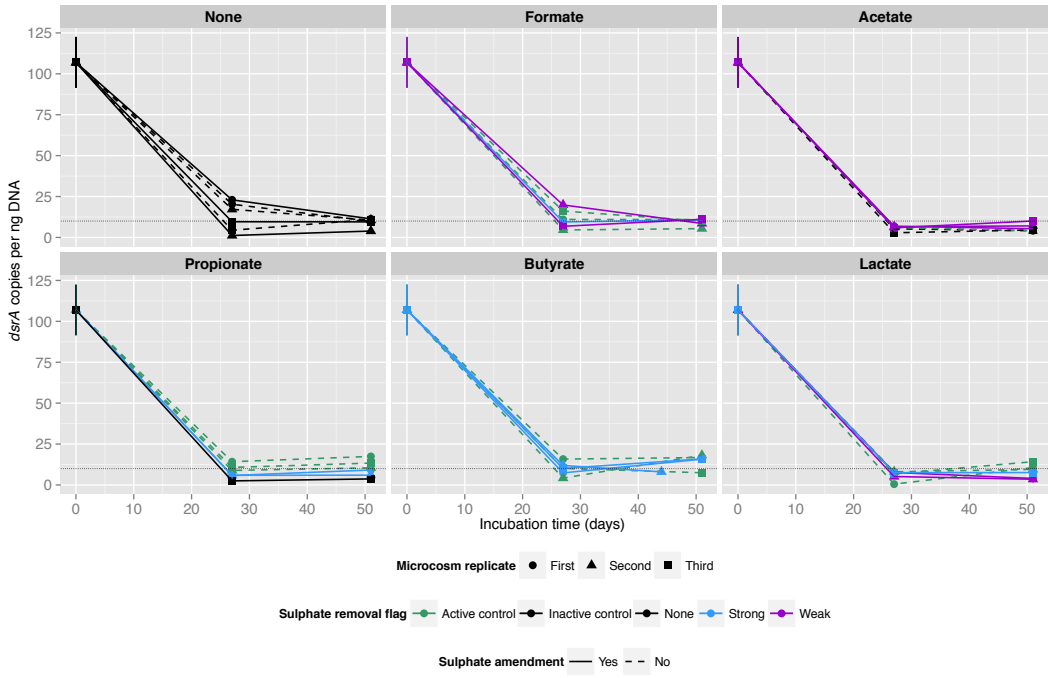

Figure 8-4
qPCR data for copy numbers of *dsrA* OTU6 for indivdual microcosm. Active control refers to micocosms without sulfate amended but rapid turnover of the indigenous sulfate pool. The horizontal dotted line marks the detection limit.

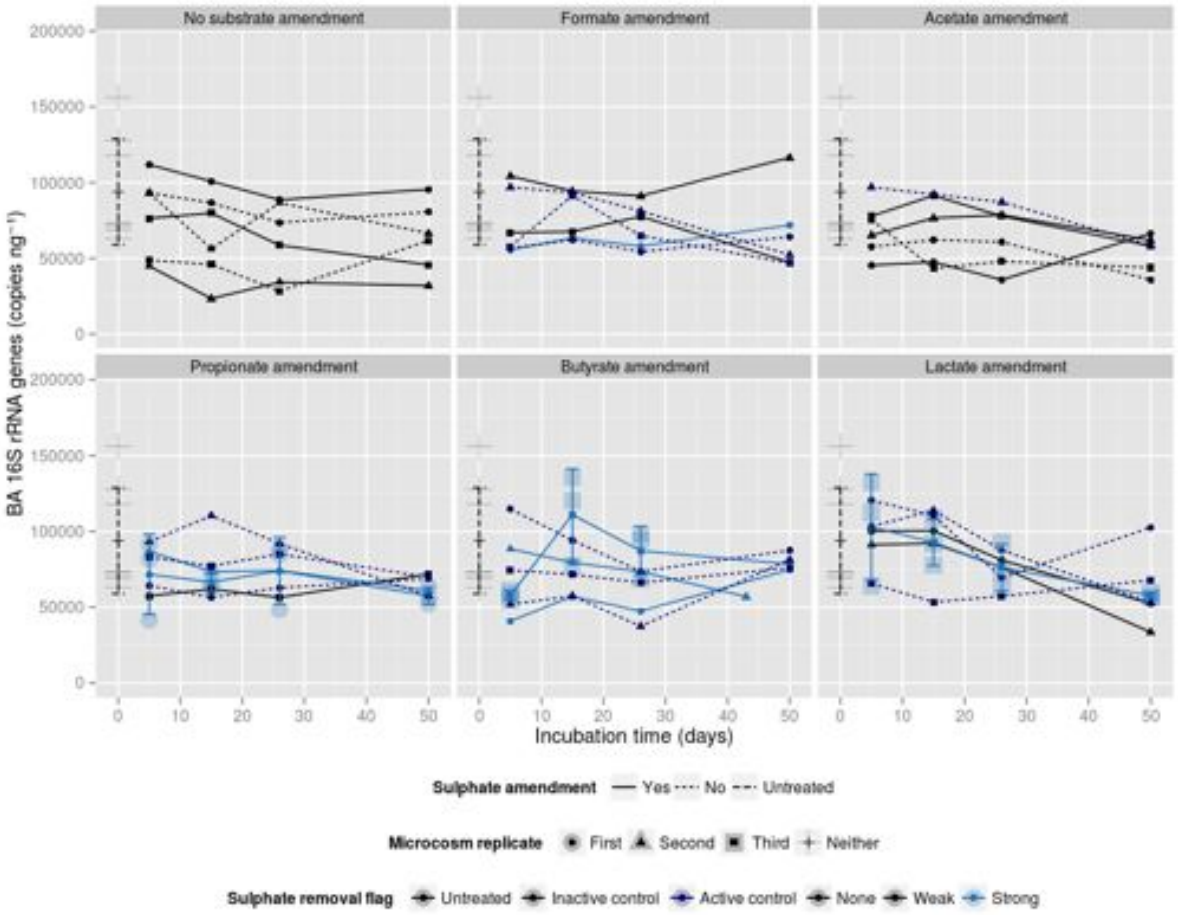

Figure 8-5
qPCR data provided by Mag. Bela Hausmann showing total *Bacterial* and *Archaeal* (BA) 16S rRNA gene copies for individual microcosms. This dataset was employed here for calculating the relative abundance of *dsrA* and *Acidobacteria* 16S rRNA genes. For further details refer to (Hausmann, 2014).

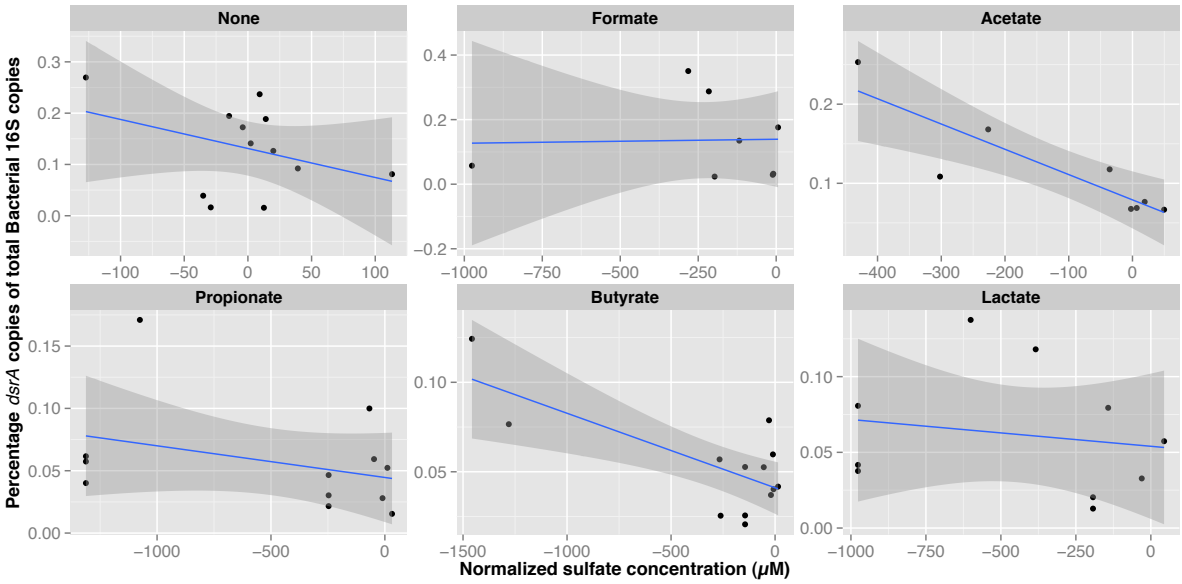

Figure 8-6
Linear models of the dataset used for correlation analysis. Data for sulfate concentrations were provided by Mag. Bela Hausmann (Hausmann, 2014).

8.2.2 qPCR *Acidobacteria* 16S rRNA gene

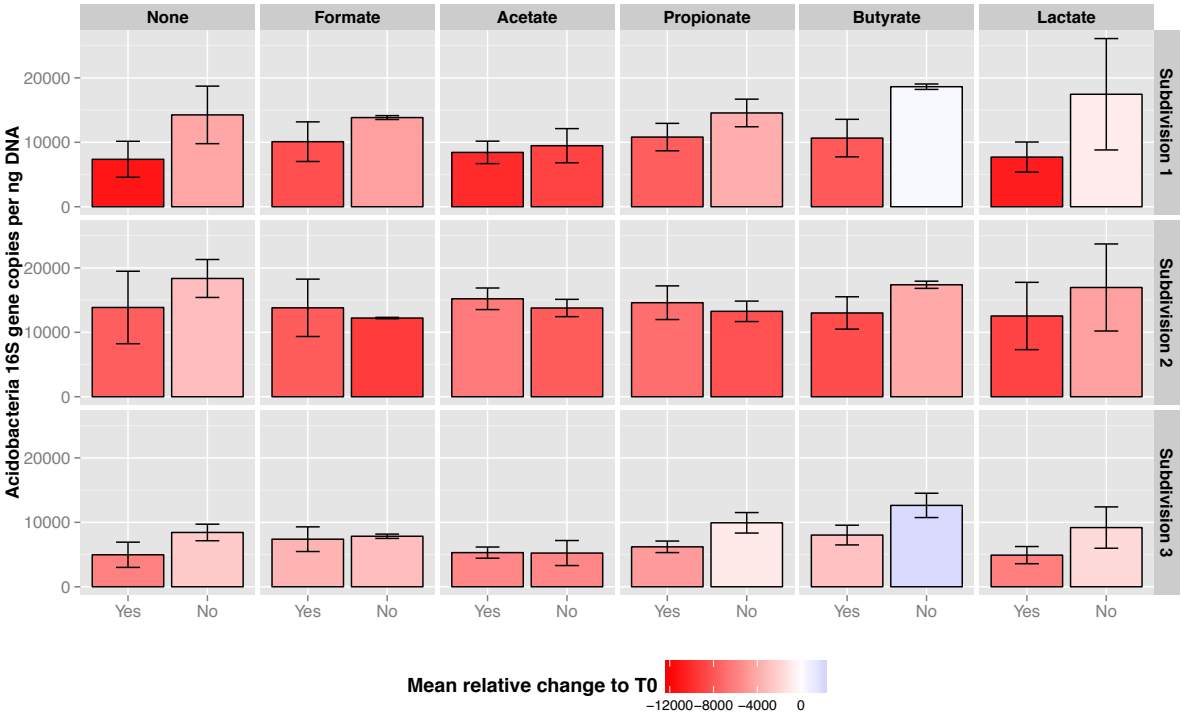

Figure 8-7
Copy values of *Acidobacteria* subdivisions 1 to 3 in microcosm experiments day 51, as determined with qPCR. Bar colour indicates the mean relative change of microcosm replicates to the mean value of the timepoint zero. Error bars denote average standard deviation.

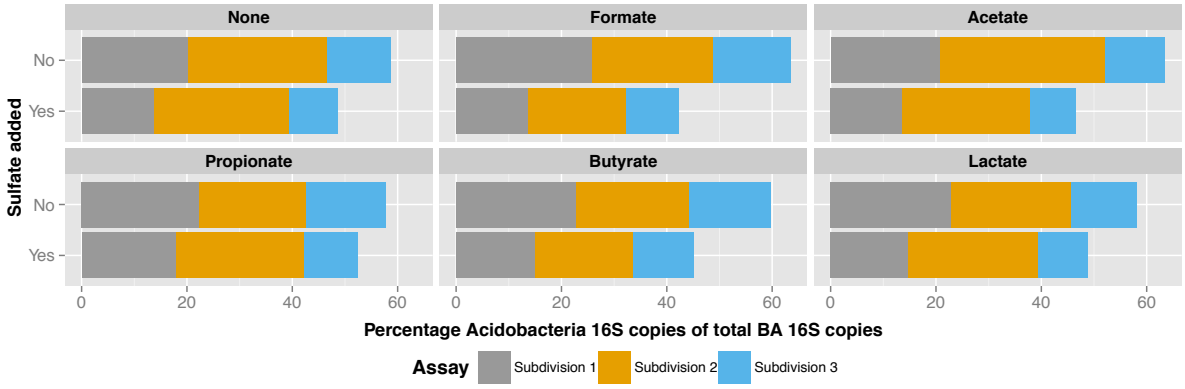

Figure 8-8
Cumulative relative abundance of *Acidobacteria* subdivions 1, 2 and 3 in microcosms after 51 days.

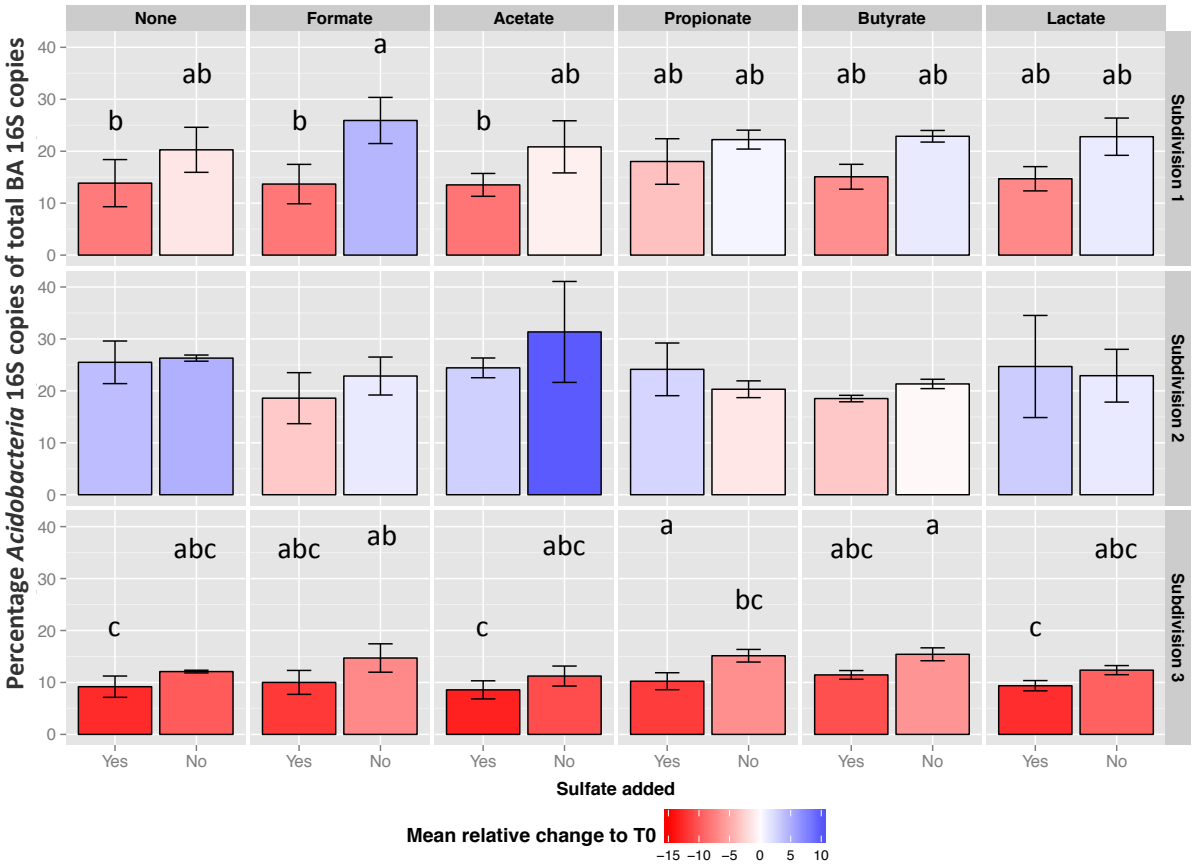

Figure 8-9
Compact letter display of results from Kruskal-Wallis one-way ANOVA of relative abundance values from *Acidobacteria* qPCR assays from microcosm experiments after 51 days. Note, that no significant differences were observed for subdivision 2.

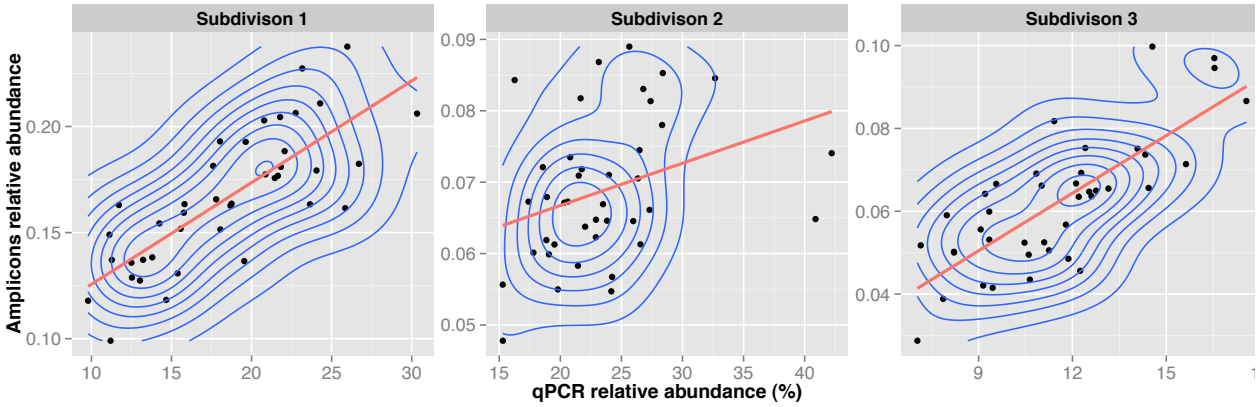

Figure 8-10
Density plots showing the distribution of samples from day 51 microcosm experiments when compared at the relative abundance level for qPCR asssays and amplicon data for *Acidobacterial* subdivisions 1, 2 and 3. The red line indicates the linear model applied to the respective dataset.

8.3 Cultivation of SRM from Schlöppnerbrunnen II

8.3.1 *Desulfosporosinus* quantitative FISH assay

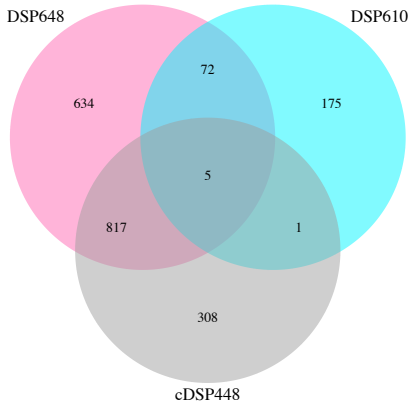

Figure 8-11
Venn diagram showing the intersections of 16S rRNA FISH probes of the *Desulfosporosinus* assay. Values represent probe hits allowing for one missmatch against the RDP databse. The 72 hits remaining in combination with cDSP648 represent exclusively *Desulfosporosinus* sequences.

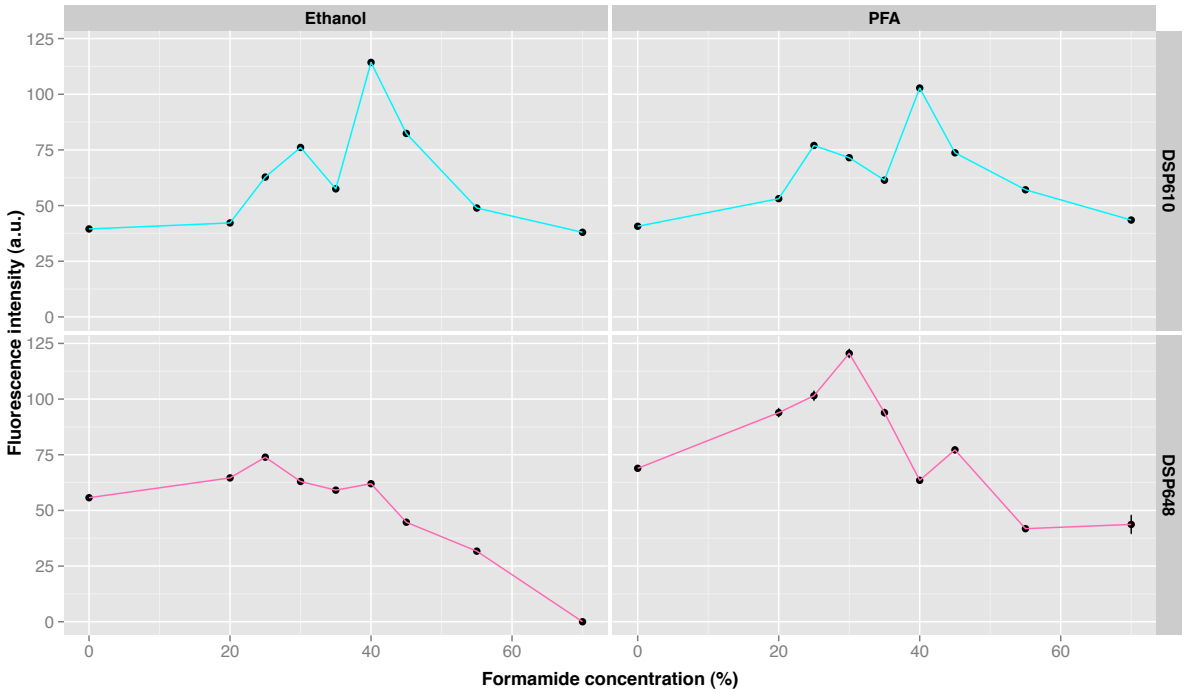

Figure 8-12
FISH Formamide series of probes DSP610 and DSP648 (with cDSP648). Note the distinctive peak at 40 % formamide of probe DSP610 for both fixatives. This pattern could also be found in previous FA series for this probe (data not shown) and could be due to a shift towards the non-hairpin conformation in the reaction equilibrium of DSP610.

8.3.2 Soil slurry enrichments and pasteurization

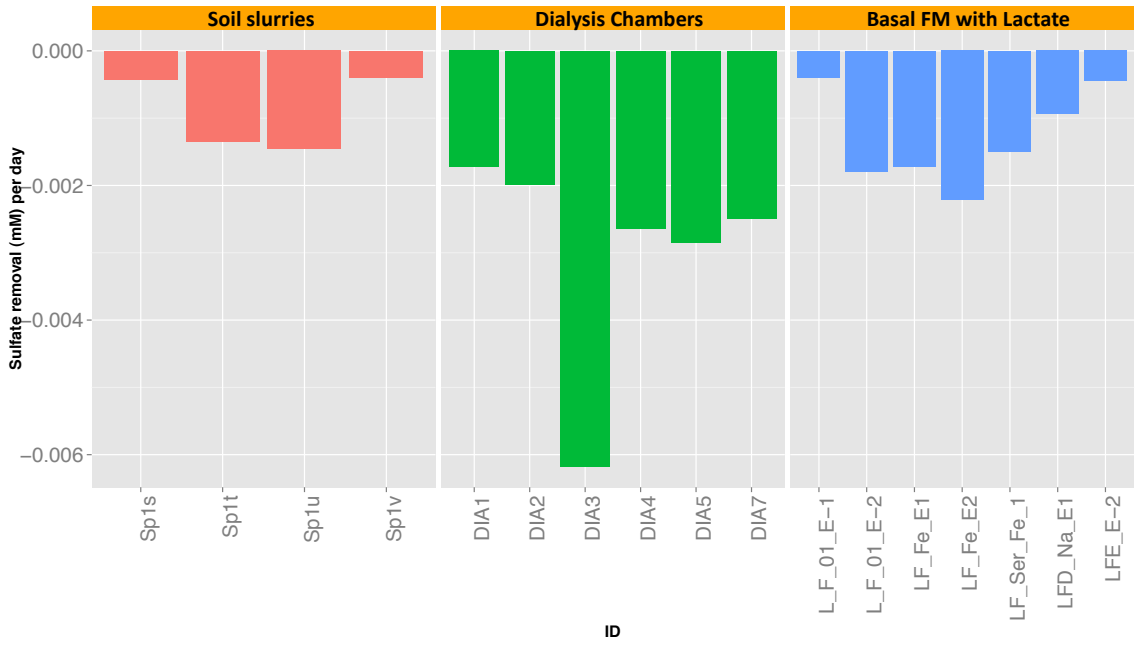

Figure 8-13
Sulfate removal rates as determined from capillary zone electrophoresis data. Rates were estimated from linear models applied to the absolute sulfate amounts in incubations. Linear models were applied only for the first sulfate amendment. For the defined media array and dilution series thereof, rates were only calculated for specimens being highly enriched in *Desulfosporosinus* cells.

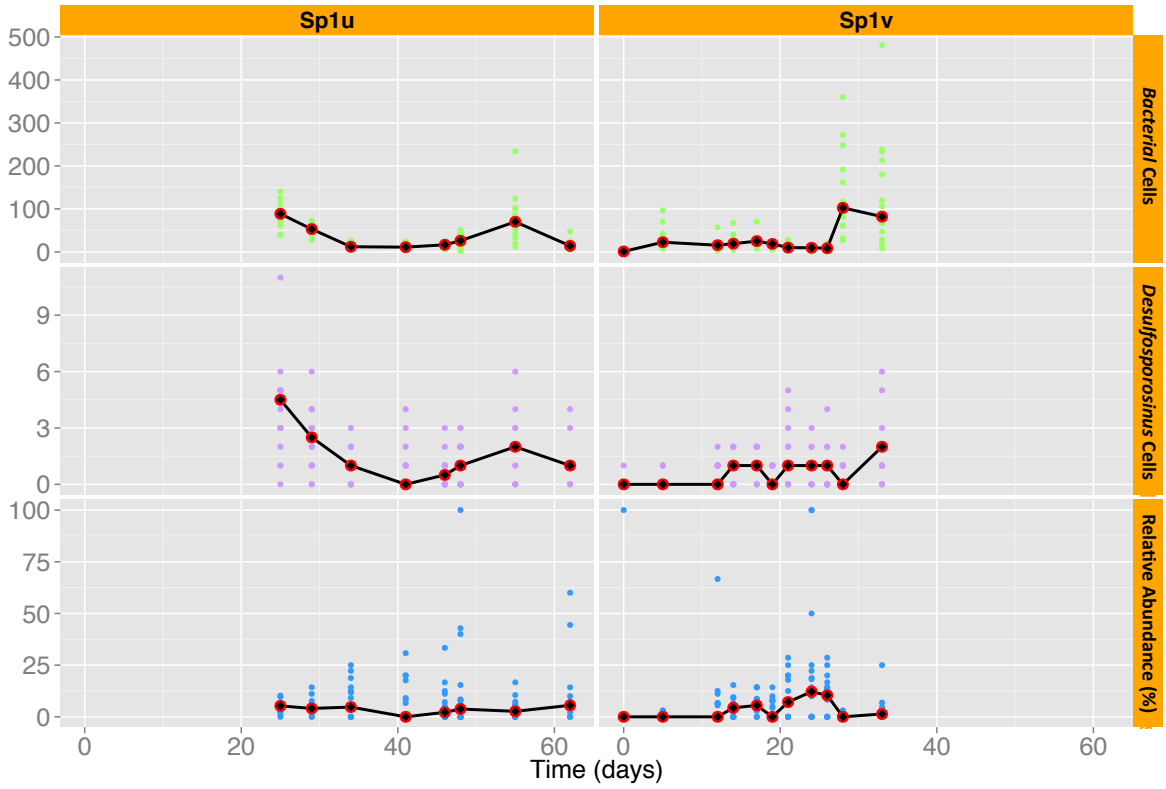

Figure 8-14
FISH quantification of soil slurry enrichments Sp1u and Sp1v. Red dots represent the median value for each timepoint. Green, lila and blue dots indicate the relaive abundance per field of view (FOV).

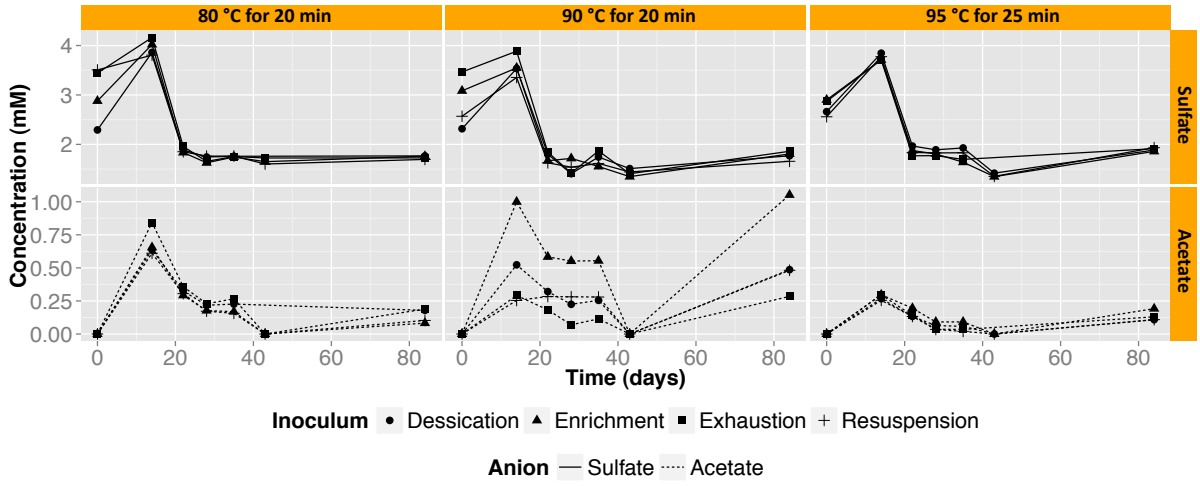

Figure 8-15
Sulfate and acetate concentrations of the pasteurization treatments. Pasteurization parameters are shown in plot headings. Inoculum denotes the sporulation treatment that was used. The inoculum "Enrichment" corresponds to soil slurry Sp1s.

8.3.3 Dialysis chambers

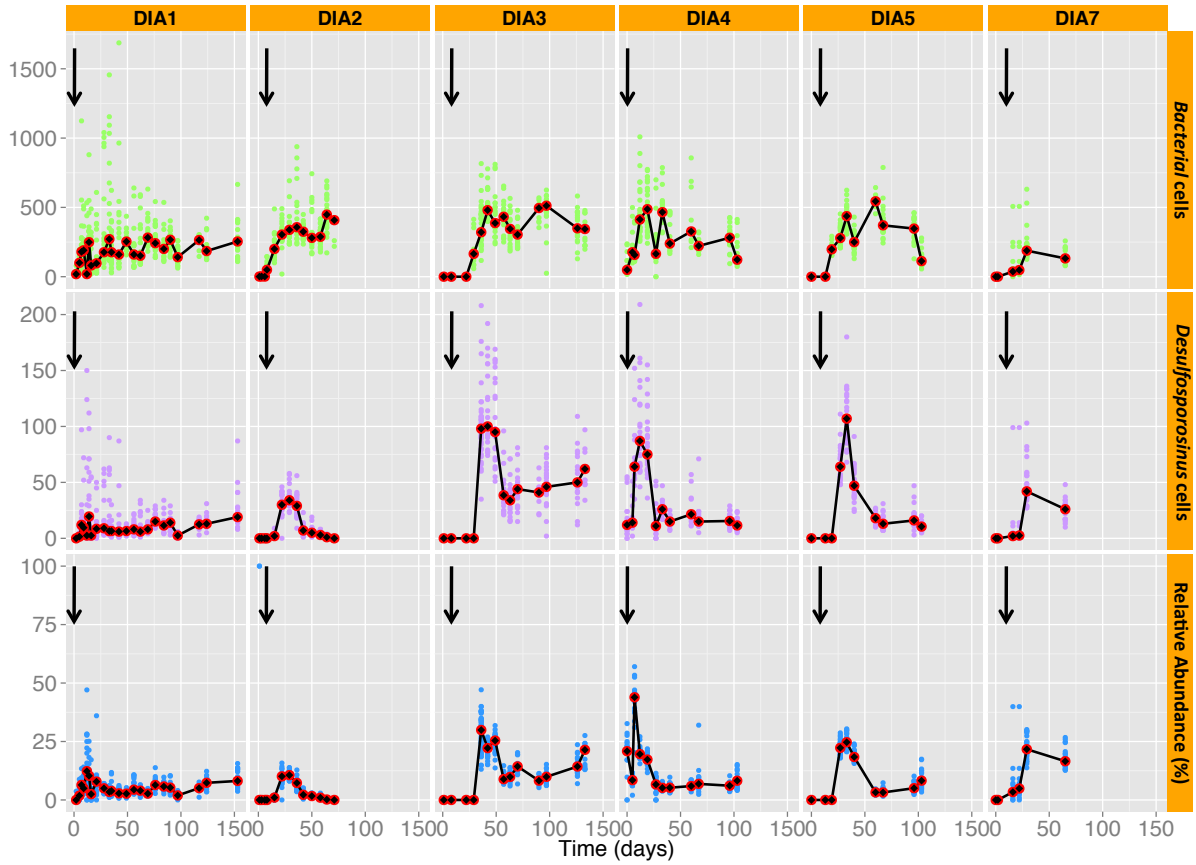

Figure 8-16
FISH quantification of *Desulfosporosinus* in dialysis chambers. Red dots represent the median value for each timepoint. Green, lila and blue dots indicate the relaive abundance per field of view (FOV). Arrows indicate the timepoint of inoculation (0 or 7 days).

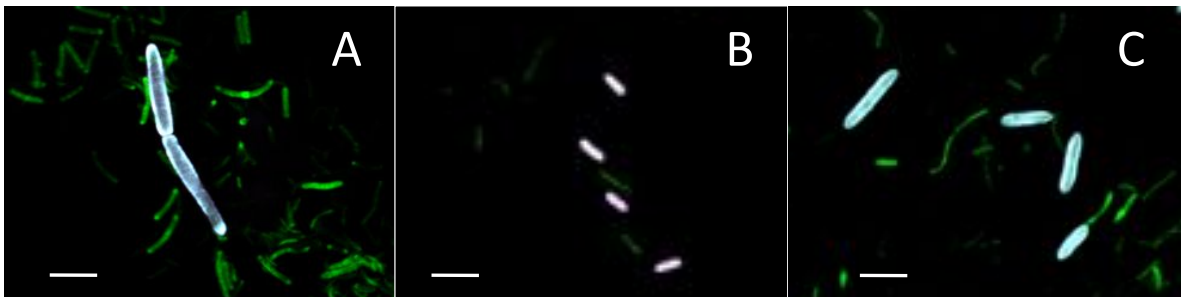

Figure 8-17
FISH images showing morphological plasticity of *Desulfosporosinus* cells growing in dialysis chambers at different incubation stages. A=initial phase (for a reference of filaments refer to Figure 3-9 and Figure 3-10), B=growth phase, C=stationary phase.
Desulfosporosinus cells stain in white-cyan. *Bacteria* in green. Probes: EUbmix-FITC, DSP648-Cy3, cDSP648, DSP610-Cy5, Scale bar: 5 µm

8.3.4 Soil agar

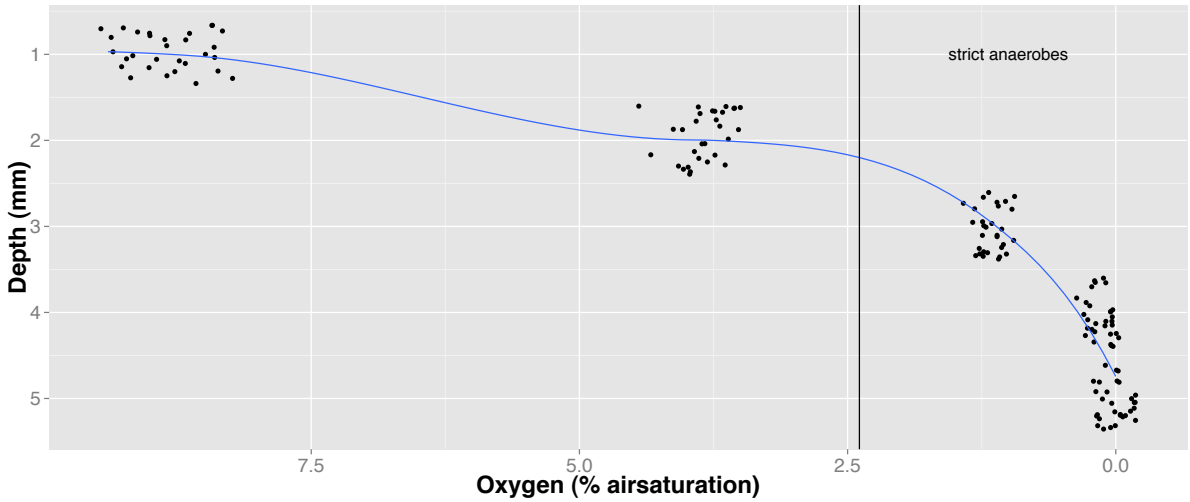

Figure 8-18
Oxygen depth profile of a soil agar plate after 10 days of anoxic incubation at 14°C. The vertical line denotes the maximum oxygen threshold permitting growth of strict anaerobes. Note that the measurement was conducted right after plates were transferred from anaerobic jars into ambient air conditions.

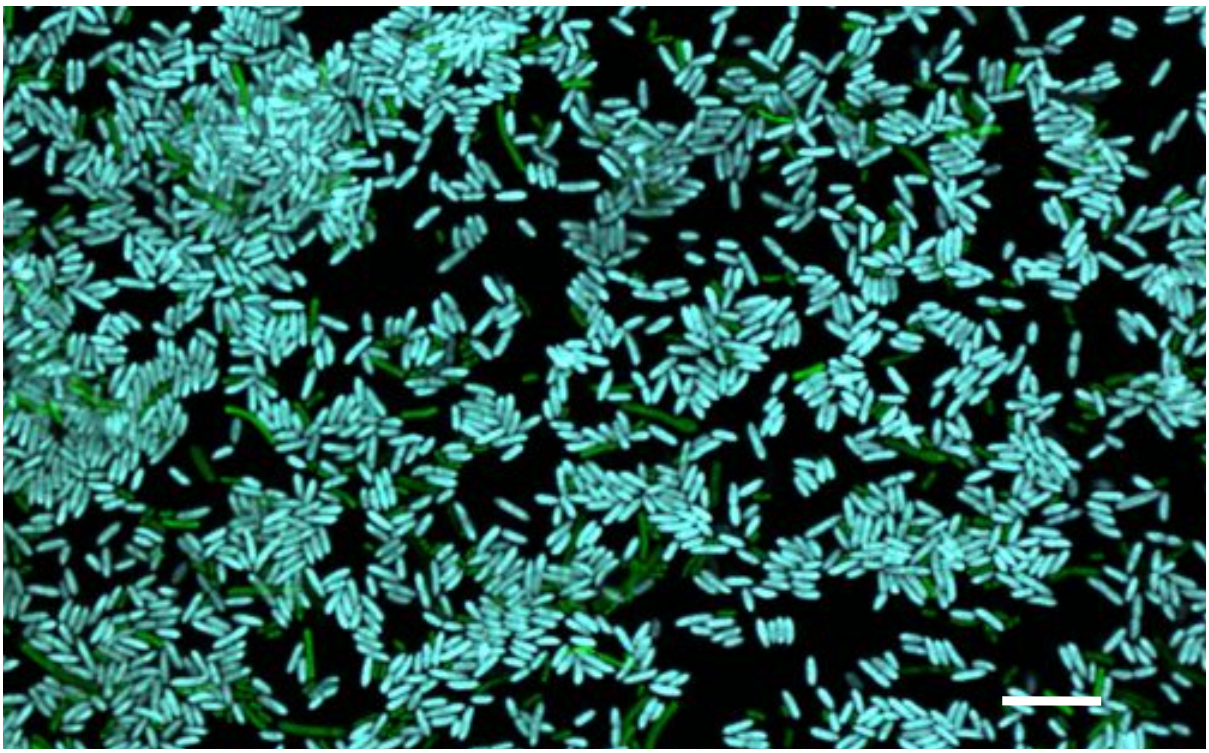

Figure 8-19
FISH analysis of Desulfosporosinus cells growing on soil agar plates. *Desulfosporosinus* cells stain in white-cyan. *Bacteria* in green. Probes: EUbmix-FITC, DSP648-Cy3, cDSP648, DSP610-Cy5. Scale bar: 10 µm

8.3.5 Defined media array

Figure 8-20
OD_{600} measurements of defined media array enrichments that exhibited an increase in optical density. Note that y-axis scales differ between individual plots. Substrate medium combinations indicated in the strip text and are abbreviated as follows. First element denotes the substrate: HC=H_2/CO_2, HA=H_2/CO_2/acetate, E=ethanol, L=lactate, B=butyrate; Second element denotes the medium type (also referenced by line colour): A=DSMZ 1250, I=aSRB, F=FM; Third element= array ID

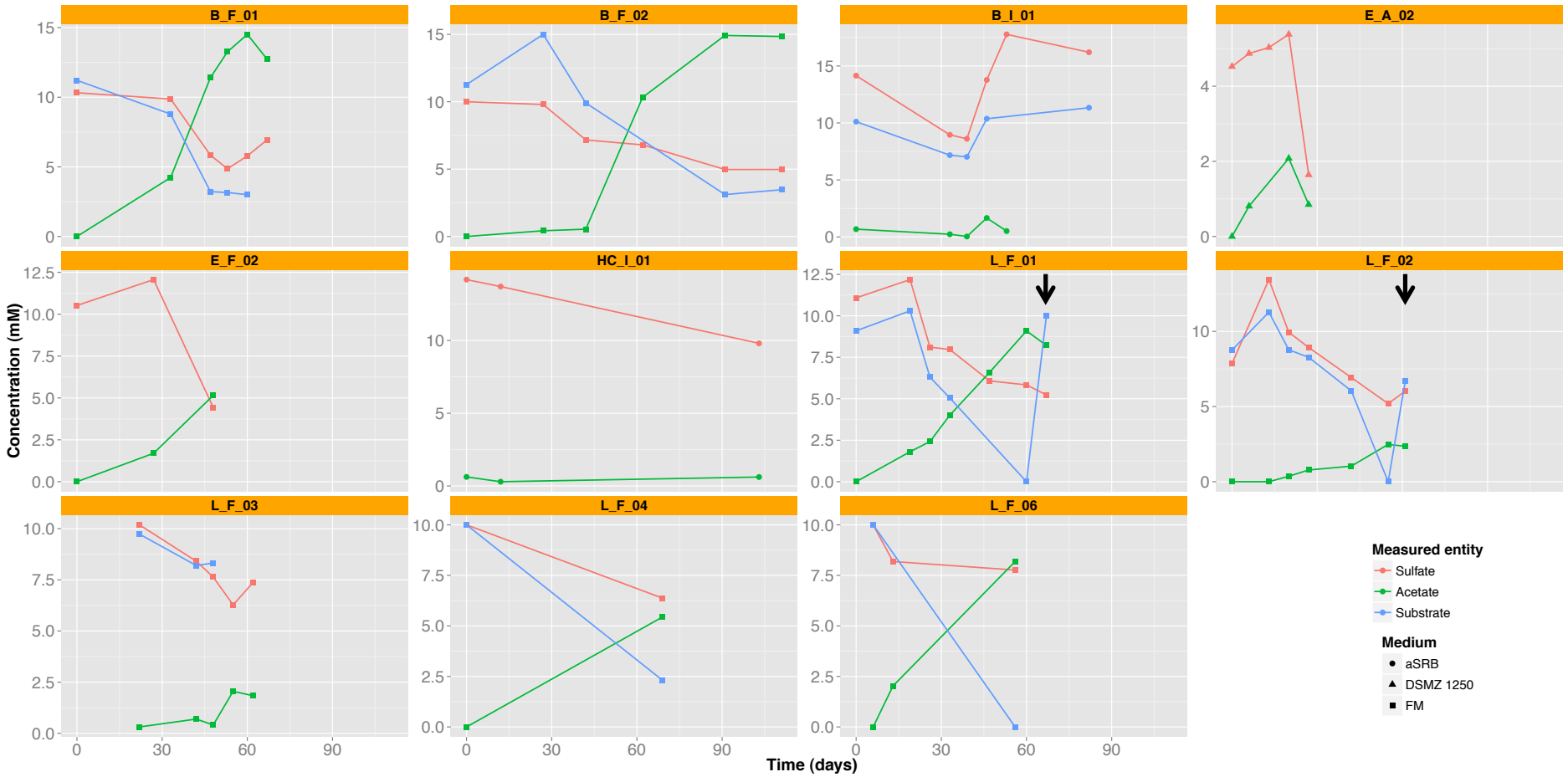

Figure 8-21
Turnover of substrates, acetate and sulfate in defined media array enrichments. Only entities exhibiting sulfate removal are shown. Note that y-axis scales differ between individual plots. Black arrows indicate timepoints of substrate addition. Substrate medium combinations indicated in the strip text and are abbreviated as follows. First element denotes the substrate: HC=H_2/CO_2, HA=H_2/CO_2/acetate, E=ethanol, L=lactate, B=butyrate; Second element denotes the medium type (also referenced by line colour): A=DSMZ 1250, I=aSRB, F=FM; Third element= array ID

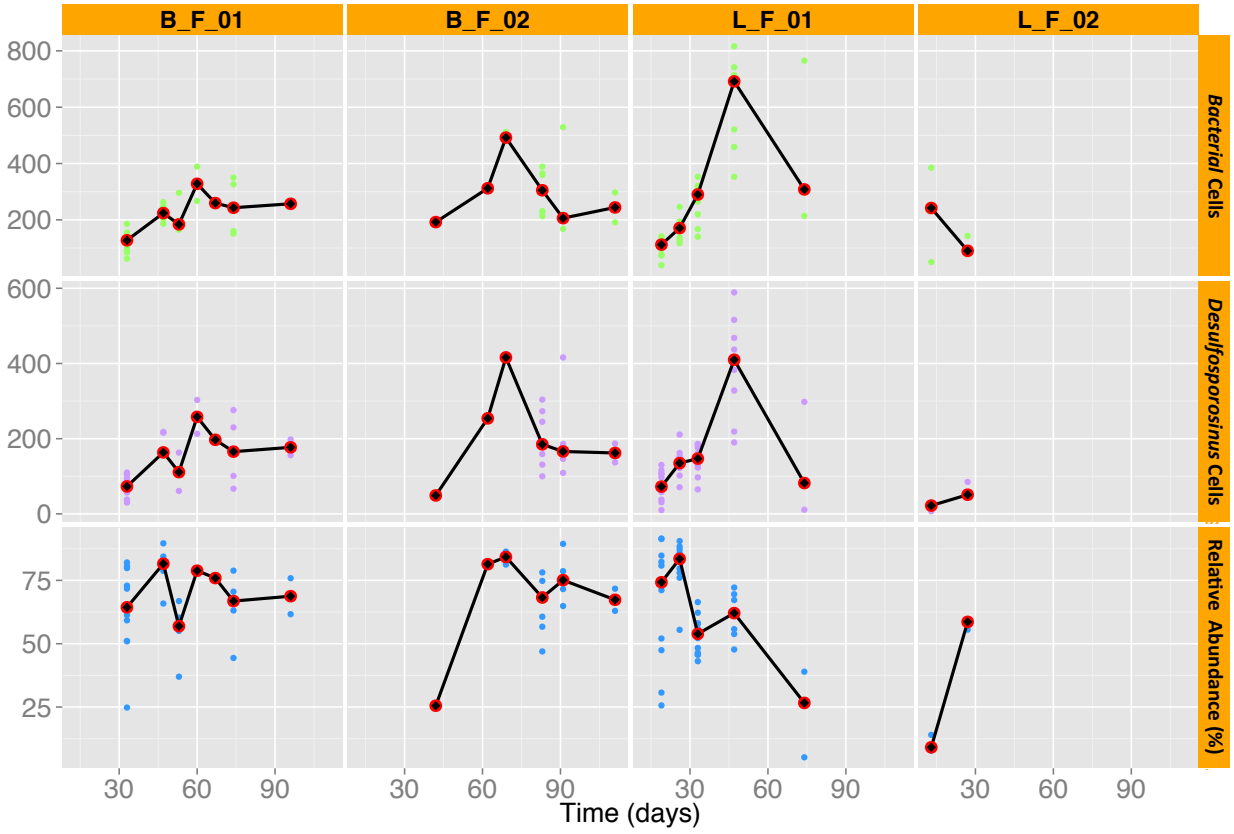

Figure 8-22
A subset of FISH quantification of defined media *Desulfosporosinus* enrichments. Red dots represent the median value for each timepoint. Green, lila and blue dots indicate the relaive abundance per field of view (FOV). Note, that only the most promising (in respect to enrichment status) combinations are provided.

8.3.6 Dilution to extinction

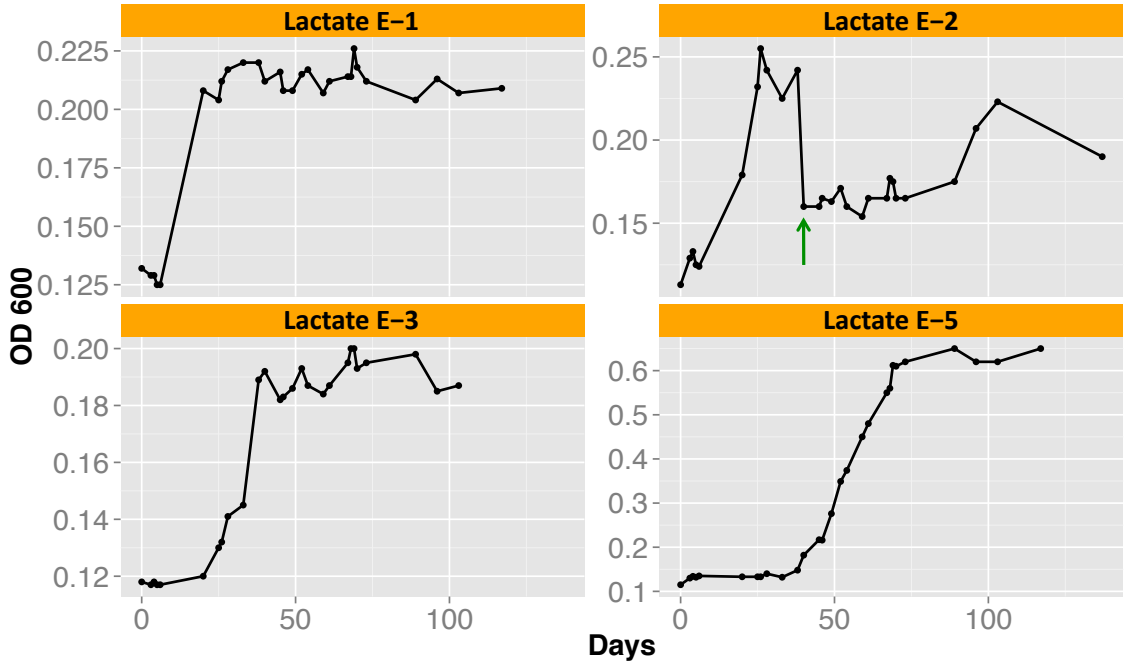

Figure 8-23
OD_{600} measurements of first generation dilution to extinction series with basal FM and lactate as electron donor. The green arrow indicates the timepoint of media addition. Specimen E-5 exhibited pronounced FeS precipitate formation due to the presence of residual iron from the degassing needle, implying the overall higher OD_{600} values.
Note that y-axis scales differ.

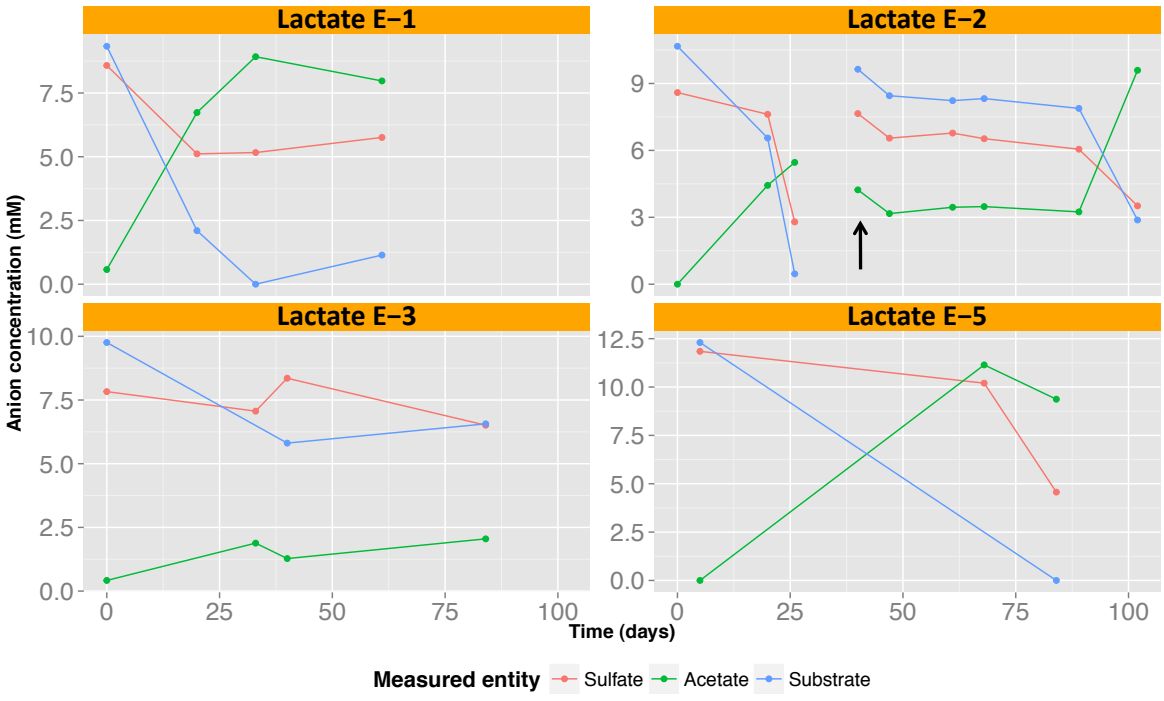

Figure 8-24
Turnover of lactate (substrate), acetate and sulfate in the first generation of dilution series with basal FM. The black arrow indicates the amendment of basal medium together with lactate and sulfate. Note that y-axis scales differ.

8.3.7 Candidate *Desulfosporosinus SbII* isolates

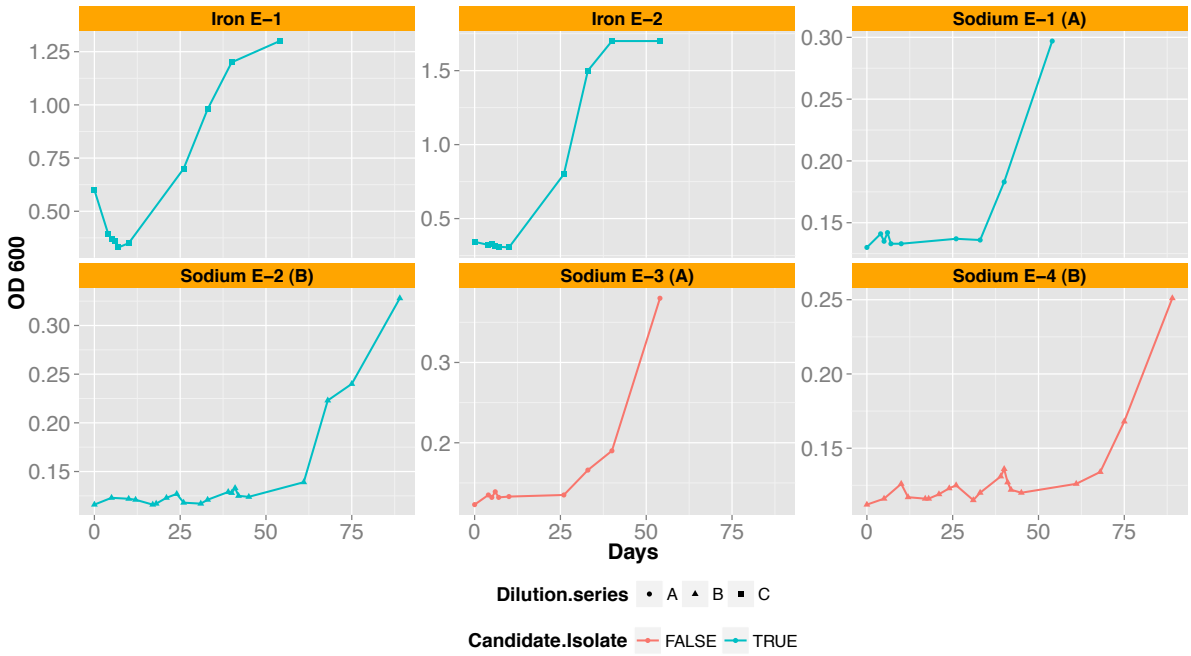

Figure 8-25
OD_{600} data of second series of dilution to extinction experiments. Headings denote the sulfate salt used for cultivation. Candidate isolates are colored in blue.

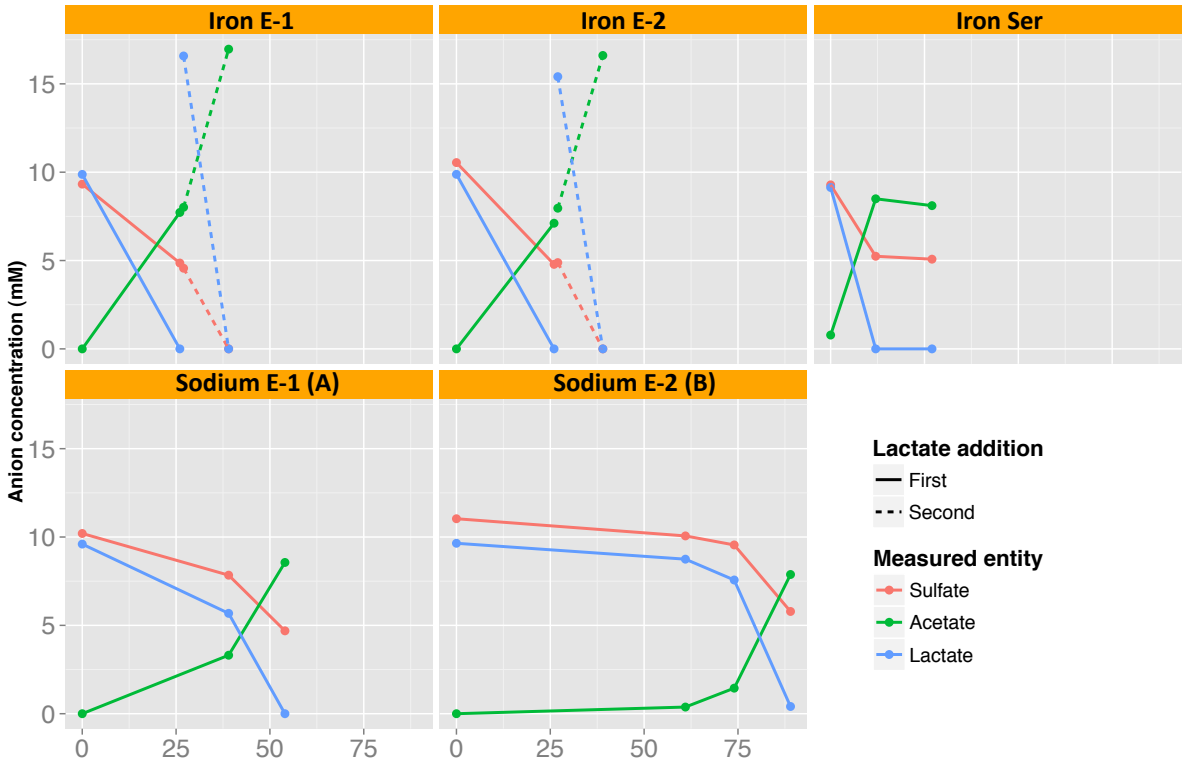

Figure 8-26
Turnover of lactate, acetate and sulfate of candidate *Desulfosporosinus* isolates from the second generation of dilution series.

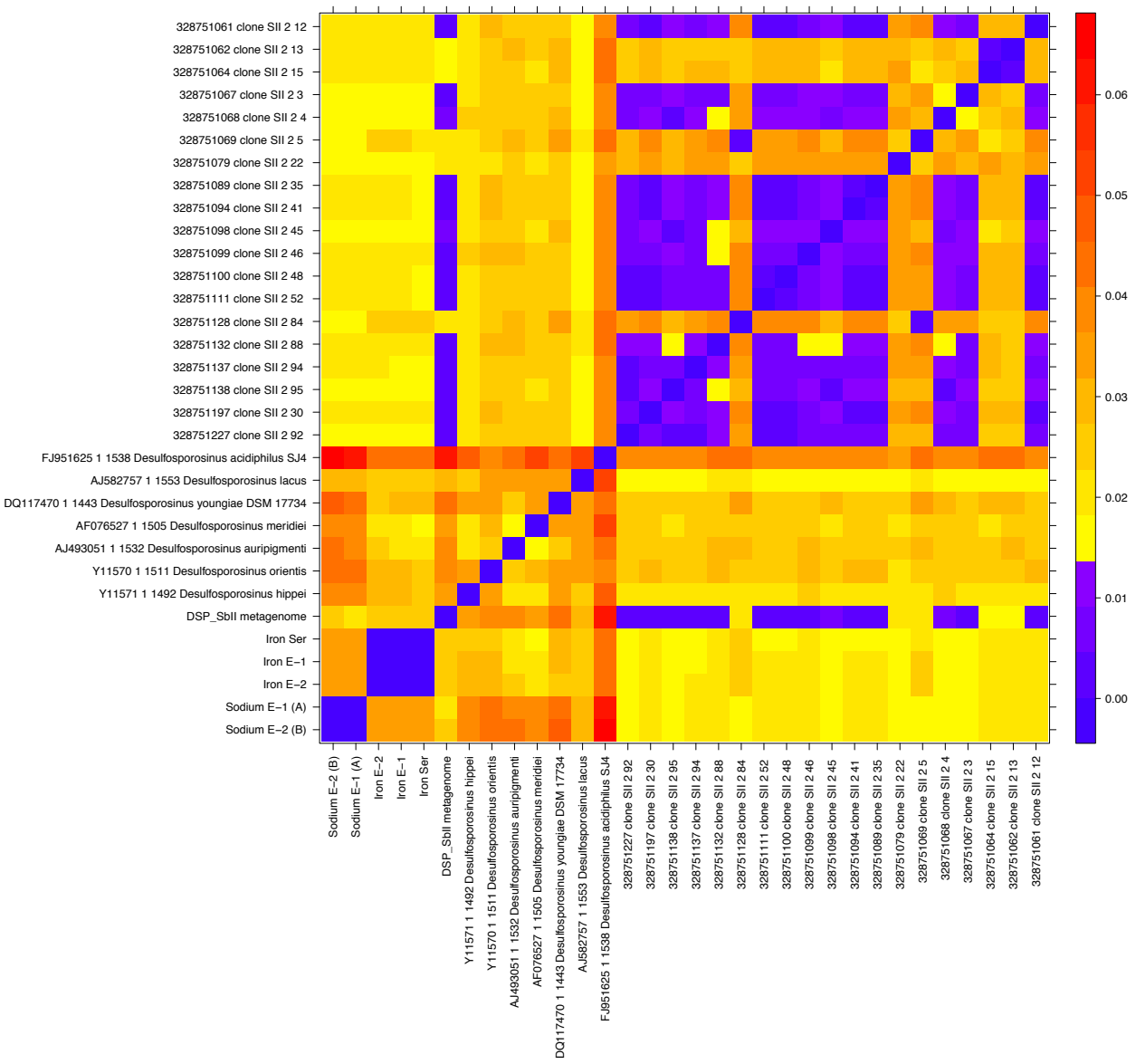

Figure 8-27
16S rRNA gene DNA distance matrix of the five candidate isolates of this study. DSP_SbII metagenome denotes a metagenomic contig obtained from Schlöppnerbrunnen II soil (Bela Hausmann). Furthermore DNA sequences of 16S rRNA gene clone libraries from Schlöppnerbrunnen II are included. For the validly described *Desulfosporosinus* type strains one representative sequence was used respectively. Distances are row, without any evoluationary model used for correction. The legend denotes the proportion of dissimilar positions. The interface between lila and yellow denotes the suggested threshold for species delimination (98.65 %), based on 16S rRNA gene DNA sequence dissimilarity.

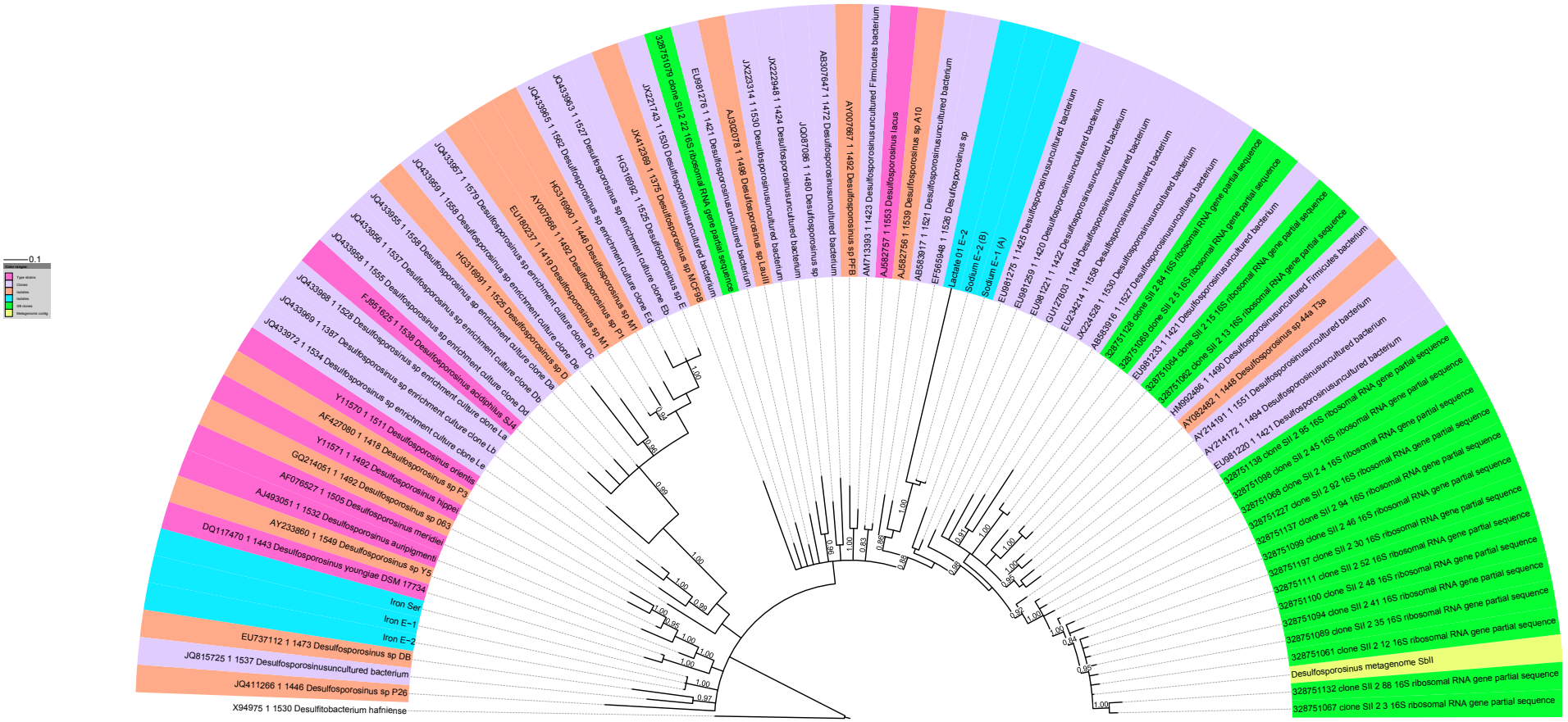

Figure 8-28

MrBayes tree, showing the phylogentic affiliation of the novel DSP-SbII candidate isolates (turquoise) to type strains of the genus*Desulfosporosinus* (pink). Note that "Lacate 01 E-2" is the highly enriched specimen from the first generation of dilution series of a *Desulfosporosinus* specific PCR product (about 1 kb in length). Not validately described, environmental *Desulfosporosinus*isolates are shown in orange. Environmental clone sequences are shown in light blue. Clones from Schlöppnerbrunnen II are shown in green. A metagenomic 16S rRNA gene contig from Schlöppnerbrunnen II soil is shown in yellow. *Desulfitobacterium hafniense* was used as an out-group (white). Posterior probability values higher than 0.8 are provided for the respective branches.

8.4 Desulfovibrio pH series

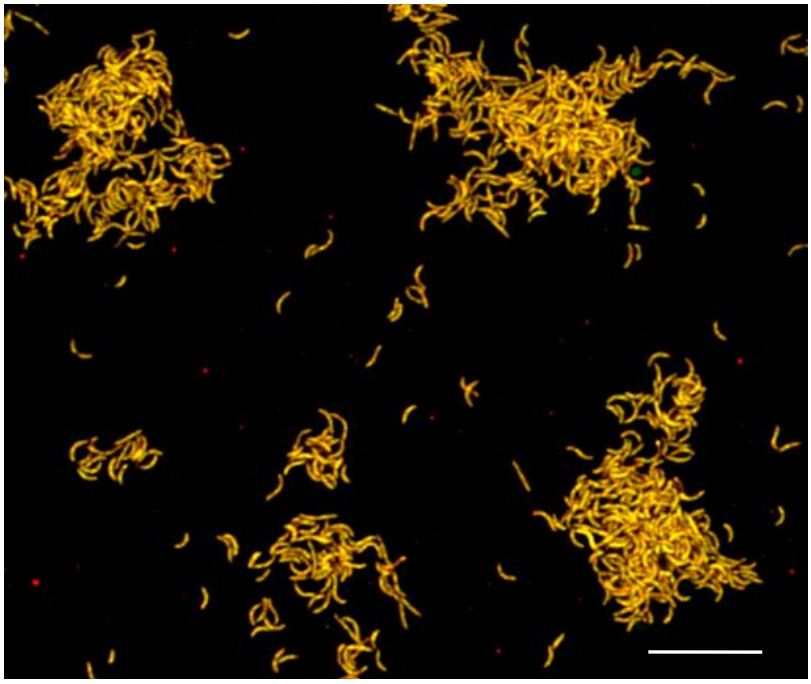

Figure 8-29
Mid exponential phase,PFA fixed *Desulfovibrio* sp. SII13a growing atneutral pH (7.1) basal FM (lactate [10 mM], sulfate [5 mM]).
Desulfovibrio cells stain yellow. The red signals are autofluorescent particles of residual FeS precipitates. Probes: EUBmix-FITC, Delta495mix-Cy3. Scalebar=10 µm

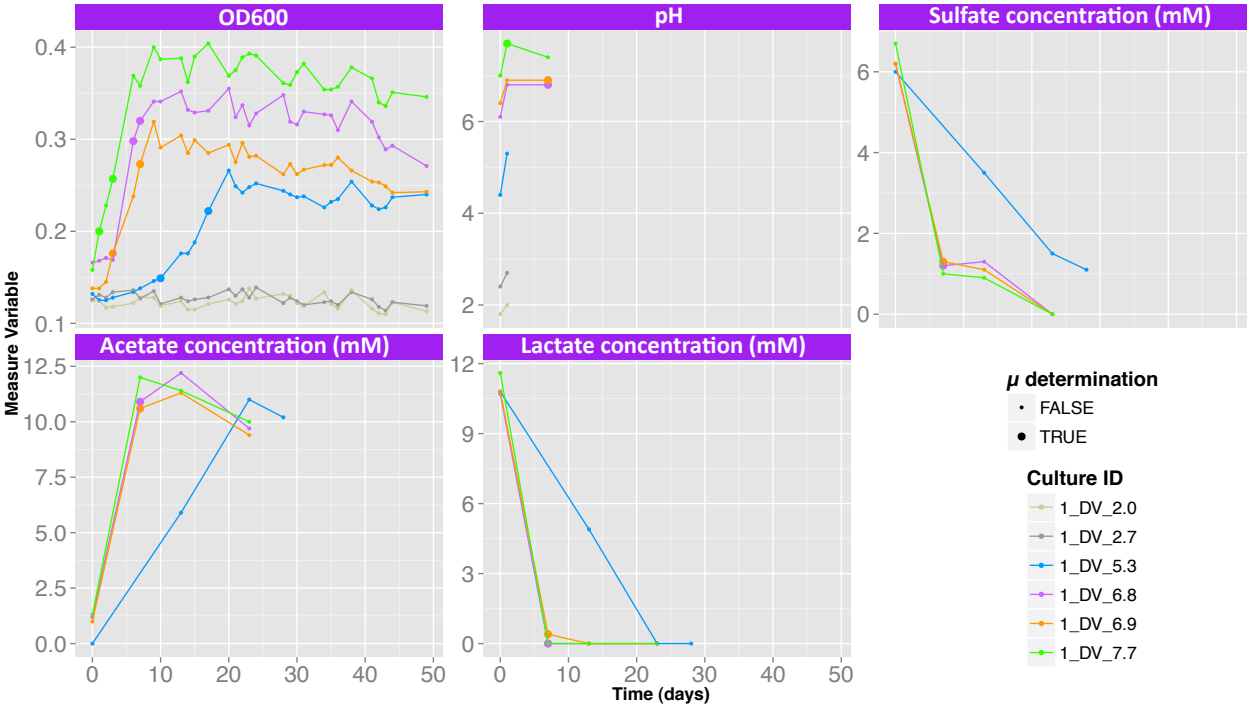

Figure 8-30
Measured parameters of first generation pH dependend growth experiment of *Desulfovibrio sp. SII13a*. The last segment numbers of culture IDs denote the pH of the medium after inoculation. Big points denote OD timepoints used for growth rate (µ) determination.

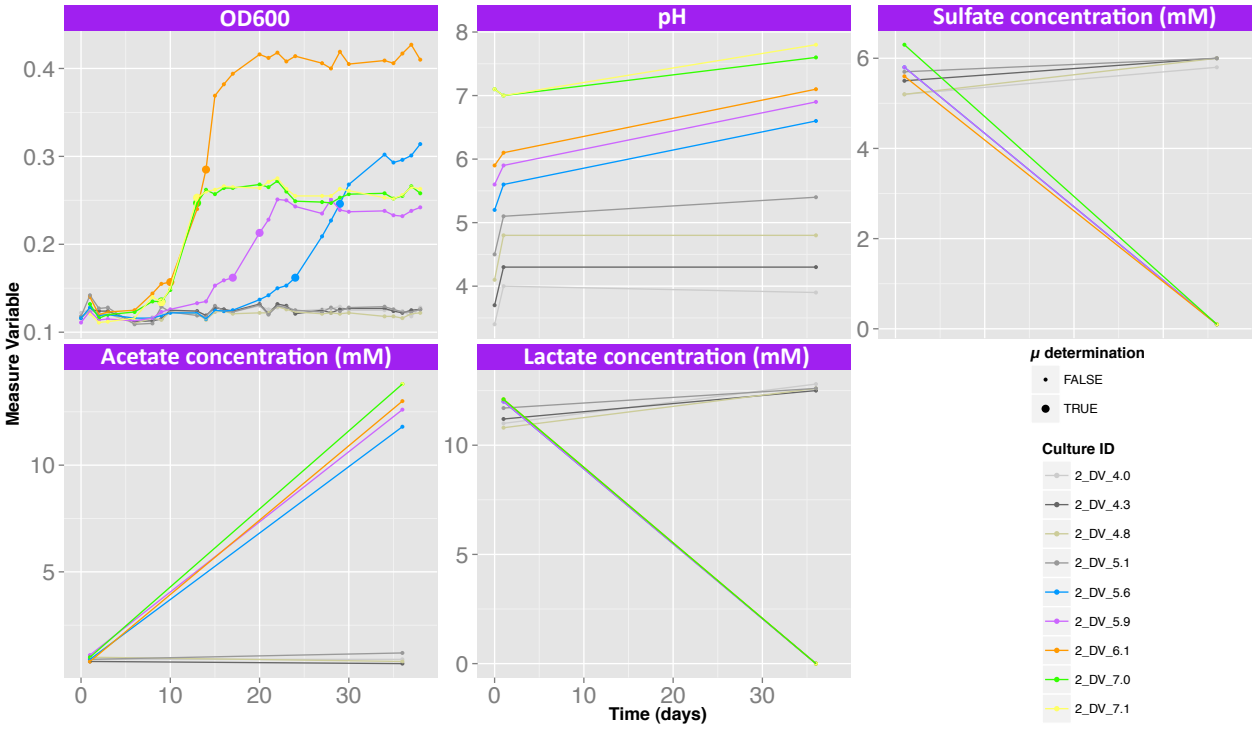

Figure 8-31
Measured parameters of the second generation of pH dependend growth experiment of *Desulfovibrio* sp. SII13a. The last segment numbers of culture IDs denote the pH of the medium after inoculation. Big points denote OD timepoints used for growth rate (μ) determination.

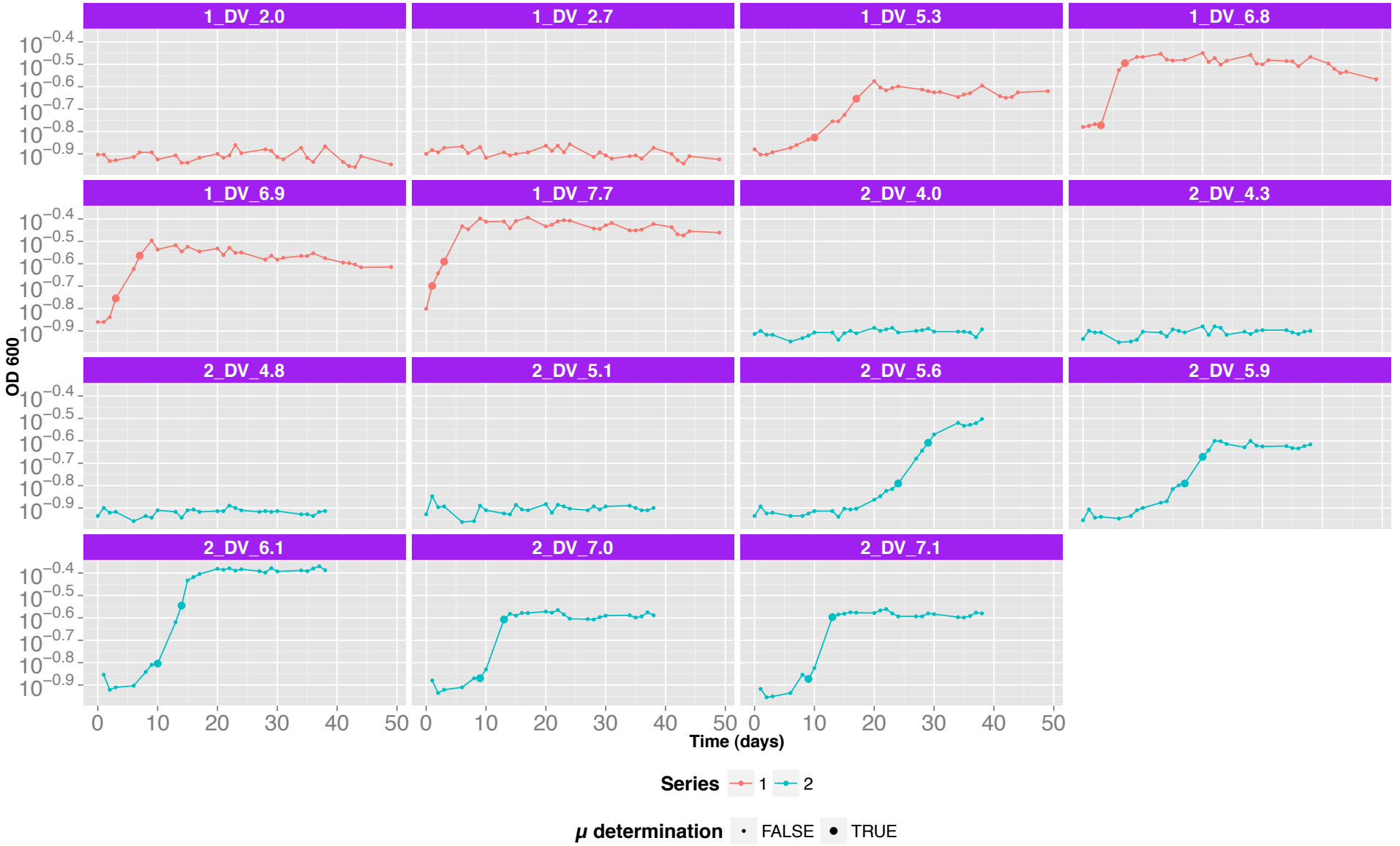

Figure 8-32
Log transformed OD_{600} data of *Desulfovibrio* sp. SII13a growing at different proton concentration. Datapoints for growth rate determination are indicated with bigh dots.

9 Curriculum vitae

Name	**Martin Huemer**
Nationality	Austria
Date of Birth	12.05.1986
Place of Birth	Freistadt, Austria
Languages	German, English, Spanish
Education	
Timeframe	*October 2011 – Summer 2014*
Institution	**Universityof Vienna**
Masterstudies	**Ecology with emphasis on microbial ecology**
Masterthesis	„ Targeted enrichment of a novel “rare biosphere“ member Desulfosporosinus species and tackling the response of potential core microbiota to anoxic regimes in an acidic fen ecosystem.
Targeted Degree	Master of Science
Timeframe	*October 2007 – September 2011*
Institution	**Universityof Vienna**
Bachelorstudies	**Biology with emphasis on ecology**
Bachelorthesis	„Analyzing Pro- and Antioxidative Effects of Juglon by Deoxyribose Degradation Assays and Cyclic Voltammetry“
Degree	Bachelor of Science
Timeframe	*October 2006 – June 2007*
Institution	**University of Vienna**
Bachelorstudies	**Cultural- and Socialanthropology**
Timeframe	*October 2005 – September 2006*
Institution	**Puplic hospital Freistadt**
Information	**Community service**
Timeframe	*September 2000 - June 2005*
Institution	**Bundesoberstufenrealgymnasium Bad Leonfelden**
Information	Curricular emphasis in Biology, Chemistry and Physics
Degree	Matura
Timeframe	*September 1996 – July 2000*
Institution	**Private secondary modern school Marianum Freistadt**
Timeframe	*September 1992 – July 1996*
Institution	**Elementary school Schenkenfelden**